School of Chemistry
FACULTY OF MATHEMATICS and PHYSICAL SCIENCES
UNIVERSITY OF LEEDS

CEDAR Prize Lecture 2007

Meteoric Smoke – where on earth is it?

John Plane

Tomas Vondrak, Sarah Broadley, Russell Saunders, Zeyu Fan

This work is supported by: NATURAL ENVIRONMENT RESEARCH COUNCIL

Papers on which this lecture is based

Removal of Meteoric Iron on Polar Mesospheric Clouds

John M. C. Plane,[1*] Benjamin J. Murray,[1] Xinzhao Chu,[2]
Chester S. Gardner[2]

Polar mesospheric clouds are thin layers of nanometer-sized ice particles that occur at altitudes between 82 and 87 kilometers in the high-latitude summer mesosphere. These clouds overlap in altitude with the layer of iron (Fe) atoms that is produced by the ablation of meteoroids entering the atmosphere. Simultaneous observations of the Fe layer and the clouds, made by lidar during midsummer at the South Pole, demonstrate that essentially complete removal of Fe atoms can occur inside the clouds. Laboratory experiments and atmospheric modeling show that this phenomenon is explained by the efficient uptake of Fe on the ice particle surface.

SCIENCE vol. 304, 426 (2004)

ATMOSPHERIC SCIENCE

An Iron Deficiency in Polar Mesospheric Clouds

Donald M. Hunten

Nature vol. **432**, 1011 (2004)

Subsequent work

Meteoric metals and PMCs:

Gardner, C.S., J.M.C. Plane, W. Pan, T. Vondrak, B.J. Murray, X. Chu, Seasonal variations of the Na and Fe layers at the South Pole and their implications for the chemistry and general circulation of the polar mesosphere, *J. Geophysical Research* **110***,* art. no. D1030210 (2005).

Murray, B. J. and J. M. C. Plane, Uptake of Fe, Na and K on low-temperature ice: implications for metal atom scavenging in the vicinity of polar mesospheric clouds, *Phys. Chem. Chem. Phys.*, 7**,** 3970-3979 (2005).

Stevens, M.H., R. R. Meier, X.-C. Chu, M. T. Deland, and J. M. C. Plane, Antarctic mesospheric clouds formed from space shuttle exhaust, *Geophys. Res. Lett.*, **32**, art. no. L13810 (2005).

Vondrak, T., Plane, J. M. C. and Meech, S. R. Photoemission from sodium on ice: A mechanism for positive and negative charge coexistence in the mesosphere. *Journal of Physical Chemistry B* **110**, 3860-3863 (2006).

Raizada, S., M. Rapp, F.-J. Lübken, J. Hoeffner, M. Zecha, and J. M. C. Plane, Effect of ice particles on the mesospheric potassium layer at Spitsbergen (78oN), *J. Geophys. Res.*, 112, art. no. D08307 (2007).

Fan, Z.Y., J. M. C. Plane, J. Gumbel, J. Stegman and E. J. Llewellyn, Satellite measurements of the global mesospheric sodium layer, *Atmos. Chem. Phys. Discuss.*, 7, 5413-5437 (2007).

Meteoric smoke

Saunders, R. W., and J. M. C. Plane, A laboratory study of meteor smoke analogues: Composition, optical properties and growth kinetics, *J. Atmos. Sol.-Terr. Phys.*, 68, 2182-2202 (2006).

Gabrielli, P., J. M. C. Plane, C. F. Boutron, S. M. Hong, G. Cozzi, P. Cescon, C. Ferrari, P. J. Crutzen, J. R. Petit, V. Y. Lipenkov, and C. Barbante, A climatic control on the accretion of meteoric and super-chondritic iridium-platinum to the Antarctic ice cap, *Earth and Planetary Science Letters*, 250, 459-469 (2006).

Saunders, R. W., P. M. Forster, and J. M.C. Plane, Potential climatic effects of meteoric smoke in the Earth's paleo-atmosphere, *Geophys. Res. Lett.*, under review.

Contents of the lecture

1. The meteoroid flux and a new model of meteoric ablation
2. The Mesospheric metal layers
3. Satellite retrievals of the global Na layer
4. Noctilucent clouds and Space Shuttle plumes
5. Meteoric smoke – how does it form, where does it go?

Path of the lecture

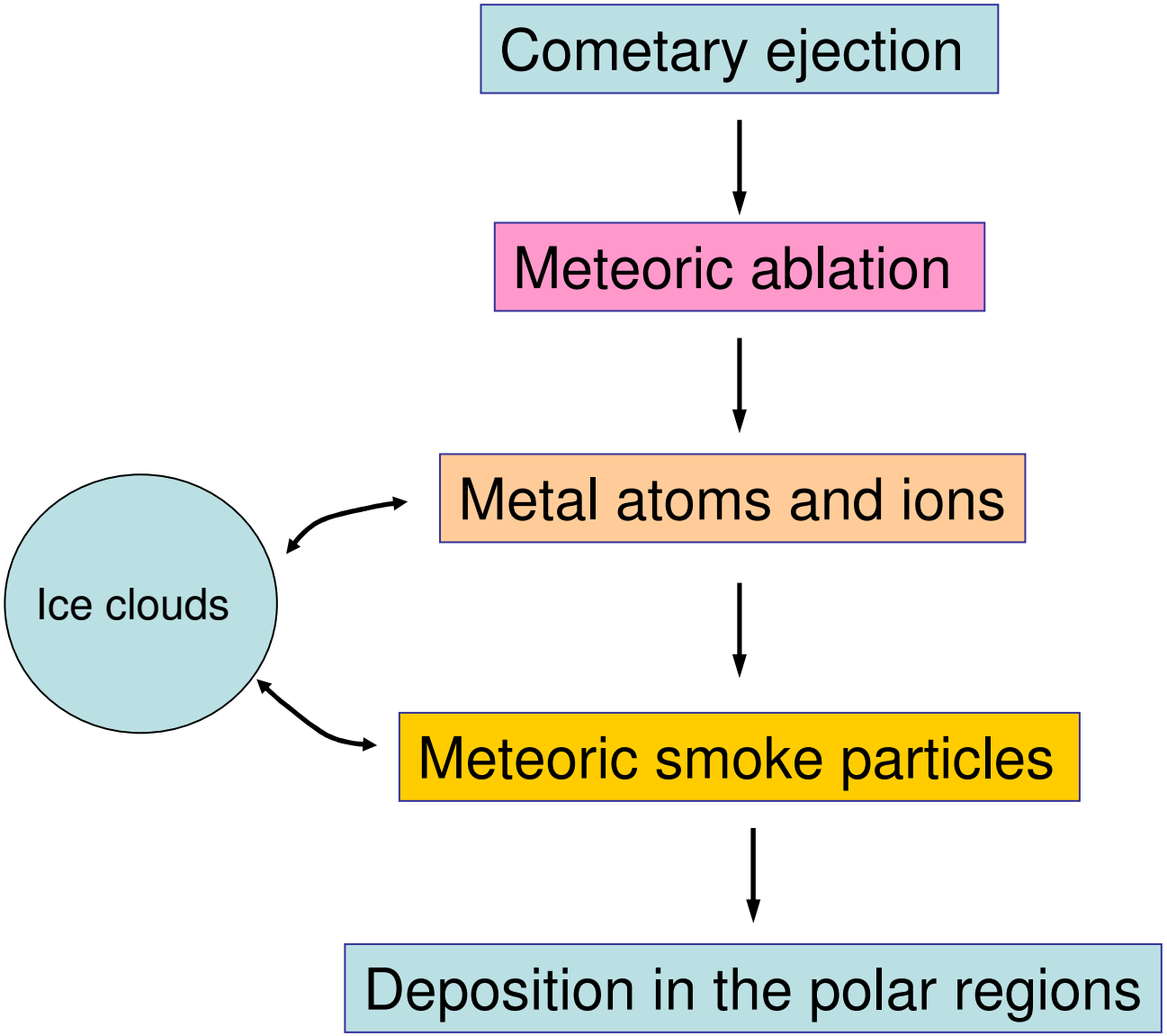

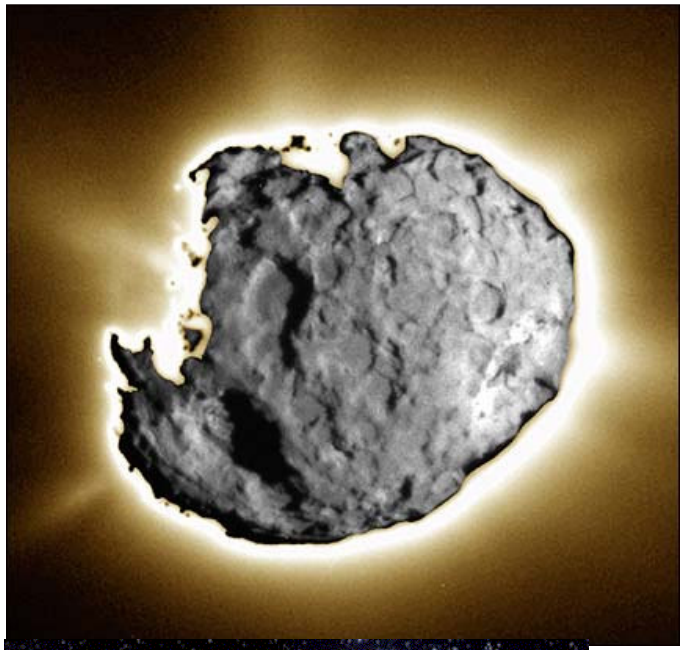

Comets are the major source of cosmic dust reaching the atmosphere

Picture of Comet Wild 2 obtained by the Nasa spacecraft Stardust 240 km away. The nucleus is ~5 km in diameter. The composite image shows an intensely active surface, jetting dust and gas streams into space.

Courtesy of John Laborde

Comets, like this photo of Comet West, leave a trail of dust behind them as they near the sun and their icy nucleus sublimates. The dust trails give rise to *meteor showers* when the earth's orbit crosses them.

Sporadic meteors make up most of the material entering the atmosphere. These originate from the asteroid belt beyond Mars, and from long-decayed cometary trails.

Although this may look like a smoky trail behind the fireball, it is actually chemiluminescence!

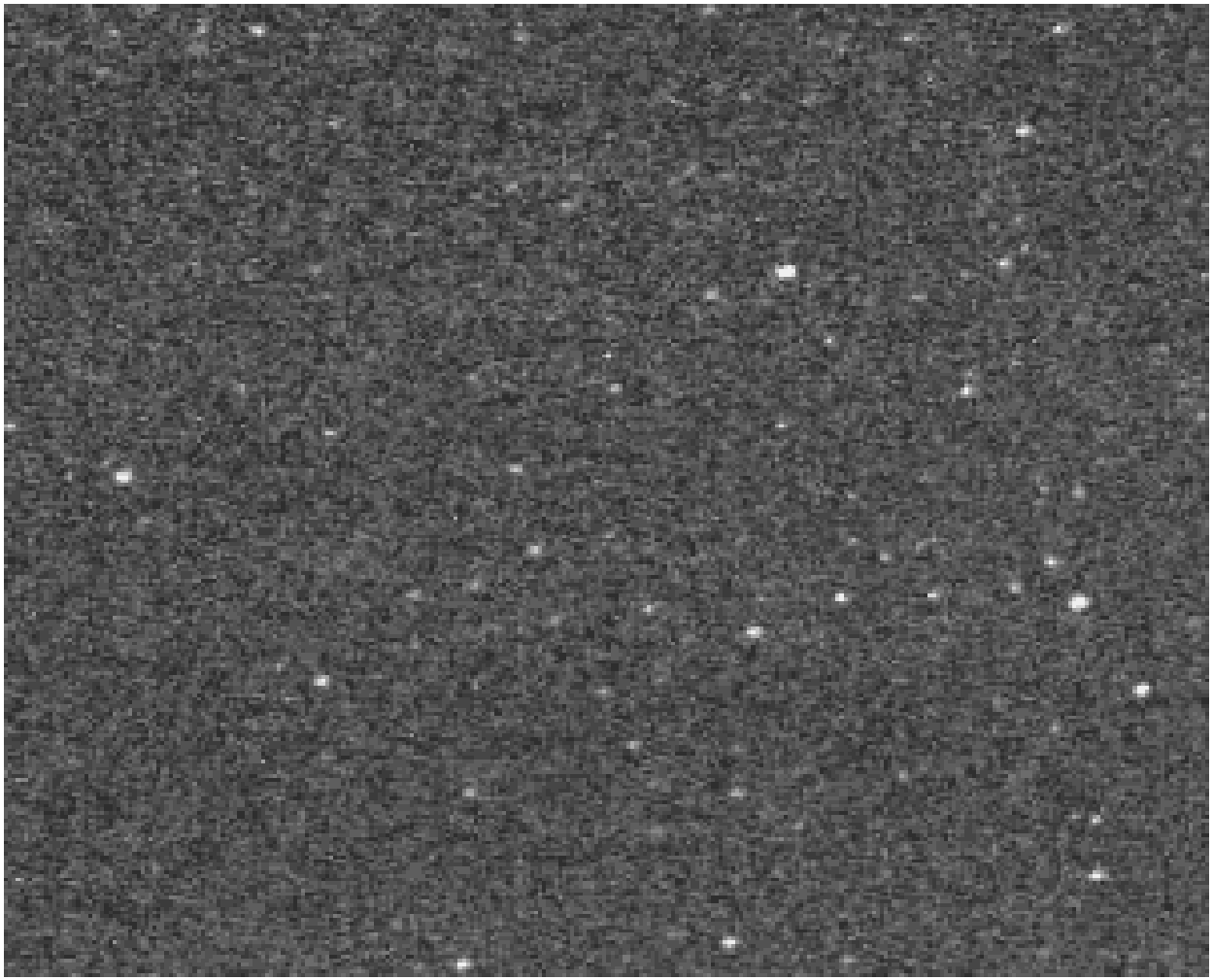

Source: www.spaceweather.com

The flux of small near-Earth objects (D < 200 m) colliding with the Earth

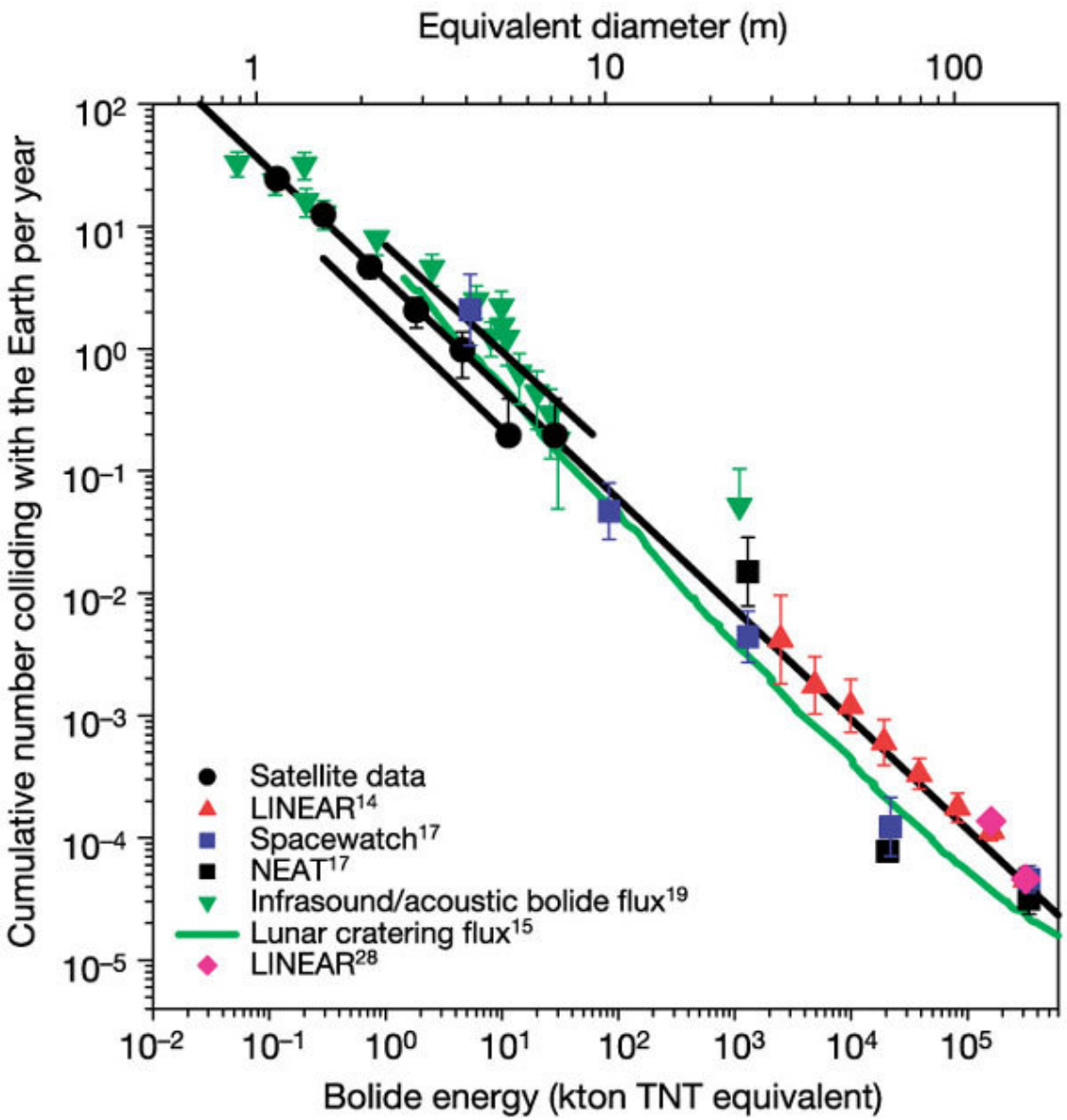

8 years of detonations recorded by infrasound, and optical flashes recorded by satellite

Power-law fit to N, the cumulative number of objects with diameters > D

$$\log N = 1.6 - 2.7 \log D$$

[Brown *et al.*, *Nature*, 2002]

The flux of small near-Earth objects over a range of 14 magnitudes of energy

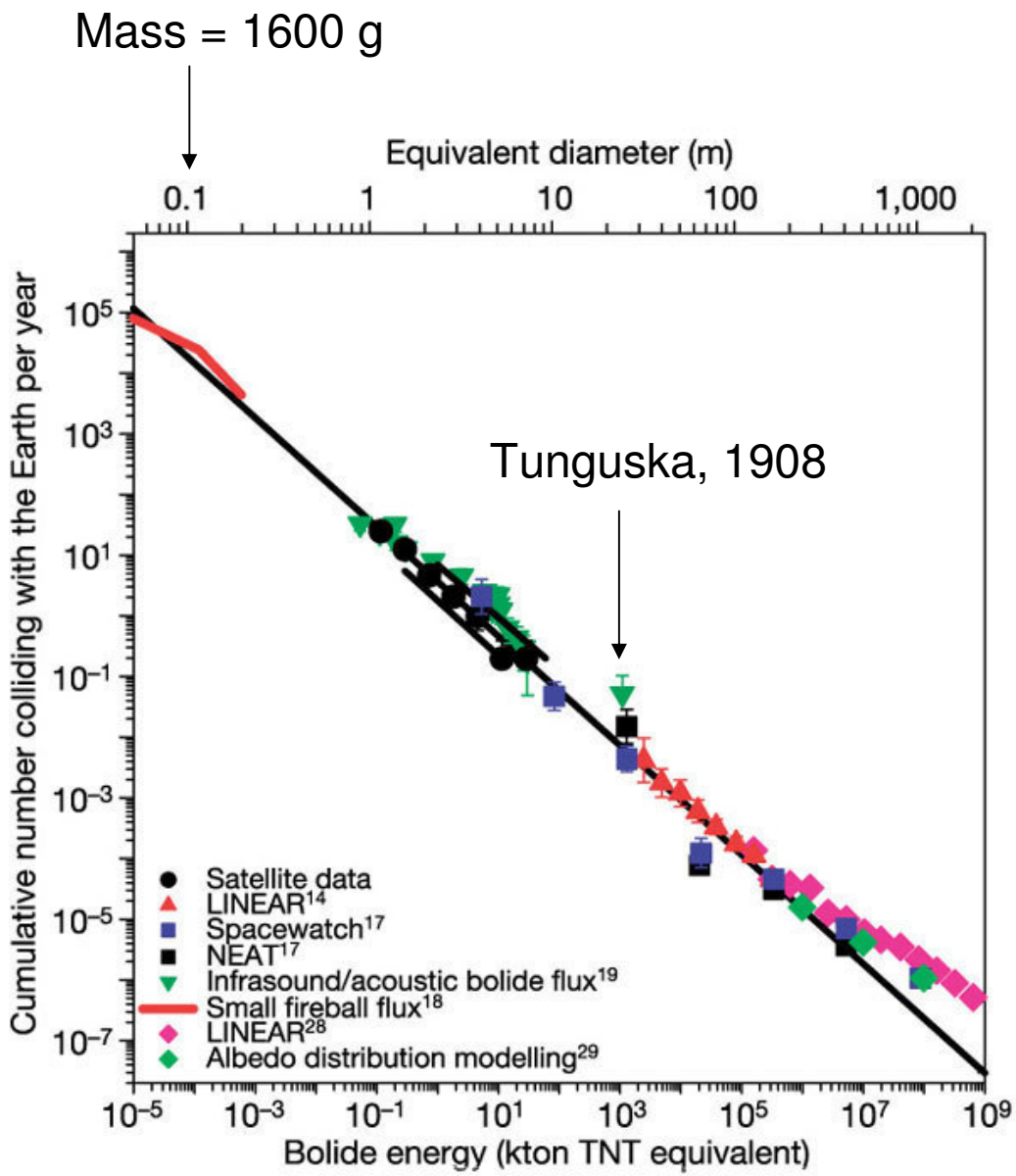

Brown *et al., Nature* 2002

The cumulative number of small meteoroids

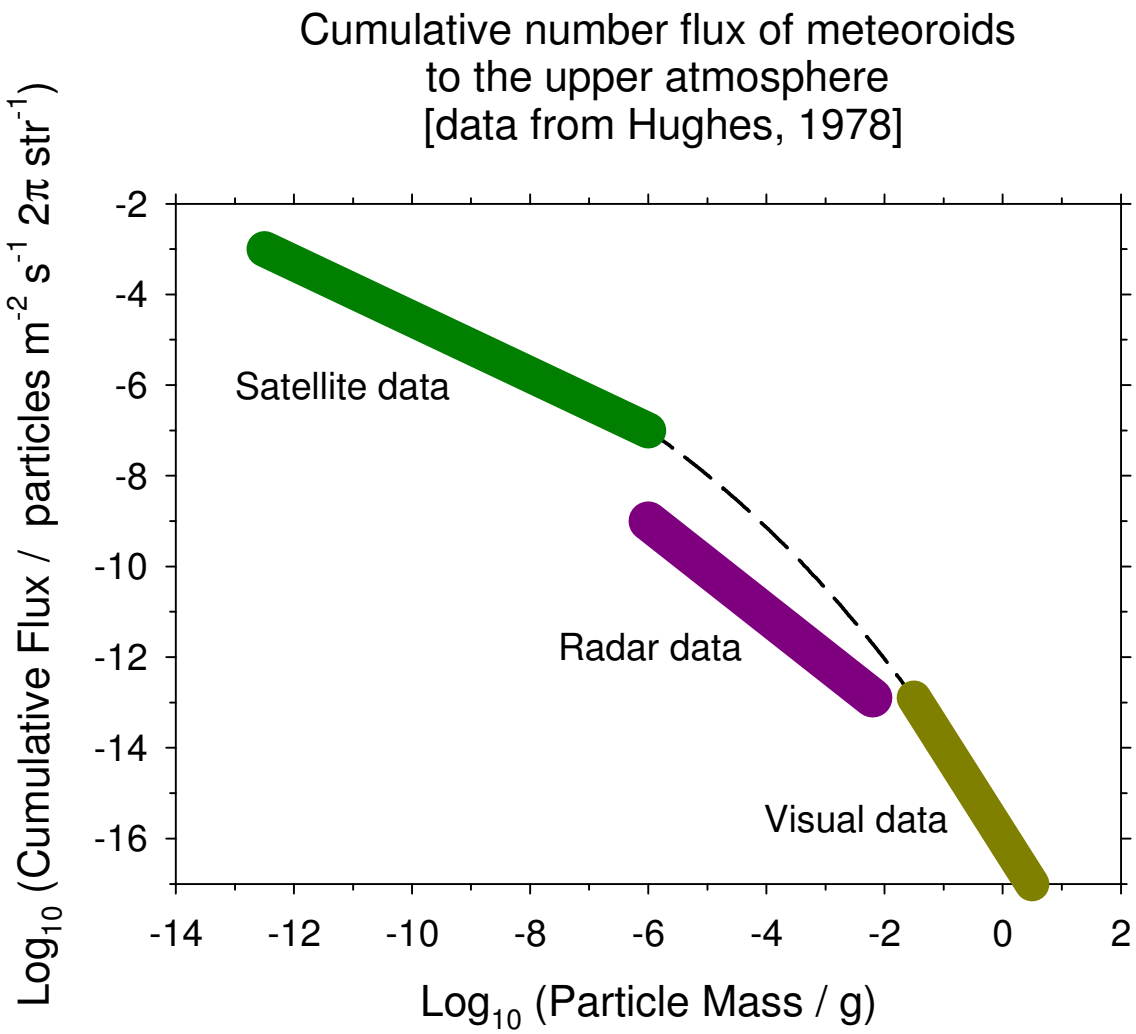

Hughes decided to ignore the radar data, and extrapolate between the satellite and visual data. Unfortunately, the largest contribution to the mass flux is around 10 μg!

Daily influx of

44 tonnes d^{-1}

The largest contribution to the incoming mass is from particles between 5 and 50 μg

Mass influx (per decade of mass) vs particle mass
[after Flynn, 2002]

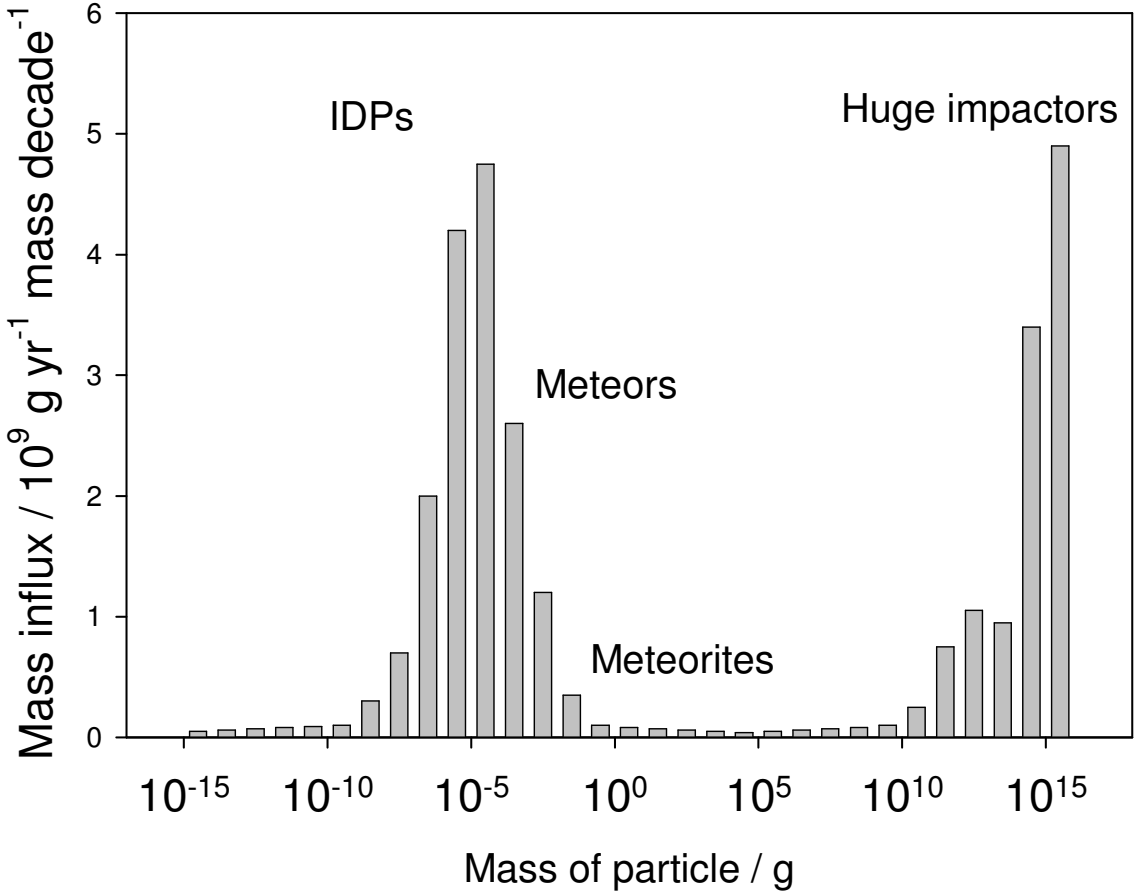

Data up to 10^{-2} g from the *Long Duration Exposure Facility*, which was exposed in space for 6 years instead of the planned 6 months, following the shuttle Challenger accident.

Produces an estimate of

110 tonnes d^{-1}

[Love and Brownlee, *Science* 1993]

A new chemical ablation model

- Classical ablation physics describes heating and melting
- Sputtering of individual atoms
- Updated MAGMA model for high temperature melts
- Mass loss rate given by Langmuir evaporation kinetics
- Impact ionization at hyperthermal energies

Solar system objects should impact on the atmosphere with velocities between 11.5 and 71.5 km s^{-1}

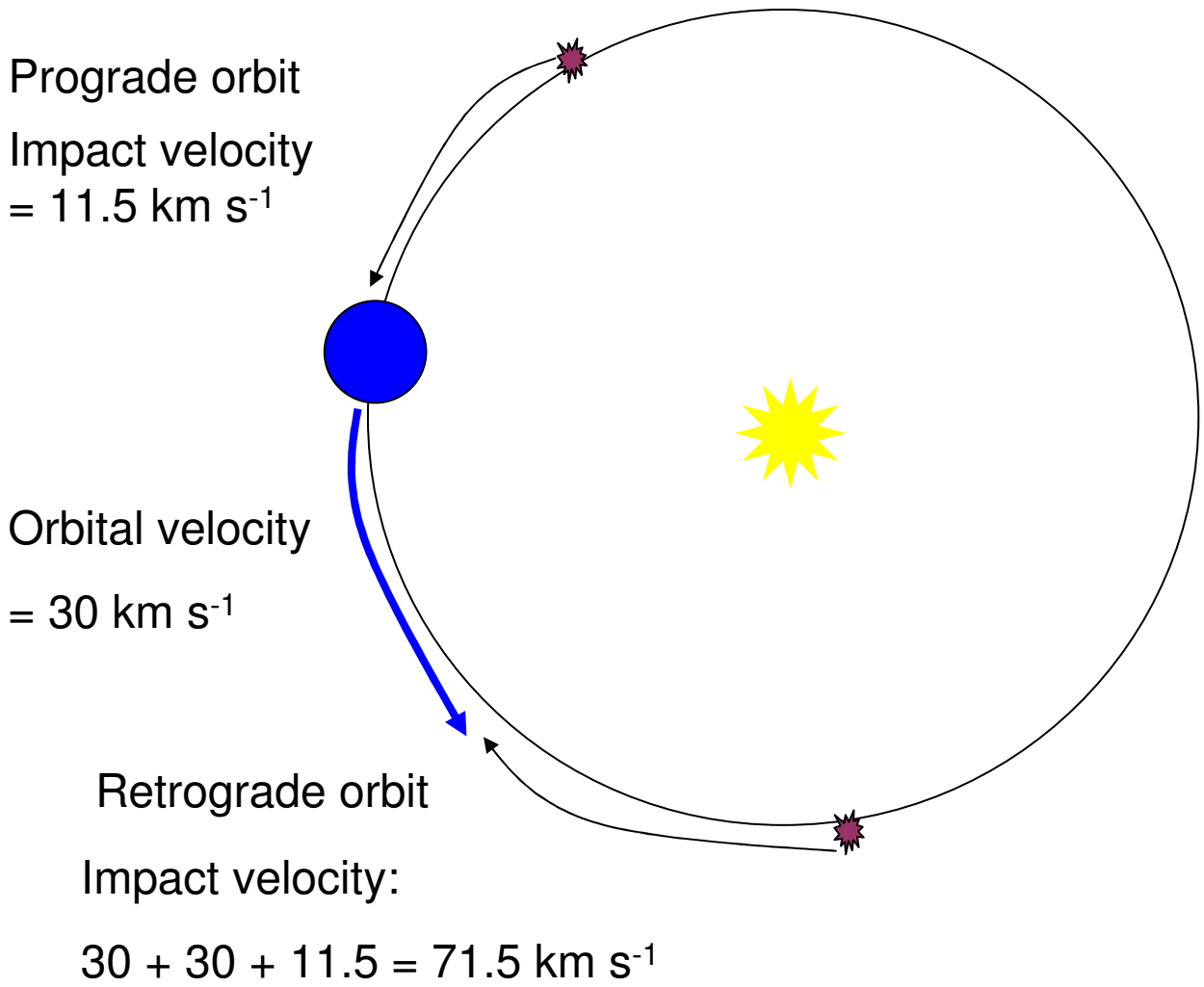

Meteoroid mass/velocity distribution taken from the Long duration exposure facility (McBride *et al.*, 1999)

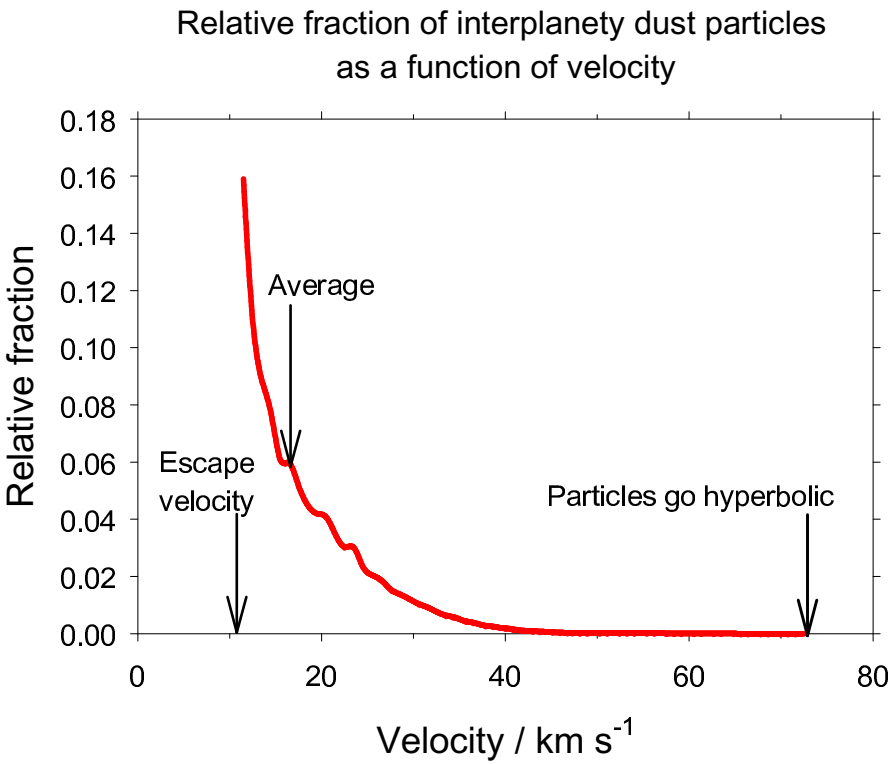

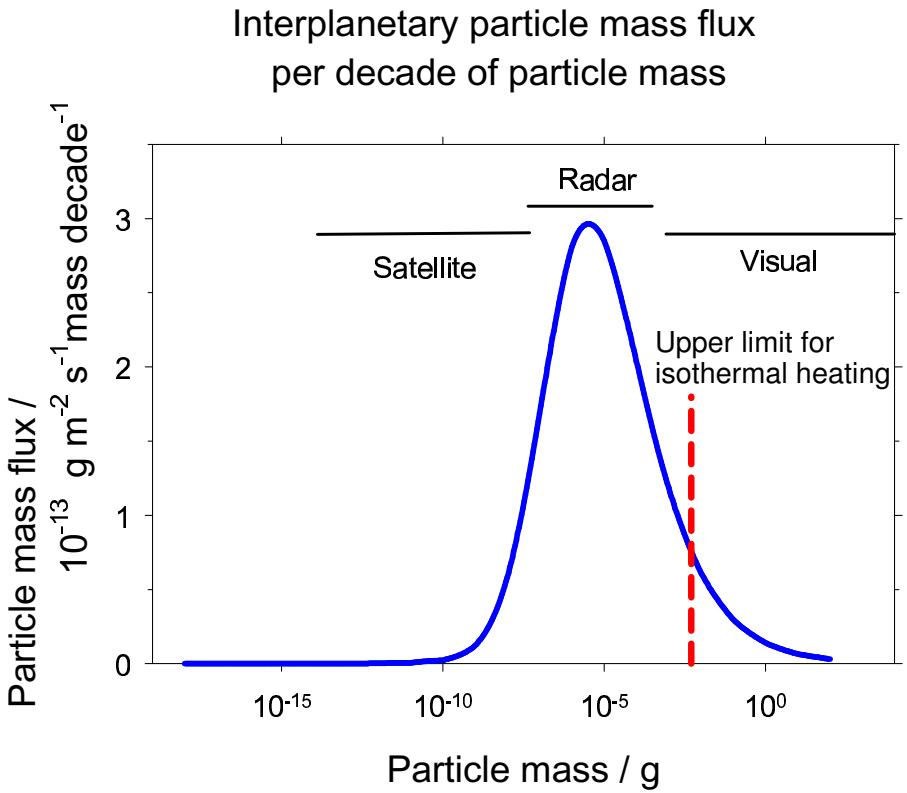

The Physics of Meteoric Ablation

The problem becomes reasonably tractable for particles less than about 250 μm in radius, because heat conductivity through the particle is fast enough for the particle to be treated as isothermal (Love and Brownlee, 1991)

The energy balance equation:

$$\frac{1}{2}\Lambda\rho_a v^3 = 4\sigma\varepsilon\left(T_s^4 - T_a^4\right) + \frac{4}{3}R\rho_m C\frac{\mathrm{d}T_m}{\mathrm{d}t}$$

Heat losses due to vaporization, heating, phase transitions

Frictional heating

Radiative heat loss

The change in velocity of the meteoroid :

$$\frac{\mathrm{d}v}{\mathrm{d}t} = -\frac{\Gamma\rho_a \pi R^2 v^2}{m} + \frac{\mu}{\left(z + r_e\right)^2}$$

Deceleration due to drag

Gravitational acceleration

Density	ρ_m = 2. x 10^3 kg m^{-3}
sublimation heat	L = 3. x 10^6 J kg^{-1}
specific heat	C = 1. x 10^3 J kg^{-1}
shape factor	A = 1.2
drag coefficient	Γ = 1.0
heat transfer coefficient	Λ = 1.0
emissivity	ε = 1.0
zenith angle	χ = 37^0

Arecibo Observatory,

Puerto Rico

The 305 m radio telescope dish can be used as an incoherent scatter radar (430 MHz). This system is so powerful that the head echoes of meteors can be observed in real time as they fly down through the beam.

From this the particle velocity and first height-of-detection are obtained.

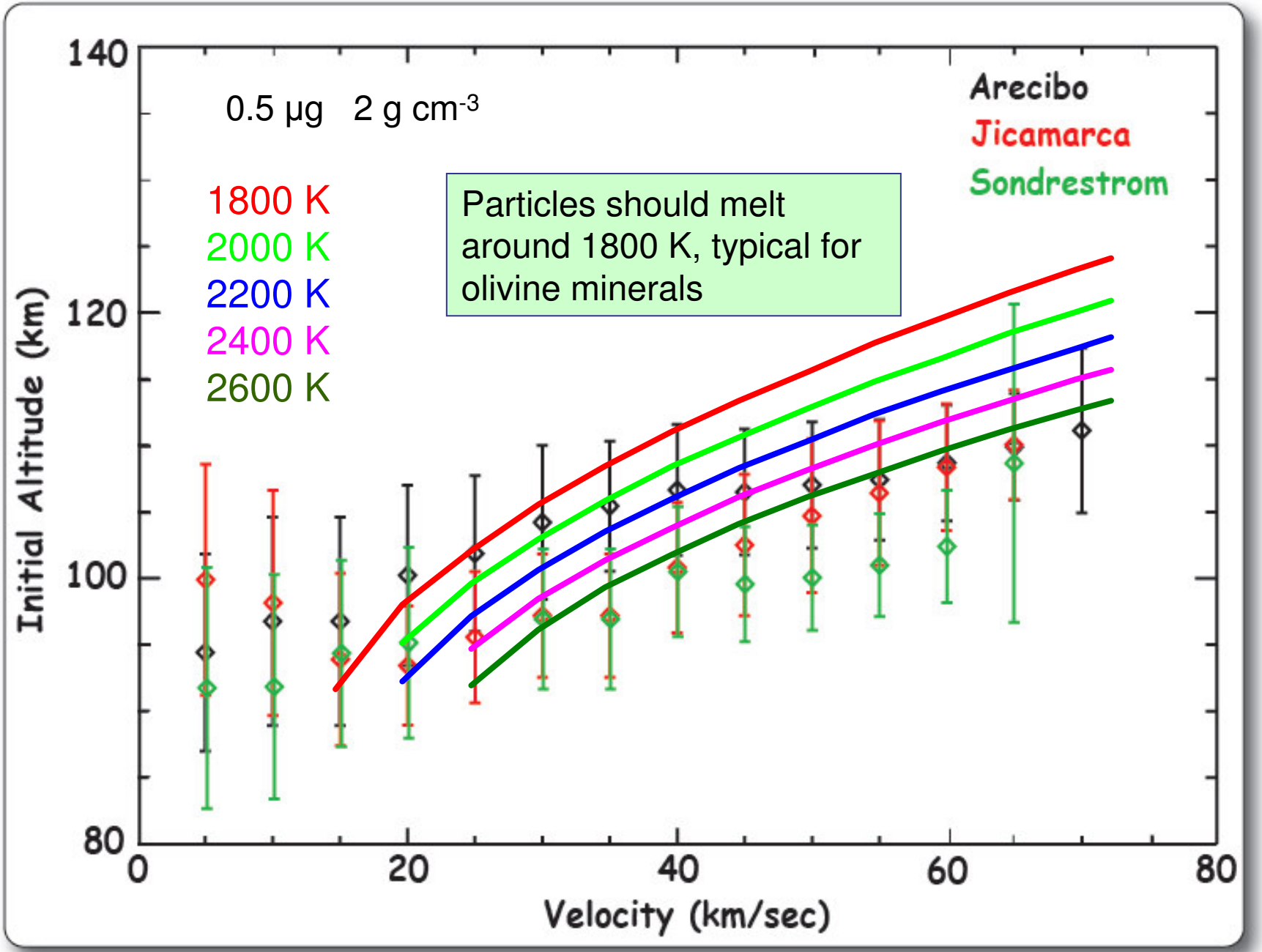

Radar data from D. Janches, CoRA

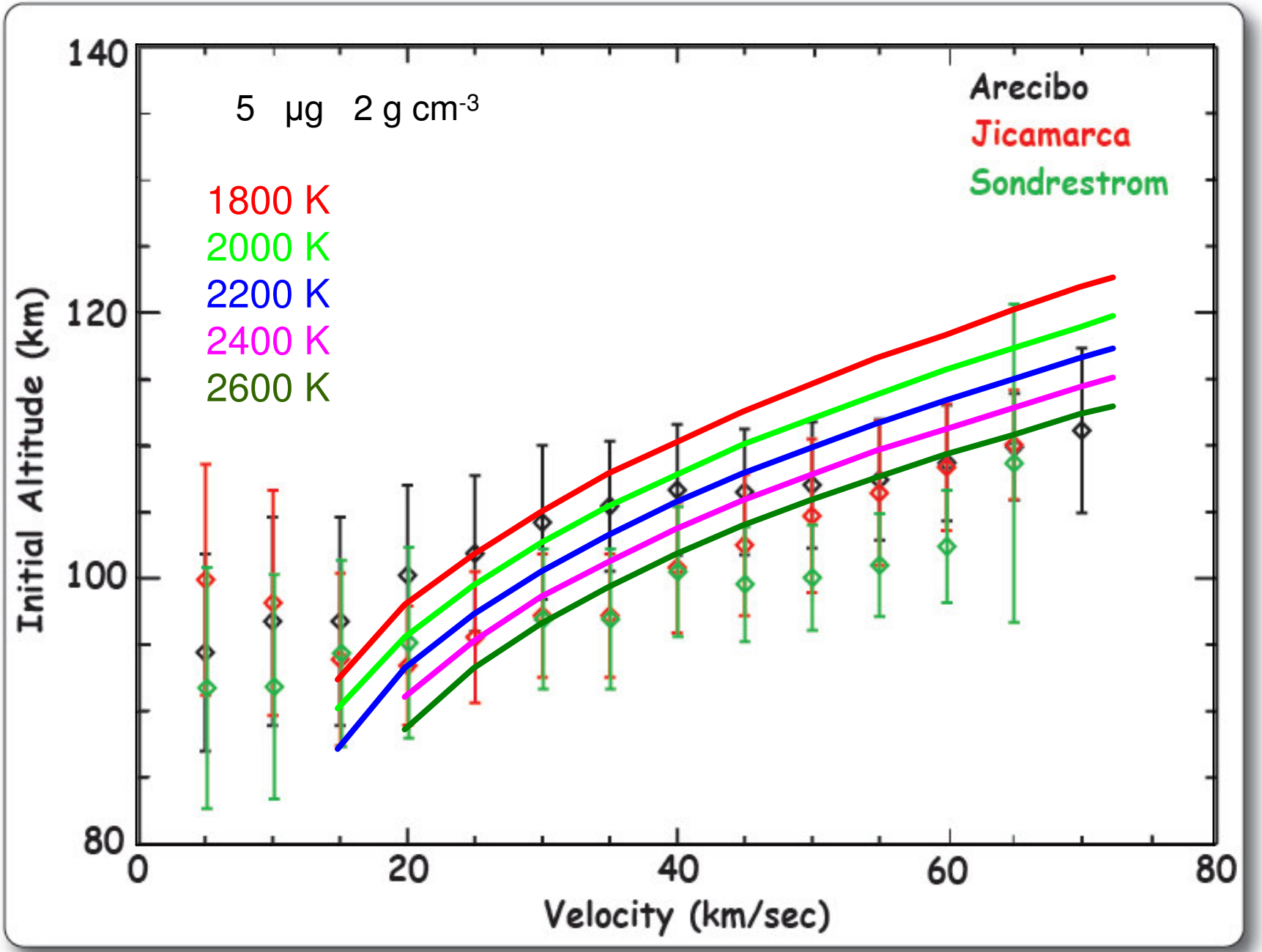

Radar data from D. Janches, CoRA

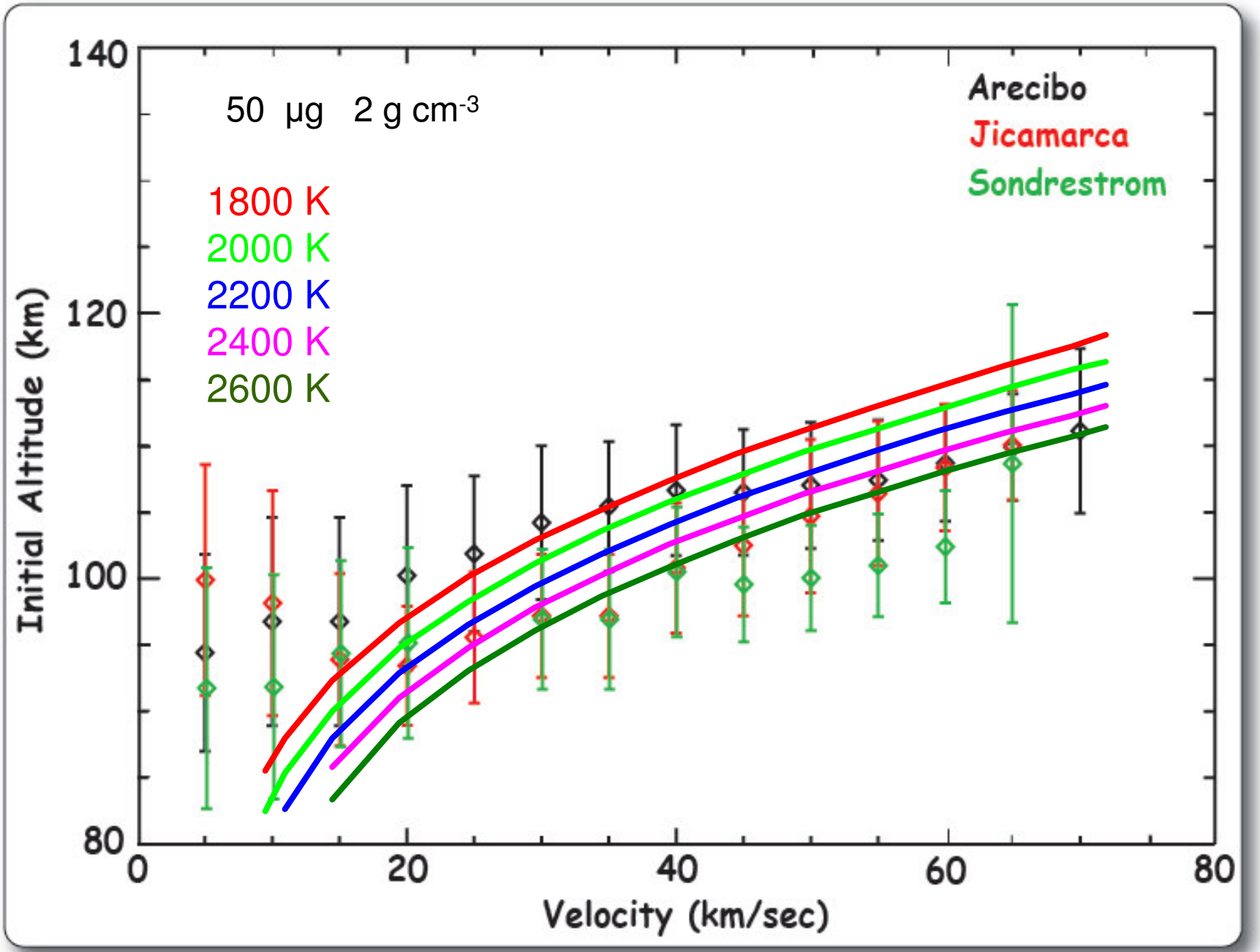

Radar data from D. Janches, CoRA

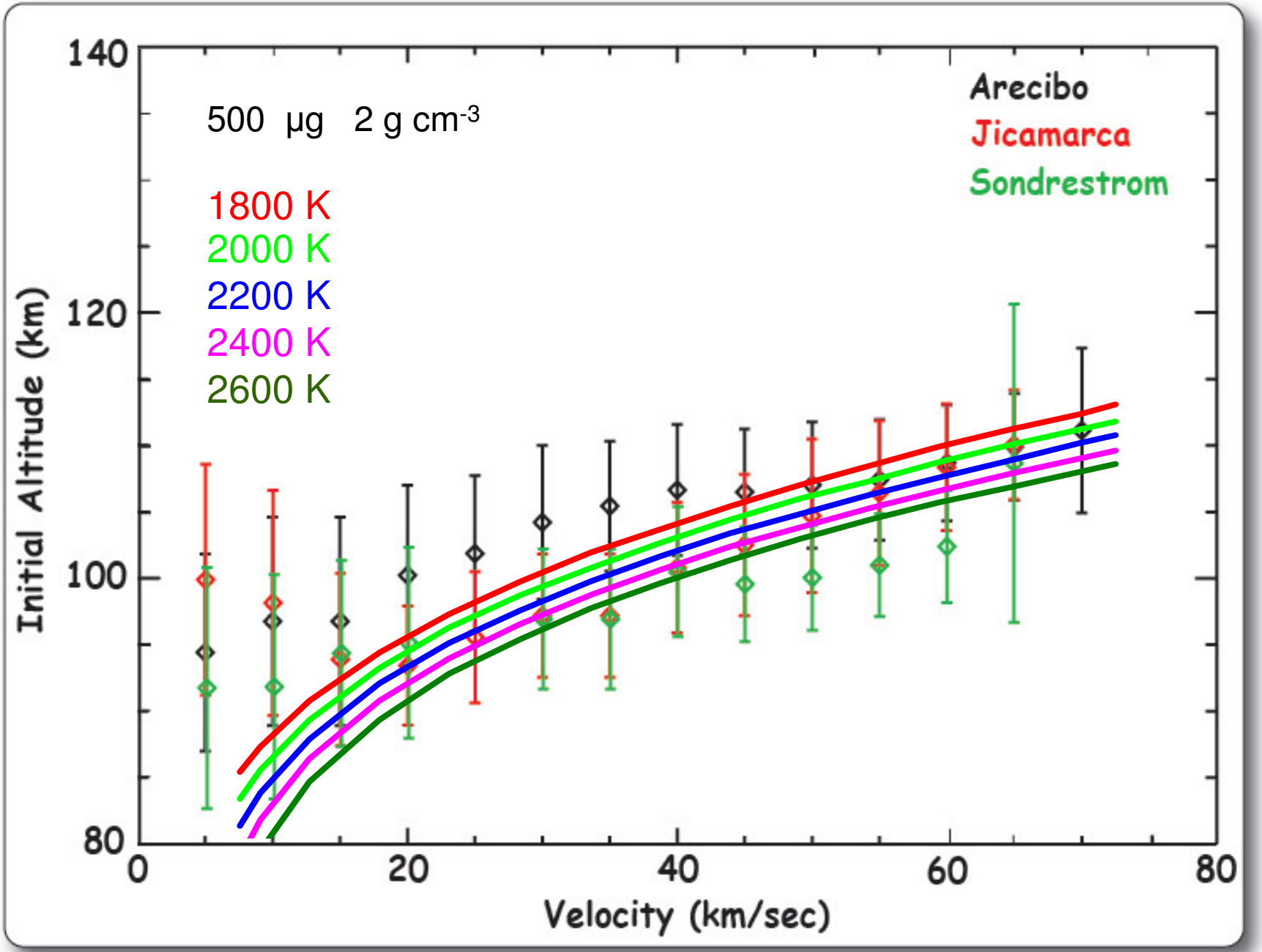

Radar data from D. Janches, CoRA

The Magma Model

Determines the thermodynamic equilibrium in a melt – gas-phase system

- calculates activity coefficients of metal oxides in non-ideal silicate and oxide melts
- establishes melt–vapour equilibrium and equilibrium between gas-phase components *simultaneously*

L. Schaefer, B. Fegley, Jr, *Icarus* **169** (2004) 216
Ideal Mixing of Complex Components: J.W. Hastie, D.W.. Bonnell, *J. Non-Crystalline Solids* **84** (1986)151

Gas-phase components in MAGMA

Atoms	Oxides	Ions
Si	SiO SiO_2	
O	O_2	
Mg	MgO	
Fe	FeO	
Ca	CaO	
Al	AlO AlO_2 Al_2O_2	
Ti	TiO TiO_2	
Na	Na_2O NaO	Na^+
K	K_2O KO	K^+

Element ablation profiles of the "typical" meteoroid: mass = 5 μg, speed = 20 km s^{-1}

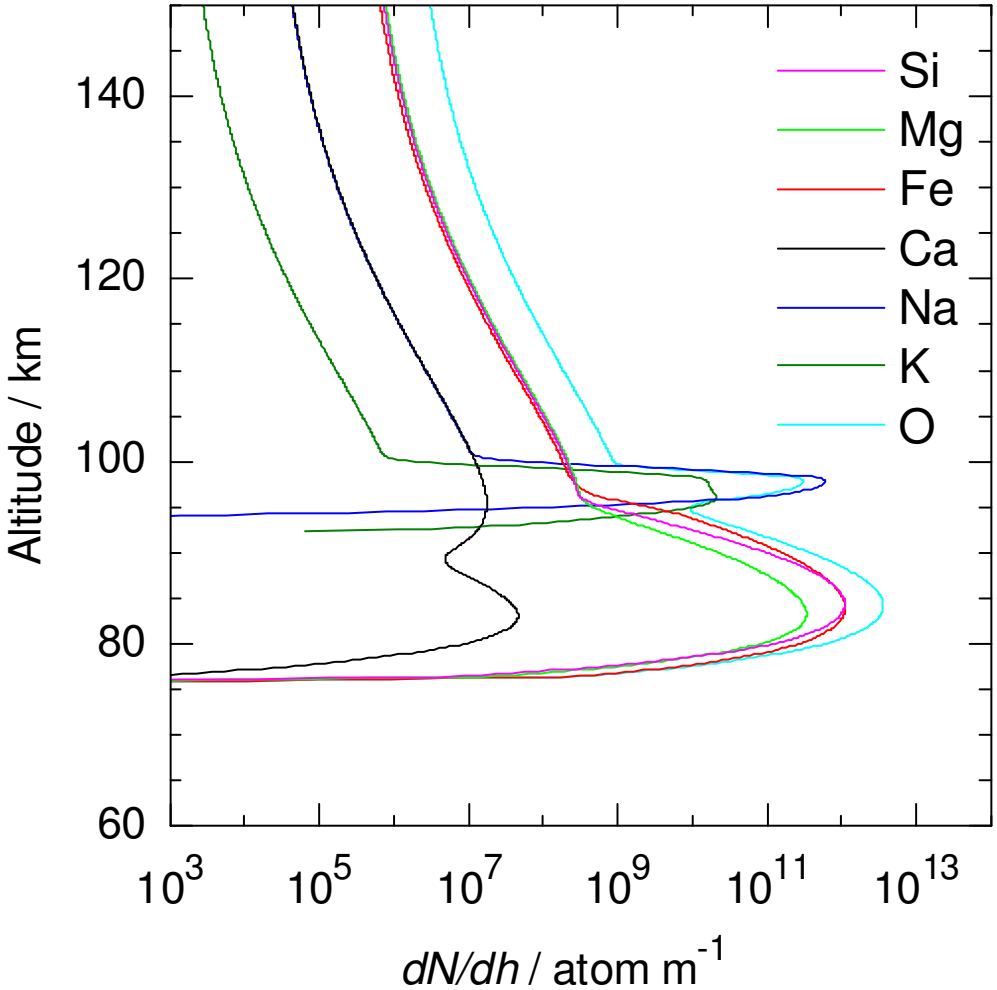

	Ablated At %	Centroid km	FWHM km
Si	100	84.7	5.6
Mg	100	84.0	5.4
Fe	100	84.5	6.4
Ca	61	(83.2)	4.7
Na	100	100.5	1.7
K	100	96.5	3.2
O	96	84.2	5.8

Differential ablation predicted

Lidar observations of meteor trials

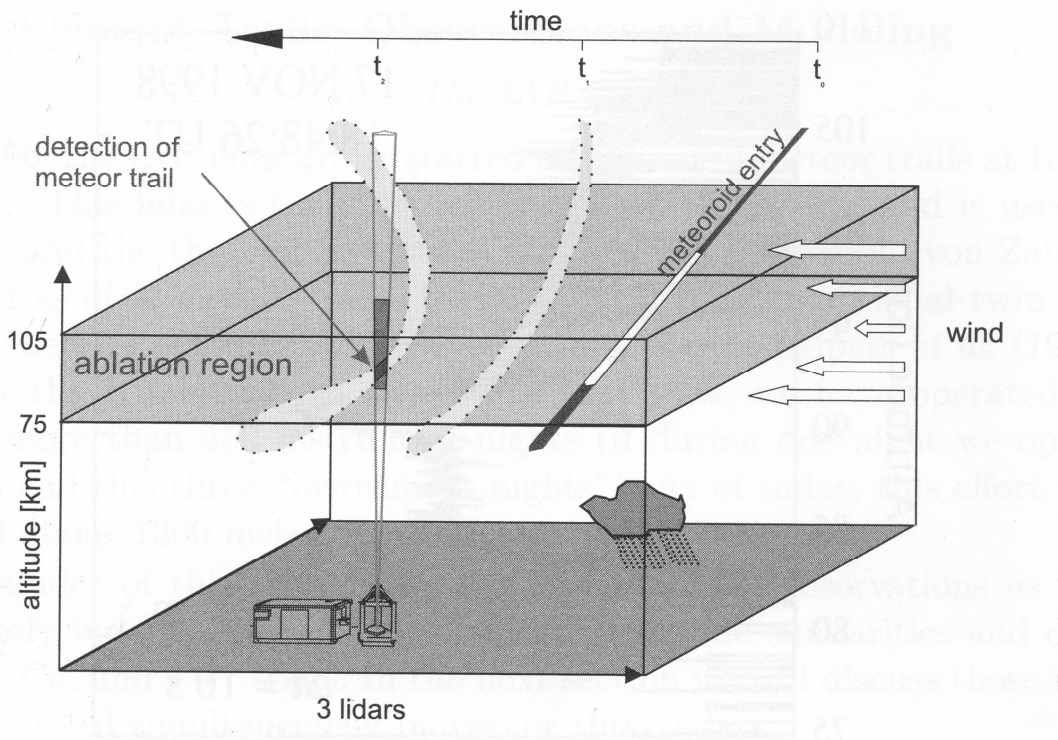

Viewing geometry of a trail evolving with time [von Zahn, 2002]

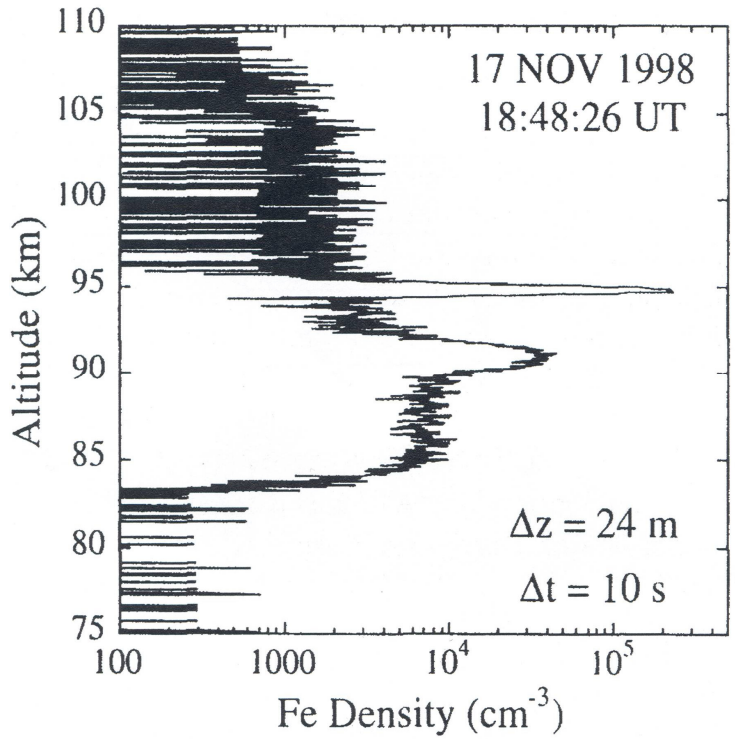

Profile on an Fe meteor trail measured by lidar [Chu *et al.*, 2002]

Lidar observation of a trail with three metals
(the only one observed out of thousands of trails)

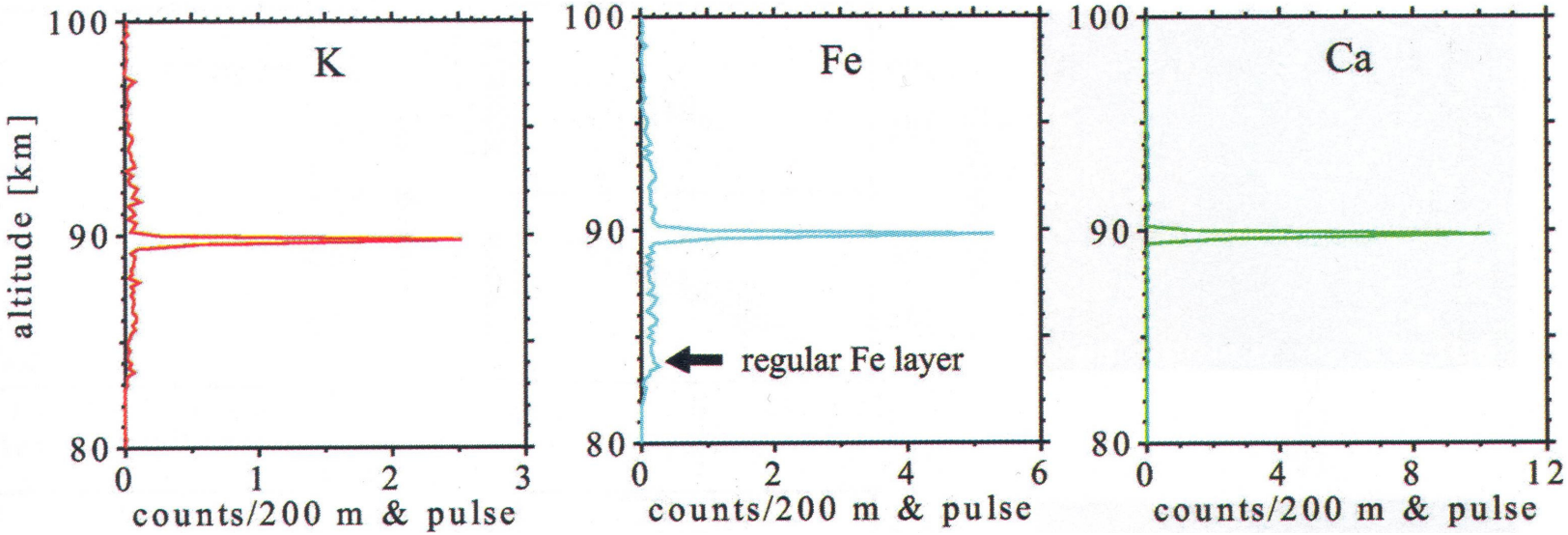

Only ~ 1% of trails show a pair of metals

⇒ differential ablation certainly occurs

U. von Zahn, in *Meteors in the Earth's Atmosphere*, Ed. E. Murad and I.P. Williams, (Cambridge University Press, 2002) 2002

Element ablation profiles integrated over the mass range 5 x 10^{-18} – 5 x 10^{-3} g, and velocity range 11 – 72 km s^{-1}

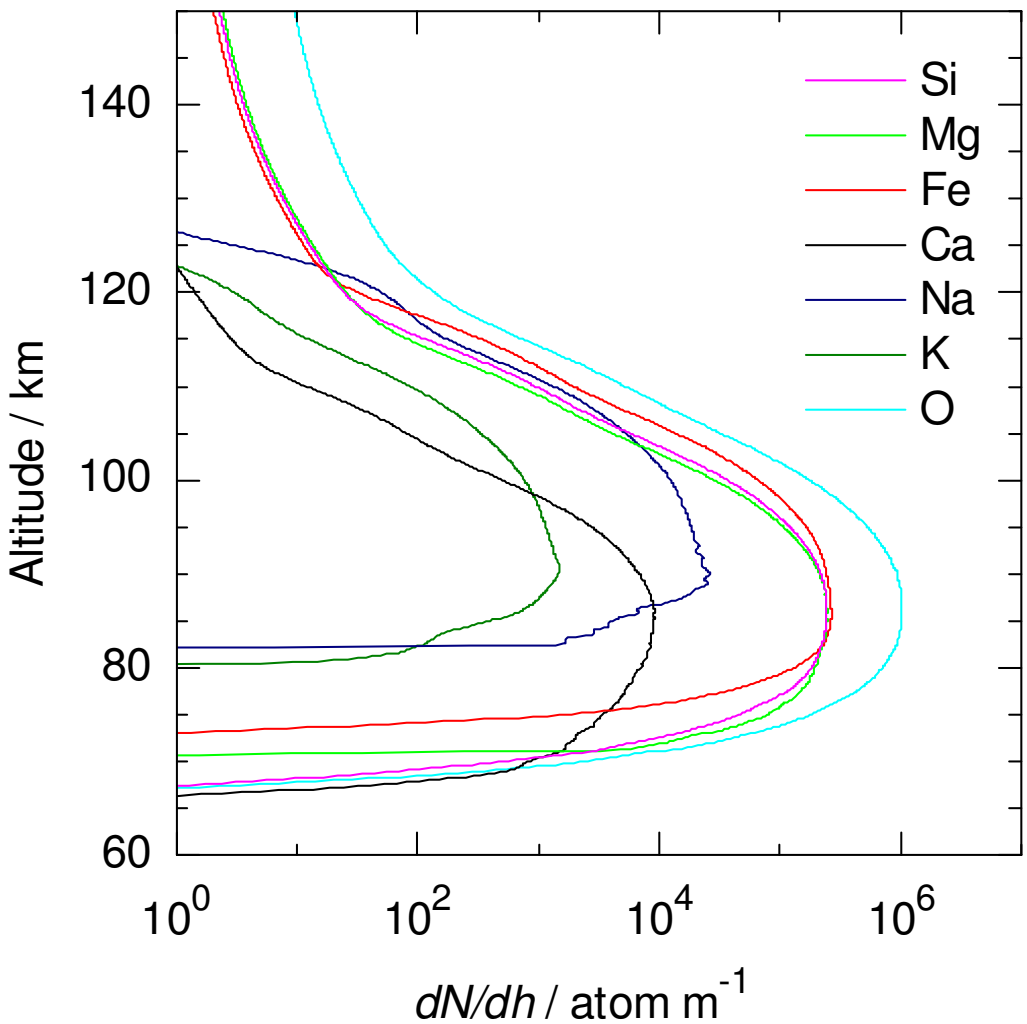

	Ablated At %	Centroid km	FWHM km
Si	70	86.9	17.2
Mg	68	86.1	17.6
Fe	82	88.9	16.4
Ca	42	84.7	16.2
Na	92	94.5	12.3
K	92	94.2	12.5
O	71	87.2	16.9

42% of the Ca ablates

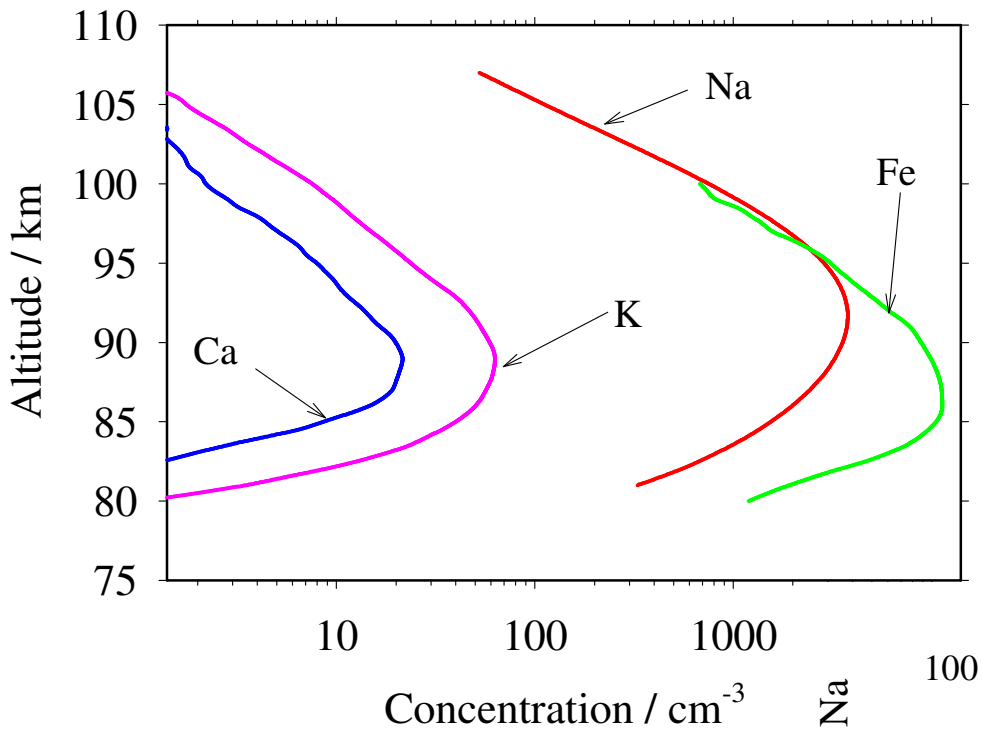

Layers of metal atoms in the mesosphere/lower thermosphere

Annual average, mid-latitude NH

The three alkali elements are roughly in their cosmic abundance: evidence that the source of the metals is meteoric.

But, what about the huge depletion of Ca?

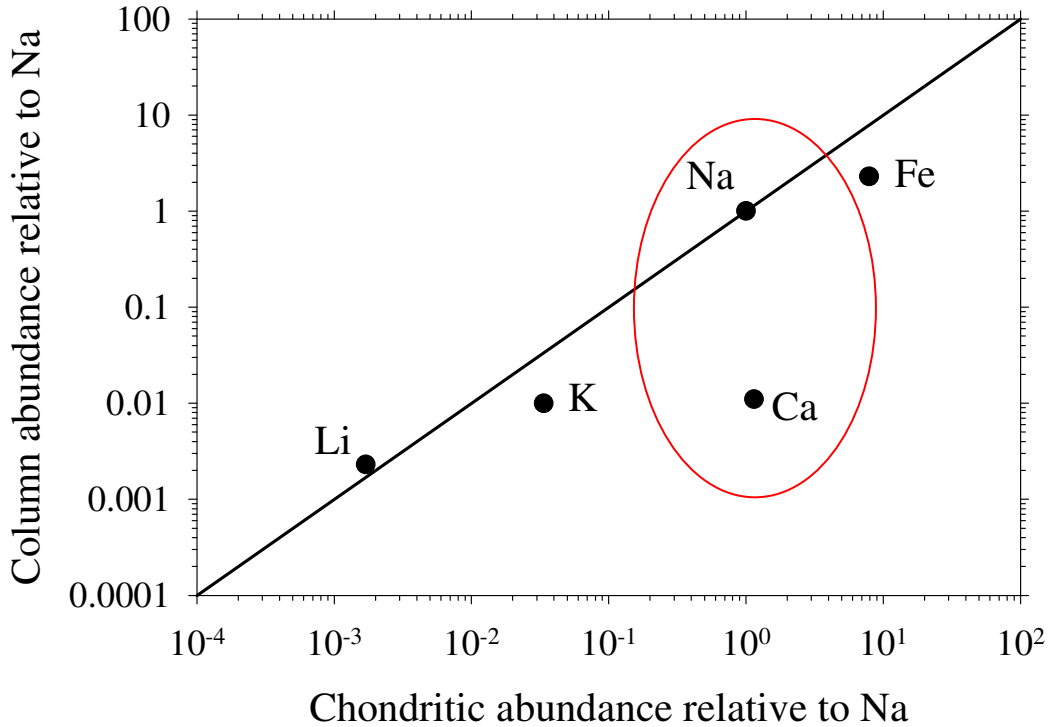

Why do metal atoms exist at all in our oxidizing atmosphere?

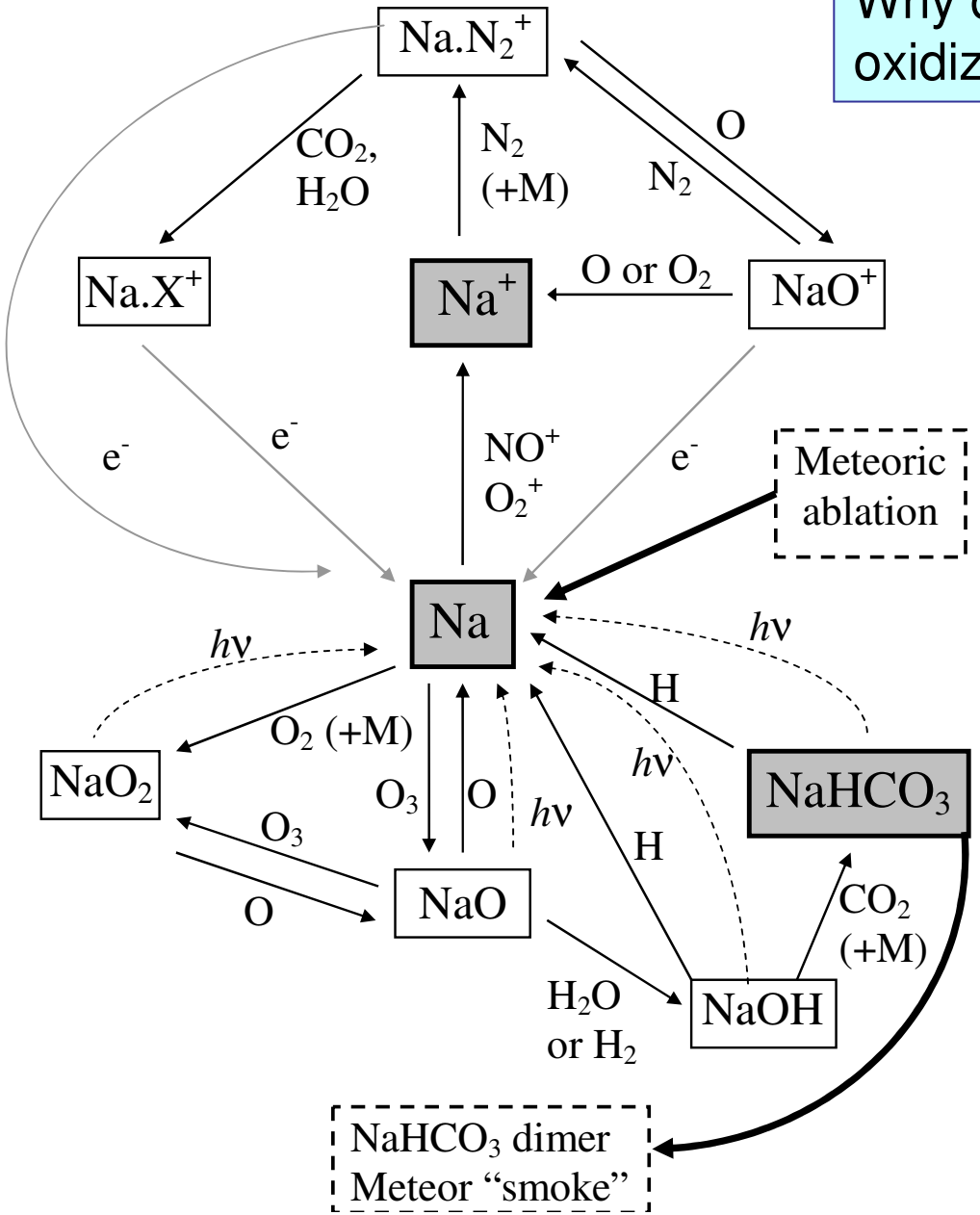

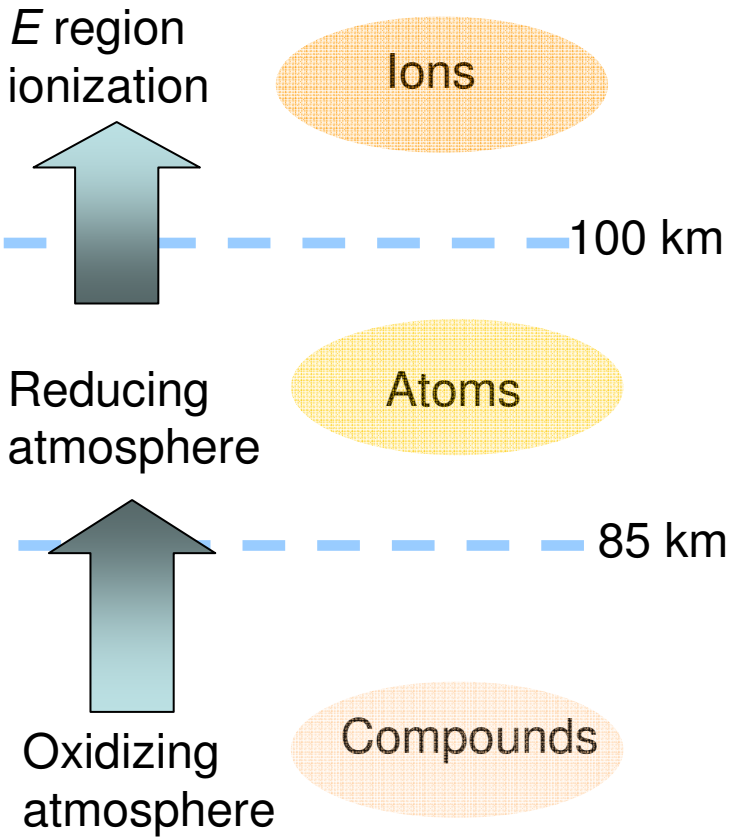

Plane, *ACP*, **4**, 627-638 (2004)

Satellite observations of the global Na layer

Method of retrieval

Gumbel, J., Z. Y. Fan, T. Waldemarsson, J. Stegman, G. Witt, E. J. Llewellyn, C.-Y. She, J. M. C. Plane, Retrieval of global mesospheric sodium densities from the Odin satellite, *Geophysical Research Letters*, **34**, Art. No. L04813, 2007.

Global Na layer

Fan, Z. Y., J. M. C. Plane, J. Gumbel, J. Stegman and E. J. Llewellyn, Satellite measurements of the global mesospheric sodium layer, *Atmos. Chem. Phys. Discuss.*, 7, 5413-5437 (2007).

Sporadic Na layers

Fan, Z.Y., J. M. C. Plane, and J. Gumbel, The global distribution of sporadic sodium layers, *Geophys. Res. Lett.*, in press.

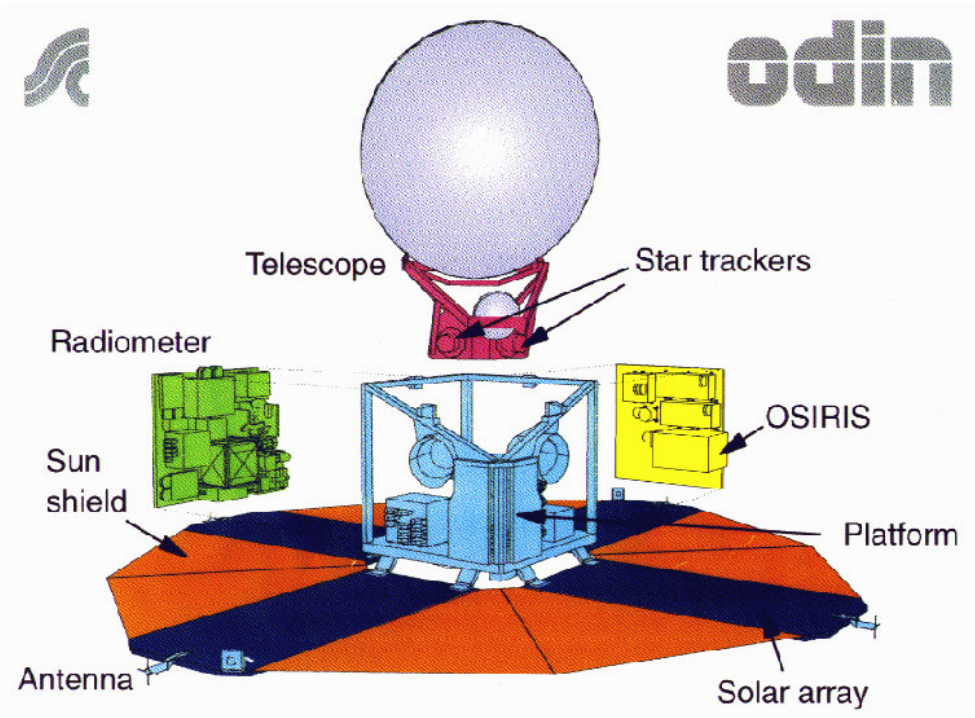

The OSIRIS UV-VIS spectrometer is carried on the ODIN satellite, which has a dual astronomy / aeronomy mission

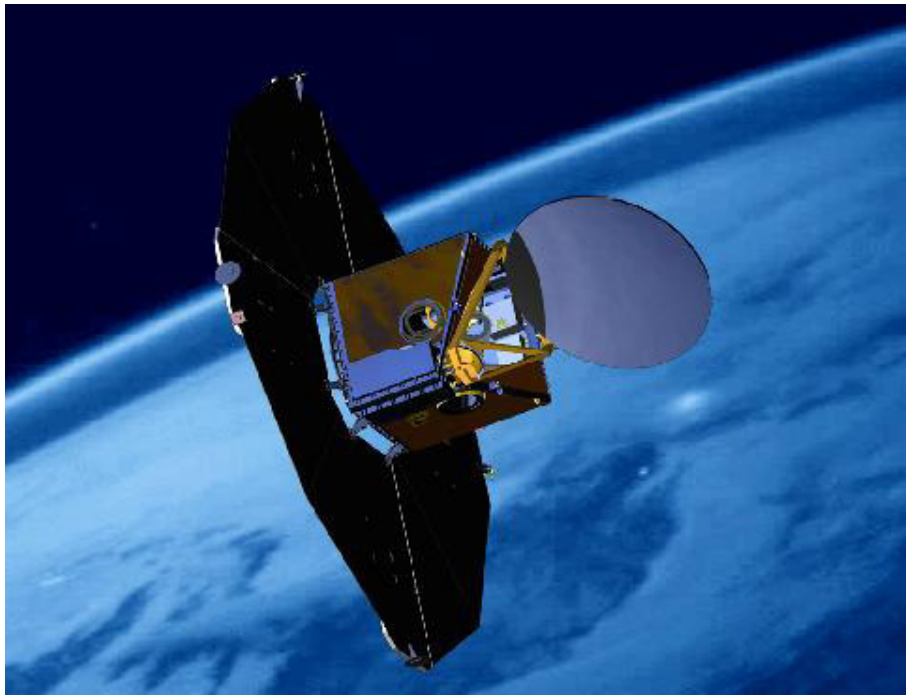

OSIRIS observations of the Na layer

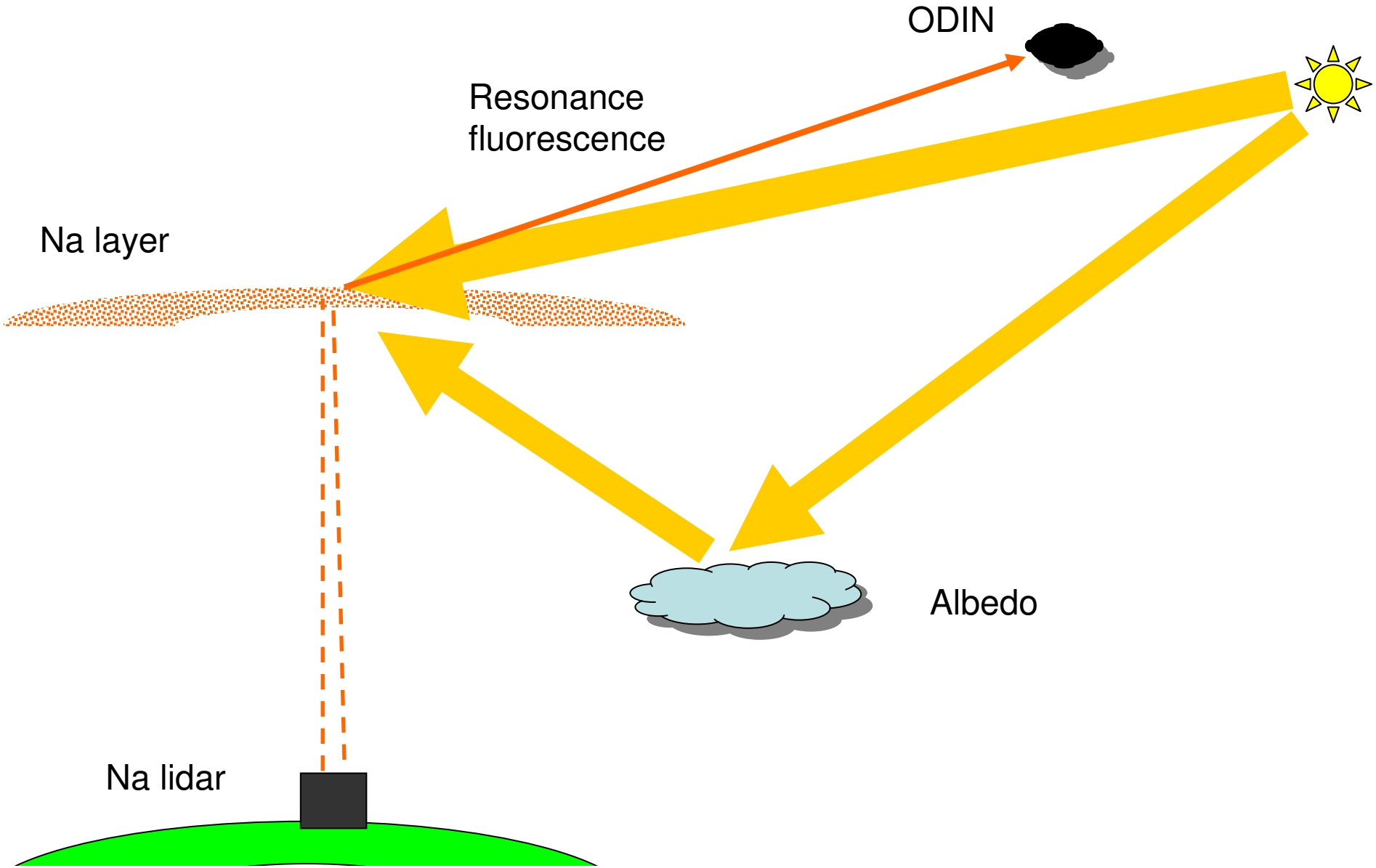

Observed radiation (550 – 610 nm) in the limb as a function of tangent height

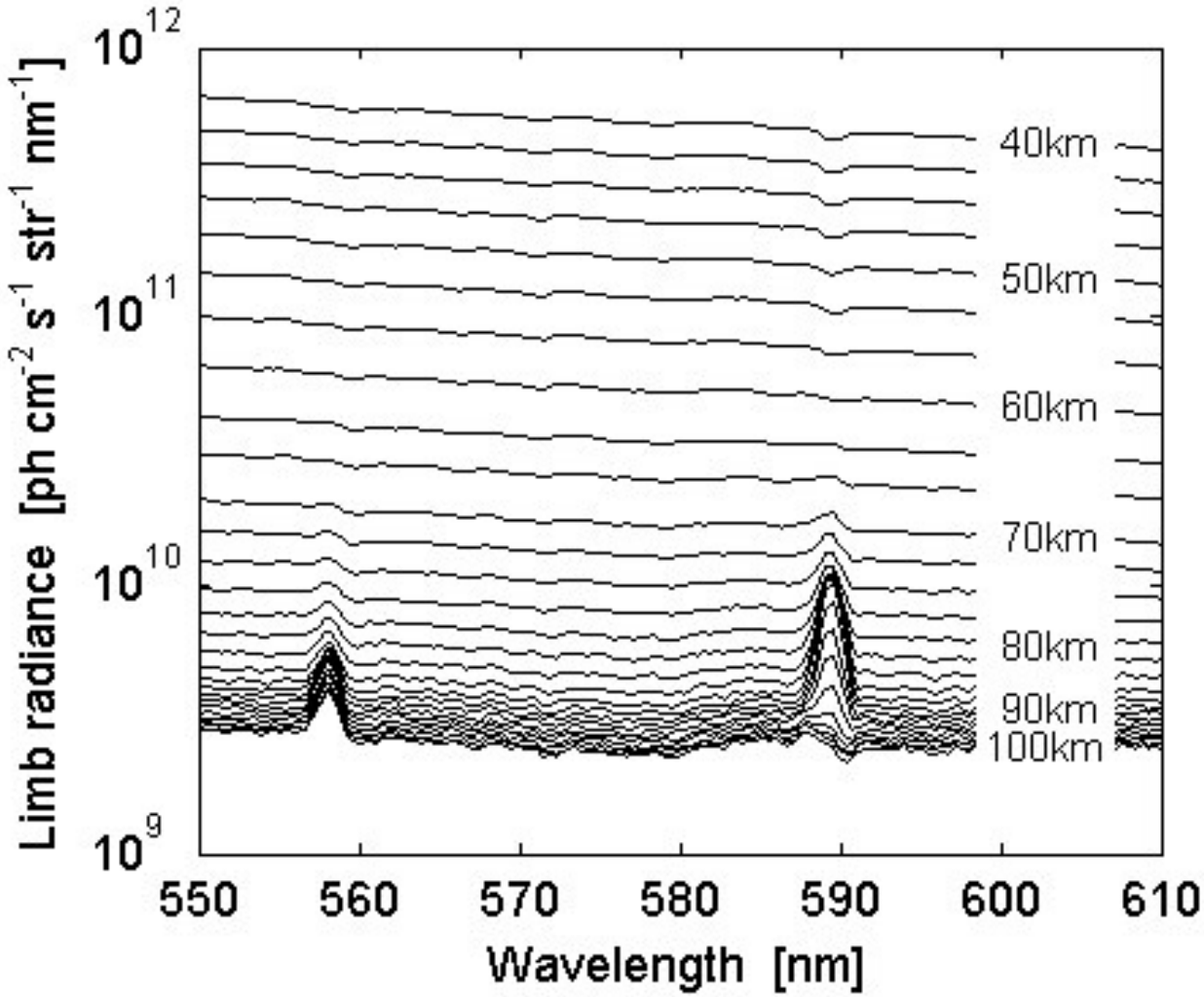

The atomic Na profile is retrieved from the radiance profile using optimal estimation theory

[Rodgers, C. D., *Inverse methods for atmospheric sounding : theory and practice*, World Scientific, Singapore (2000)]

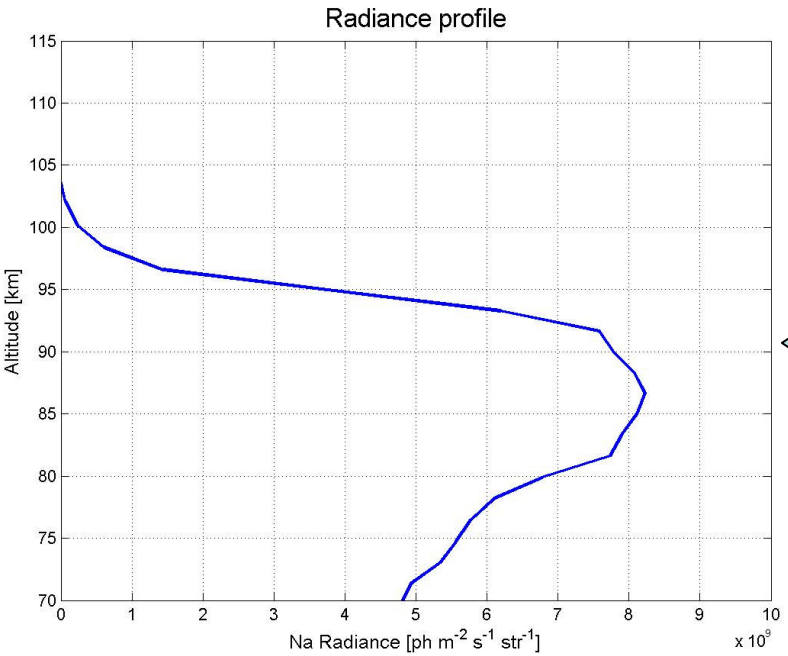

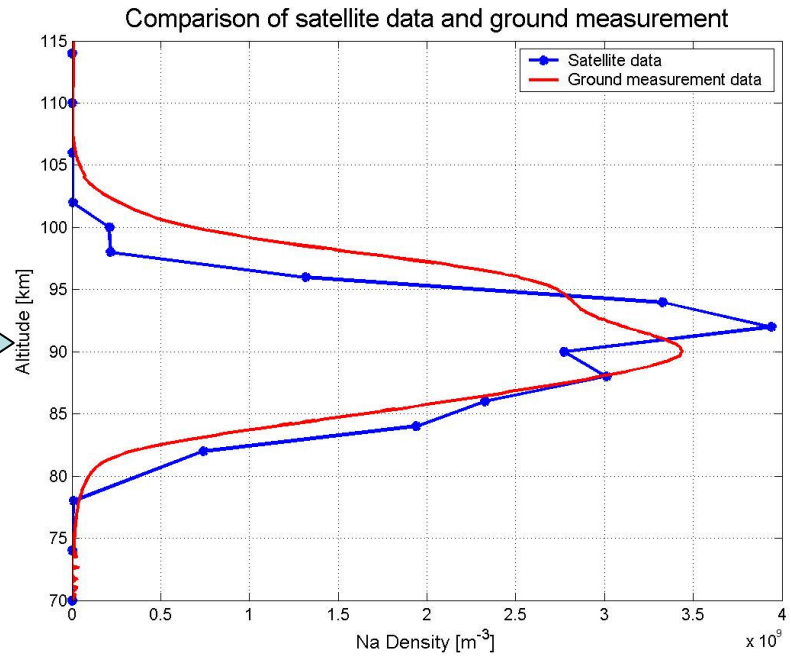

The retrieval algorithm was ground-truthed by comparing with overflights of the Ft. Collins Na lidar

Error analysis and validation

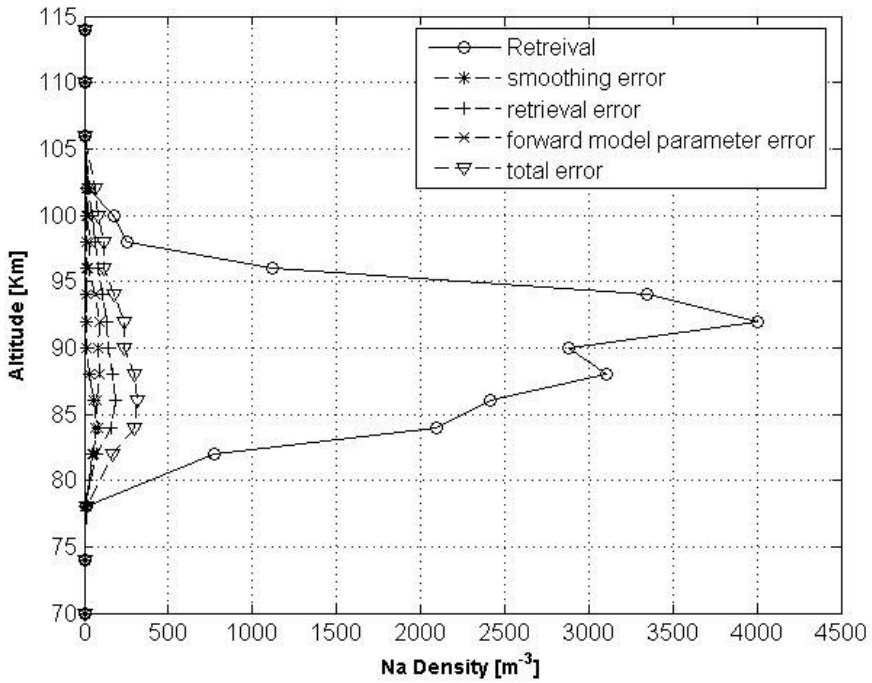

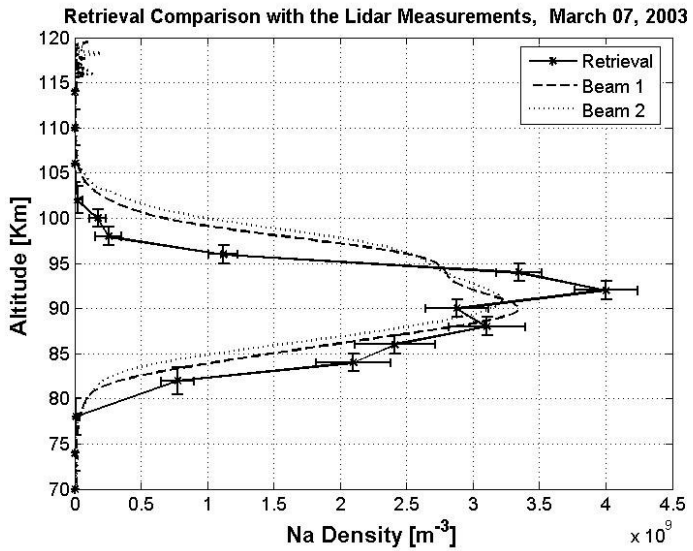

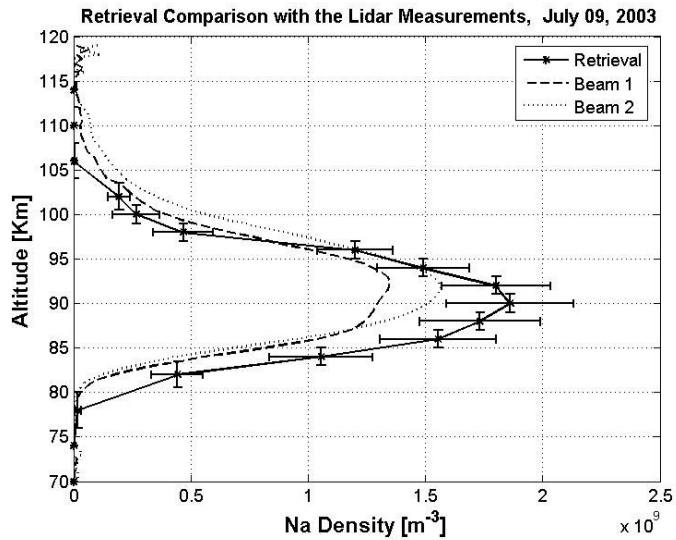

Monthly variation of Na column abundance for the years 2003 - 04

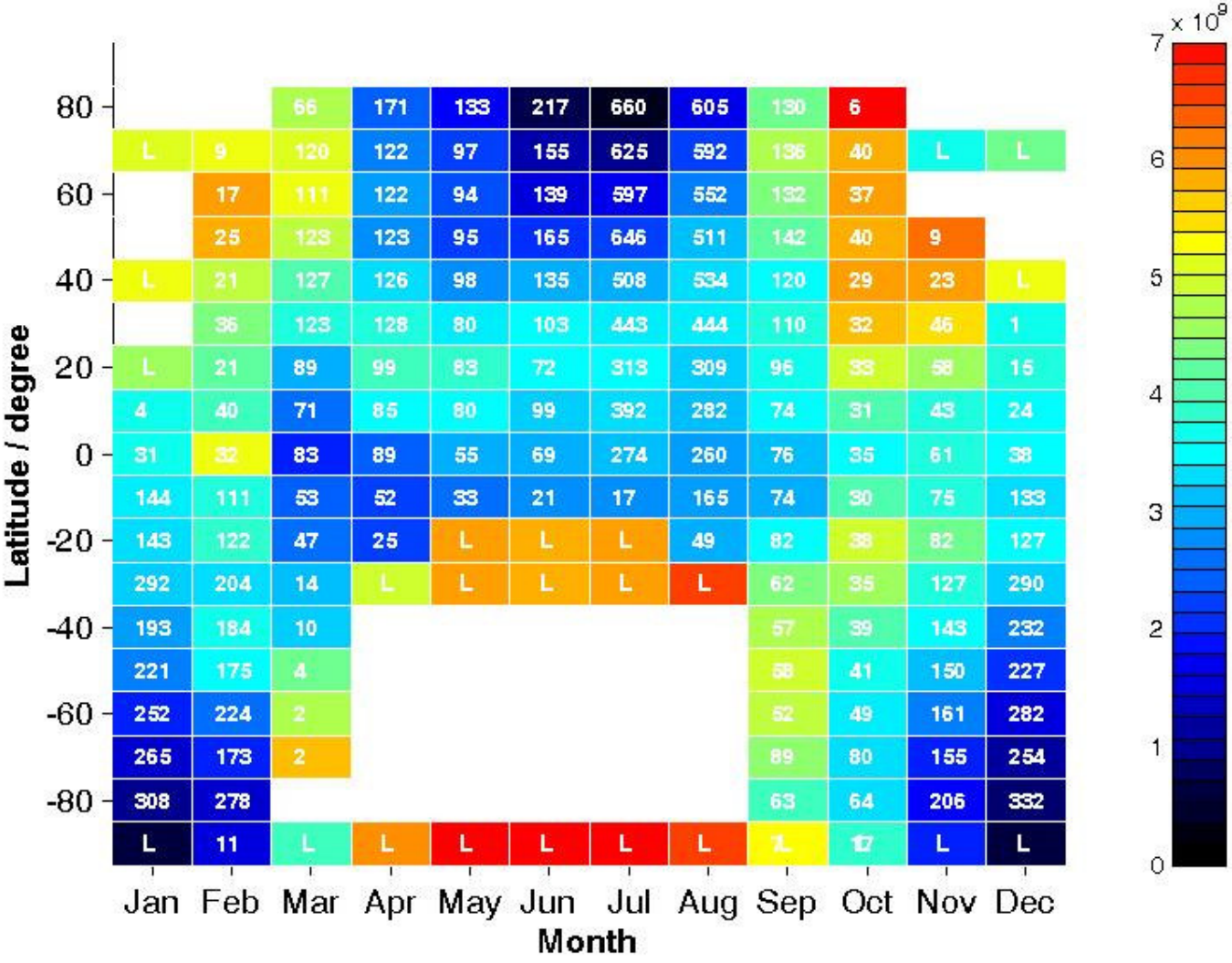

L = lidar measurements

Na layer at mid to high latitudes

40 – 80° N, March - September

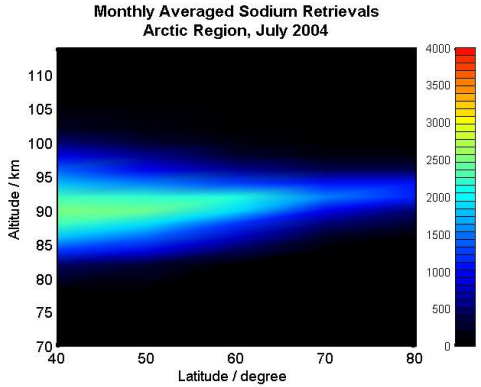

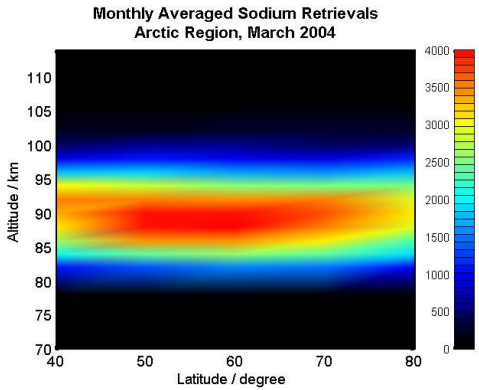

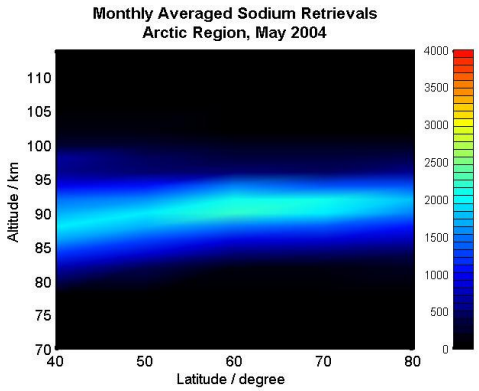

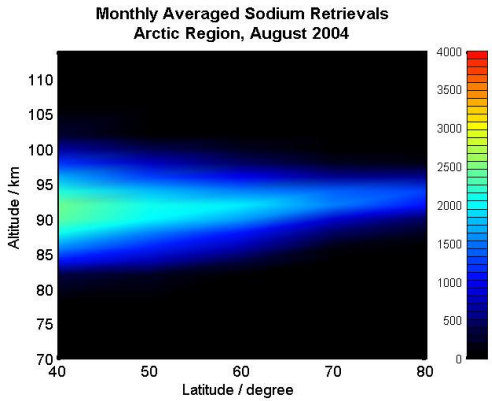

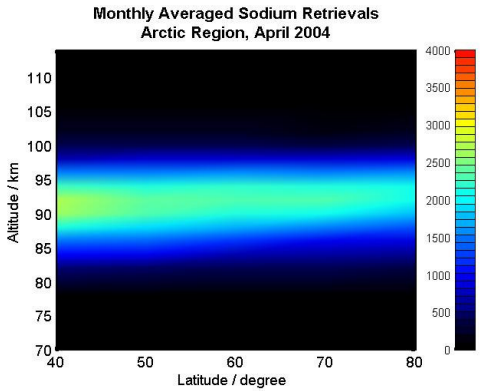

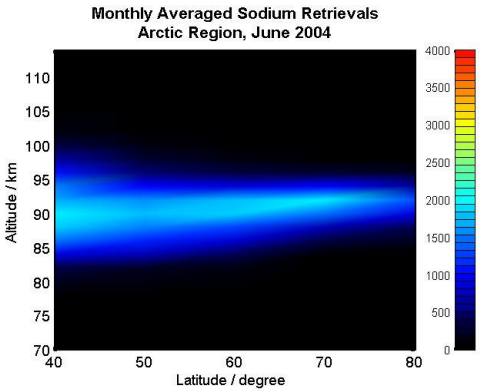

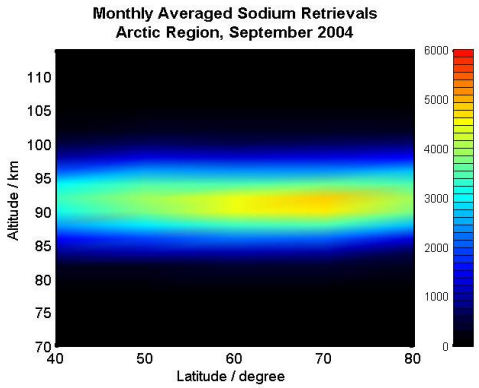

Na loss during summer at high latitudes

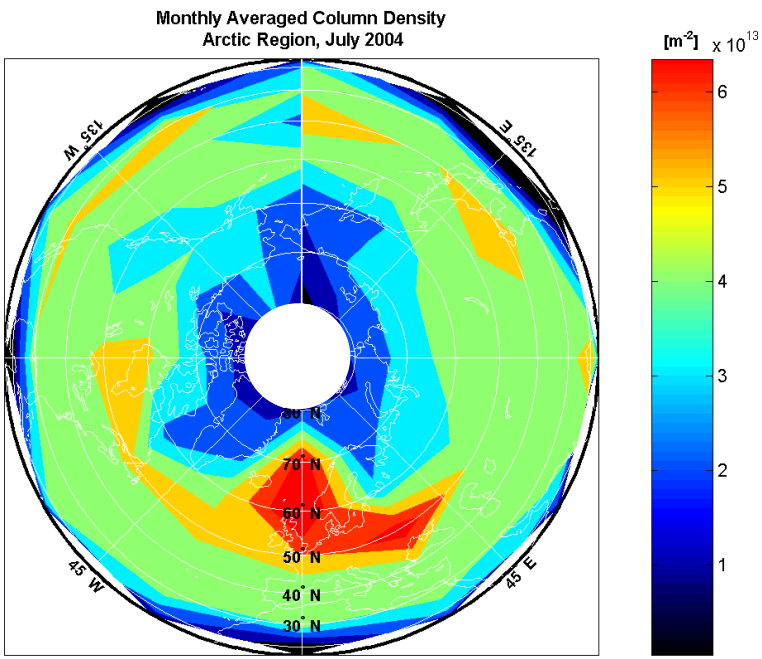

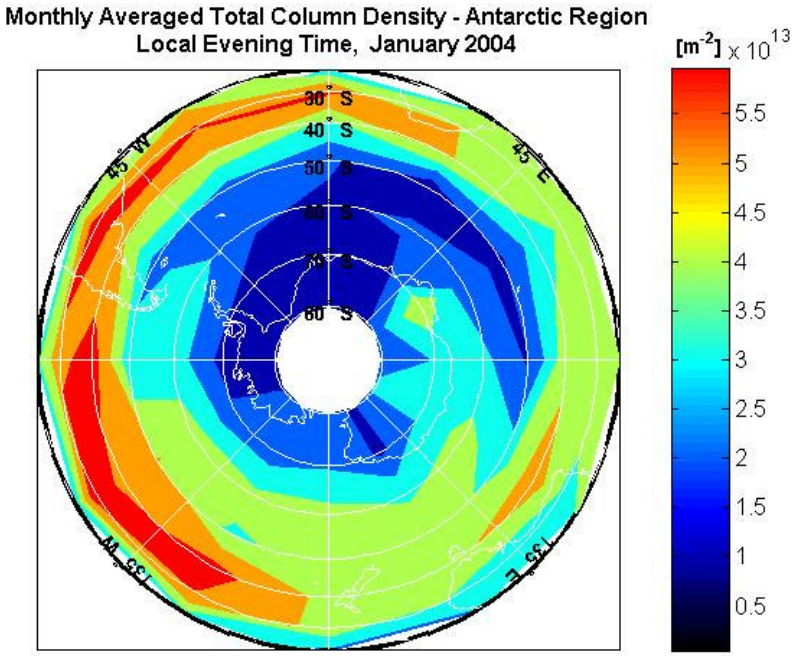

Satellite measurements of sporadic Na layers (SSLs)

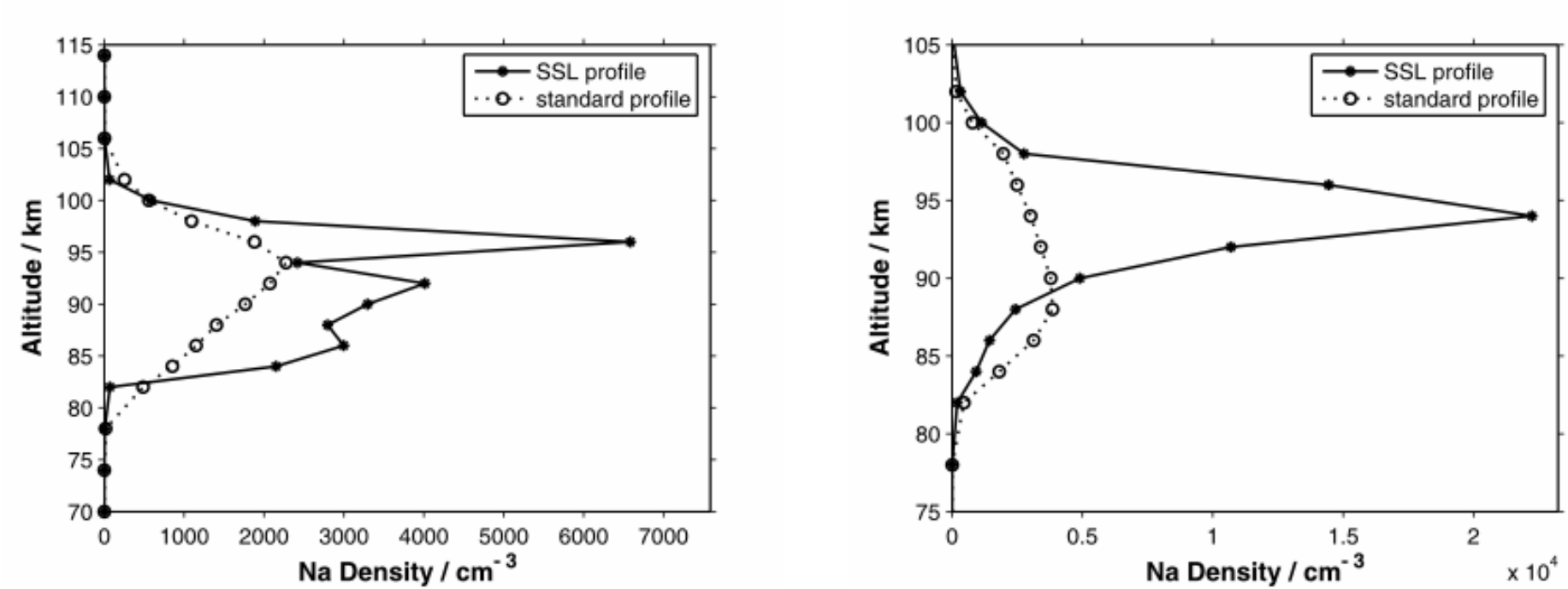

SSLs are strong enhancements over the background Na layer which are typically short-lived. The layers peak between 90 and 105 km. They can either appear as a discrete narrow layer (left panel), or be so large that they dominate the entire Na layer (right panel).

SSL occurrence frequency

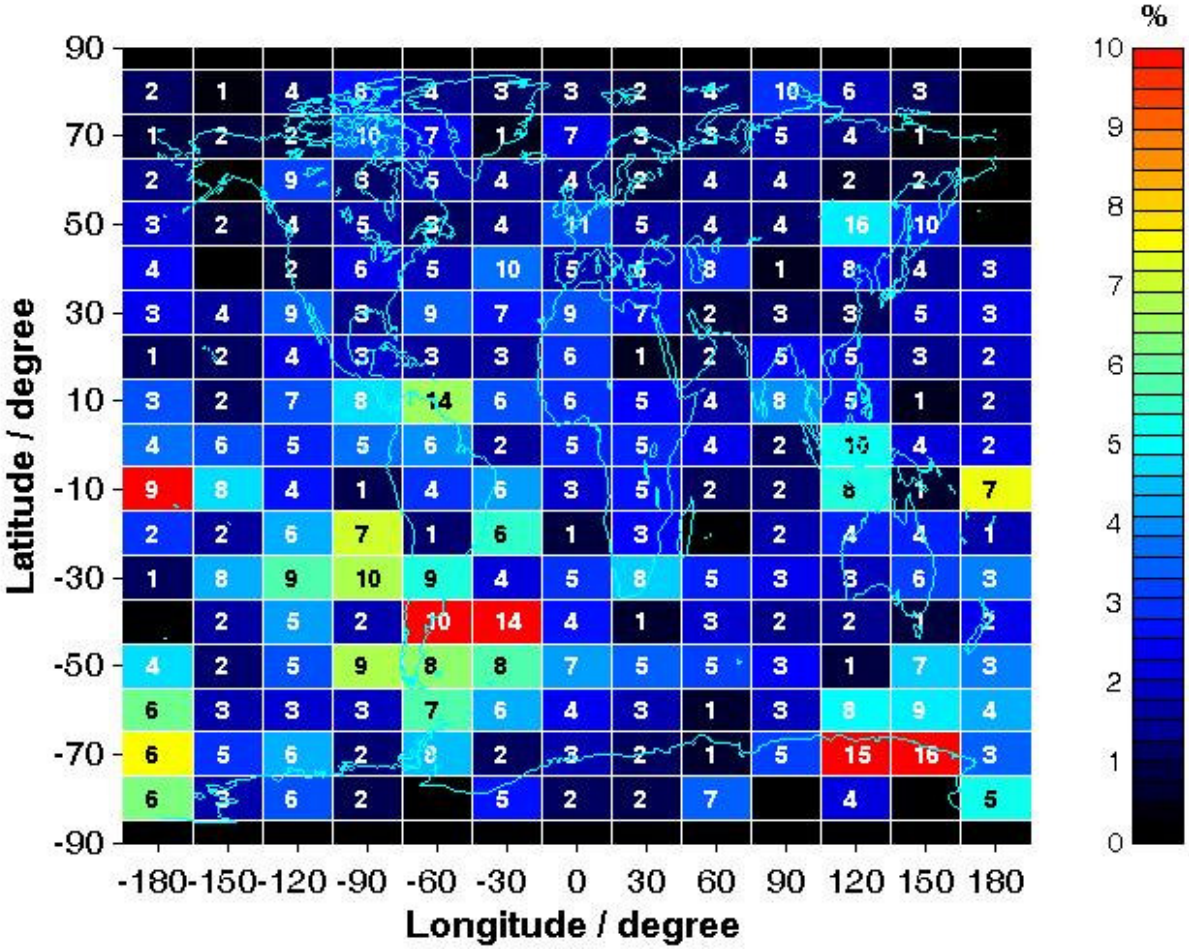

Measurements at ~0600 and 1800 LT

No wintertime data above ~20°

The occurrence rate is much higher in the southern hemisphere, particularly over South America and around Antarctica. There is a reasonably strong correlation with sporadic *E* occurrence. Gravity wave activity may also play a role.

Polar Mesospheric (or Noctilucent) Clouds

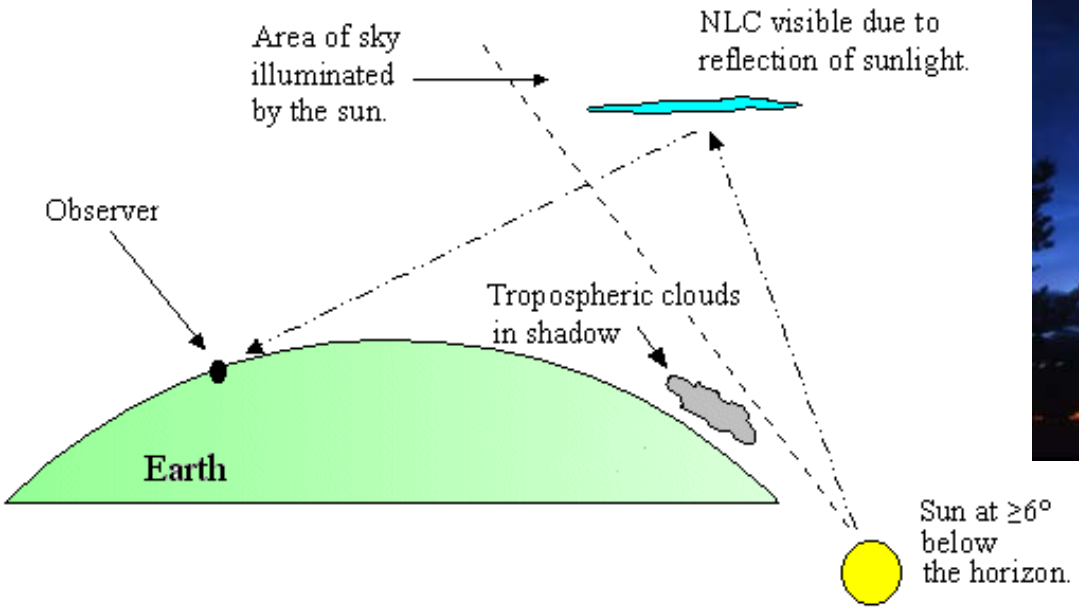

- observed in mid-summer at high latitudes (>55°) when the solar depression angle is greater than about 6° (i.e. around local midnight)
- first observed in 1885, a year after the Mt. Krakatoa eruption
- height has been 82 – 84 km since 1885

Are PMCs an early warning of climate change?

Satellite measurements show they are increasing in brightness, and probably occurrence frequency.

Is this because of decreasing *T*, increasing [H_2O], or a change in CN number density ?

PMCs overlap with the layers of metal atoms above 80 km.

How do they interact?

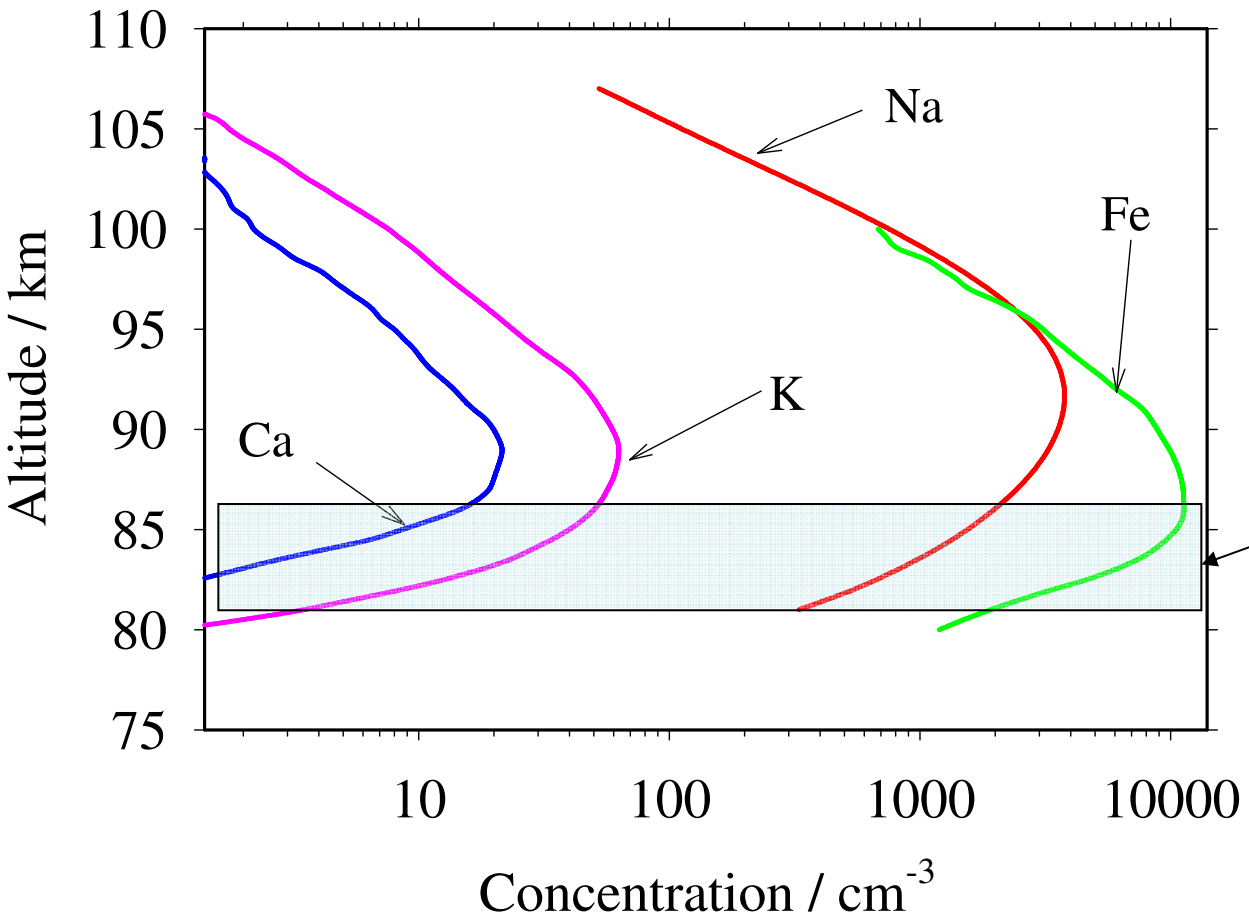

Annual average layers of metal atoms in the mesosphere/lower thermosphere

Height range of polar mesospheric clouds

Meteoric metals and PMCs

Plane, J.M.C., B.J. Murray, X.Z. Chu, and C.S. Gardner, Removal of meteoric iron on polar mesospheric clouds, *Science*, 304, 426-428 (2004).

Lübken, F.J., and J. Höffner, Experimental evidence for ice particle interaction with metal atoms at the high latitude summer mesopause region, *Geophys. Res. Lett.*, 31, L08103, (2004).

Gardner, C.S., J.M.C. Plane, W. Pan, T. Vondrak, B.J. Murray, X. Chu, Seasonal variations of the Na and Fe layers at the South Pole and their implications for the chemistry and general circulation of the polar mesosphere, *J. Geophysical Research* **110***,* art. no. D1030210 (2005).

She, C. Y., B. P. Williams, P. Hoffmann, R. Latteck, G. Baumgarten, J. D. Vance, J. Fiedler, P. Acott, D. C. Fritts, F.-J. Lübken, Simultaneous observation of sodium atoms, NLC and PMSE in the summer mesopause region above ALOMAR, Norway (69N, 12E), *J. Atmos. Solar-Terr. Phys.*, 68, 93-101, (2006)

Raizada, S., M. Rapp, F.-J. Lübken, J. Höffner, M. Zecha, and J. M. C. Plane, Effect of ice particles on the mesospheric potassium layer at Spitsbergen (78oN), *J. Geophys. Res.*, 112, art. no. D08307 (2007).

What happens to metal atoms inside the ice clouds?

South Pole atmospheric observatory – University of Illinois Boltzmann lidar

Lidar observations of atomic Fe by resonant scattering at 372 nm

Lidar observations of PMCs by Mie scattering at 374 nm

The Fe Layer in the presence of PMC

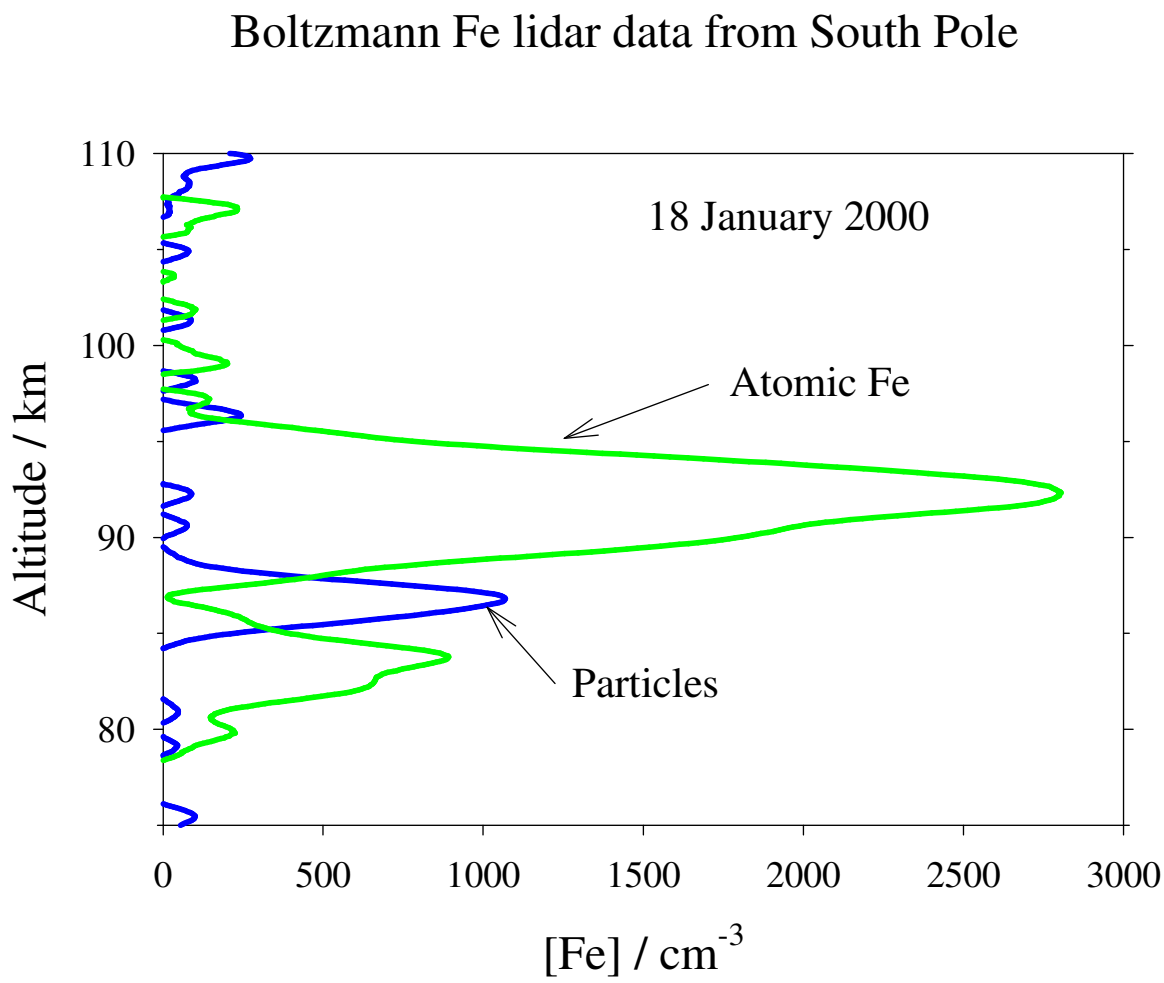

Uptake coefficient needs to be at least 0.1 to compete with meteoric input

The uptake coefficient of Fe atoms on ice

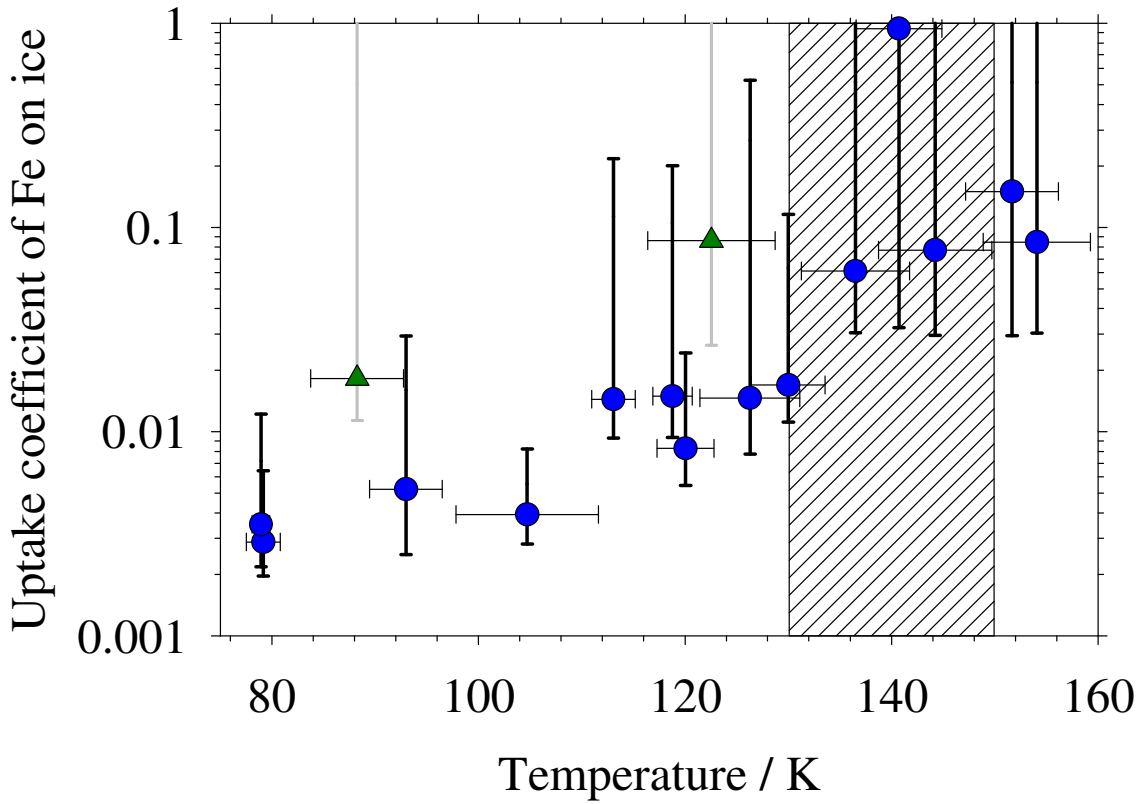

The uptake coefficient or "sticking probability" was measured in the lab using a fast flow tube with ice-coated walls. The ice was either cubic crystalline (blue points) or amorphous (green points). The errors become large once the uptake coefficient approaches 0.1, because uptake is no longer rate-limiting

Murray and Plane, *PCCP,* 7**,** 3970-3979 (2005).

Modelling the Fe layer at South Pole during summer

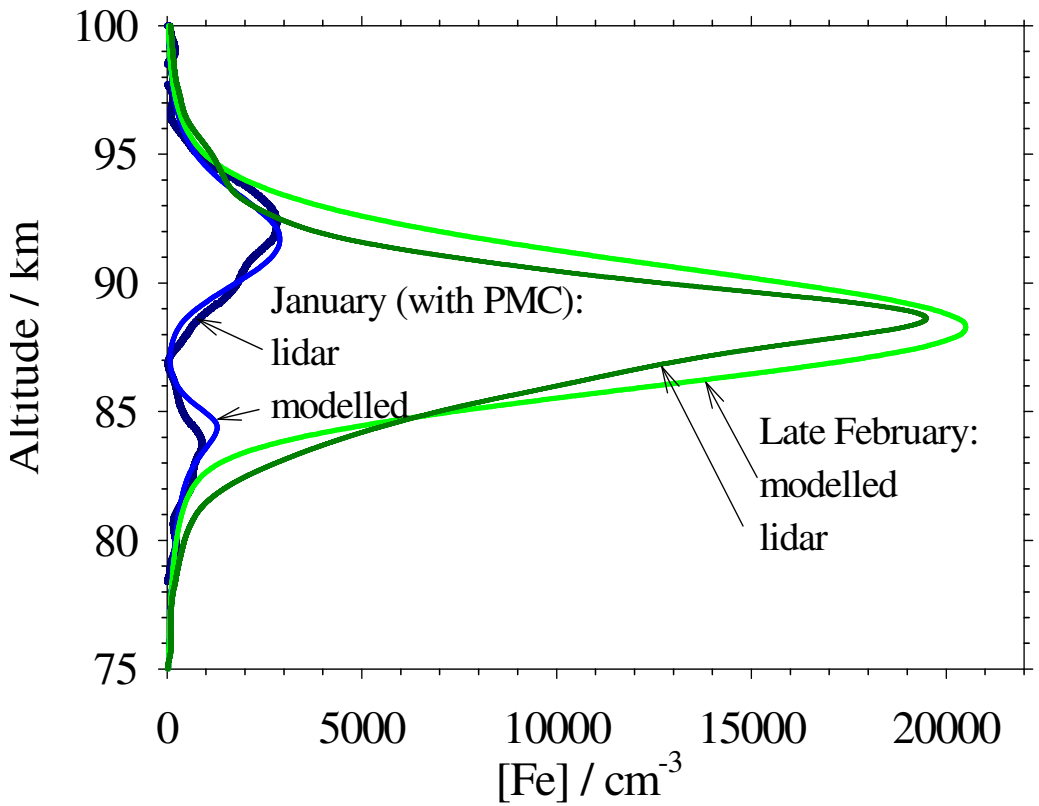

Good agreement between model and observations:

Substantial Fe removal in presence of PMC (January)

cf. Fe layer in absence of PMC (February)

Fe ablation flux = 1.1 x 10^4 atom cm^{-2} s^{-1}
γ(Fe and Fe species on ice) = 1

Plane *et al.*, *Science* 304, 426 (2004)

The K layer and NLCs

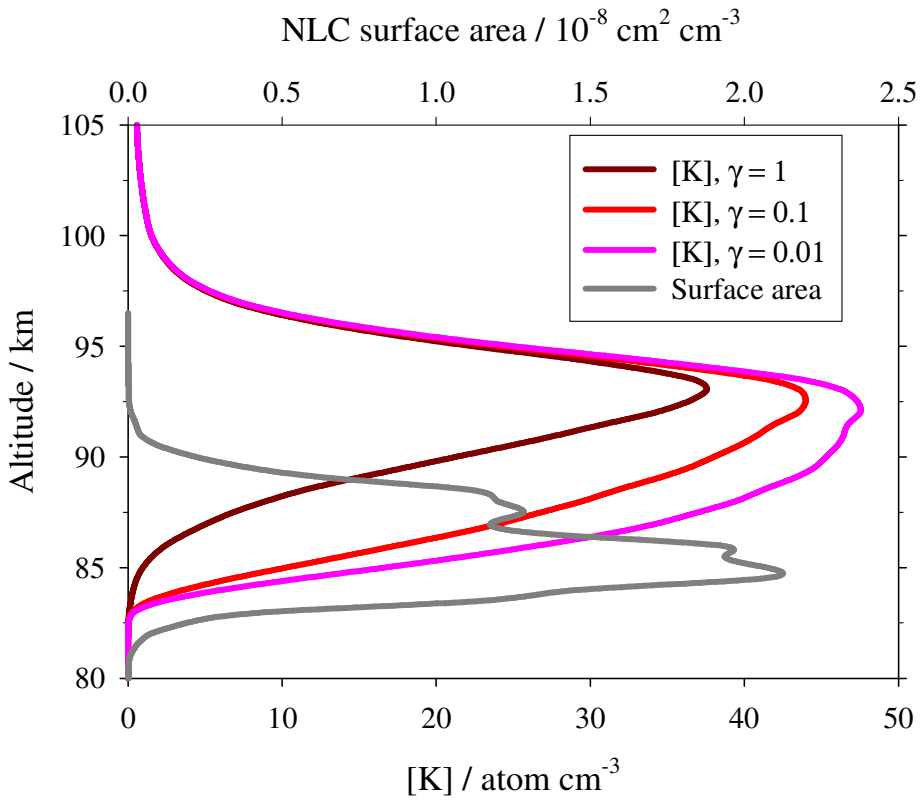

The modeled K profile at 79°N during July when the uptake coefficient of K on ice, *γ*, is set to 1, 0.1 and 0.01.

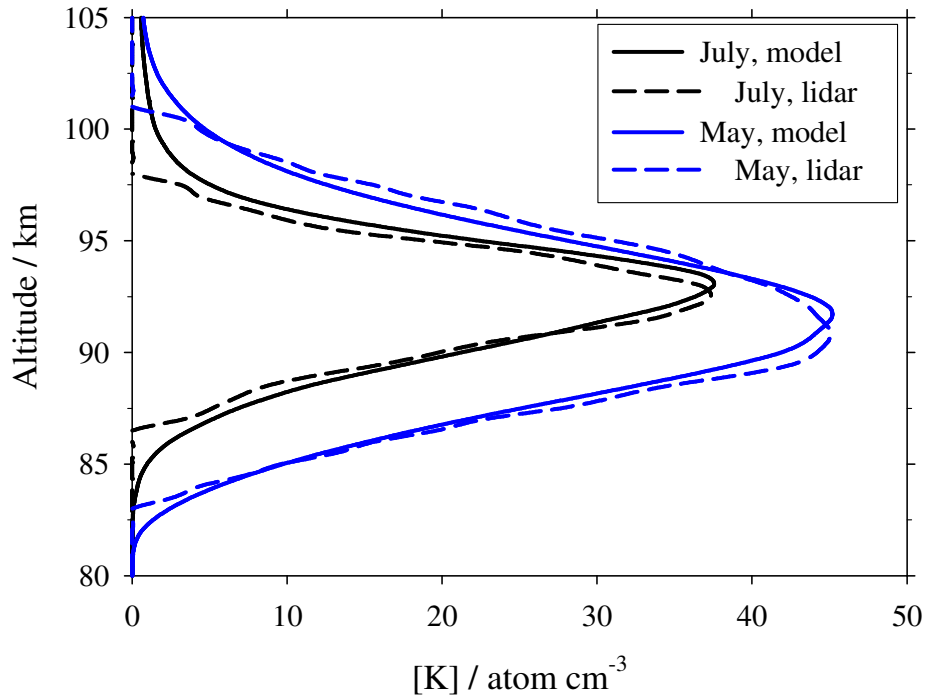

Comparison of modeled and measured K profiles at 79°N in early May (blue lines) and July (black lines).

Raizada et al. *J. Geophys. Res.*, 112, art. no. D08307 (2007)

What about the seasonal variability of the Na and Fe layers at South Pole?

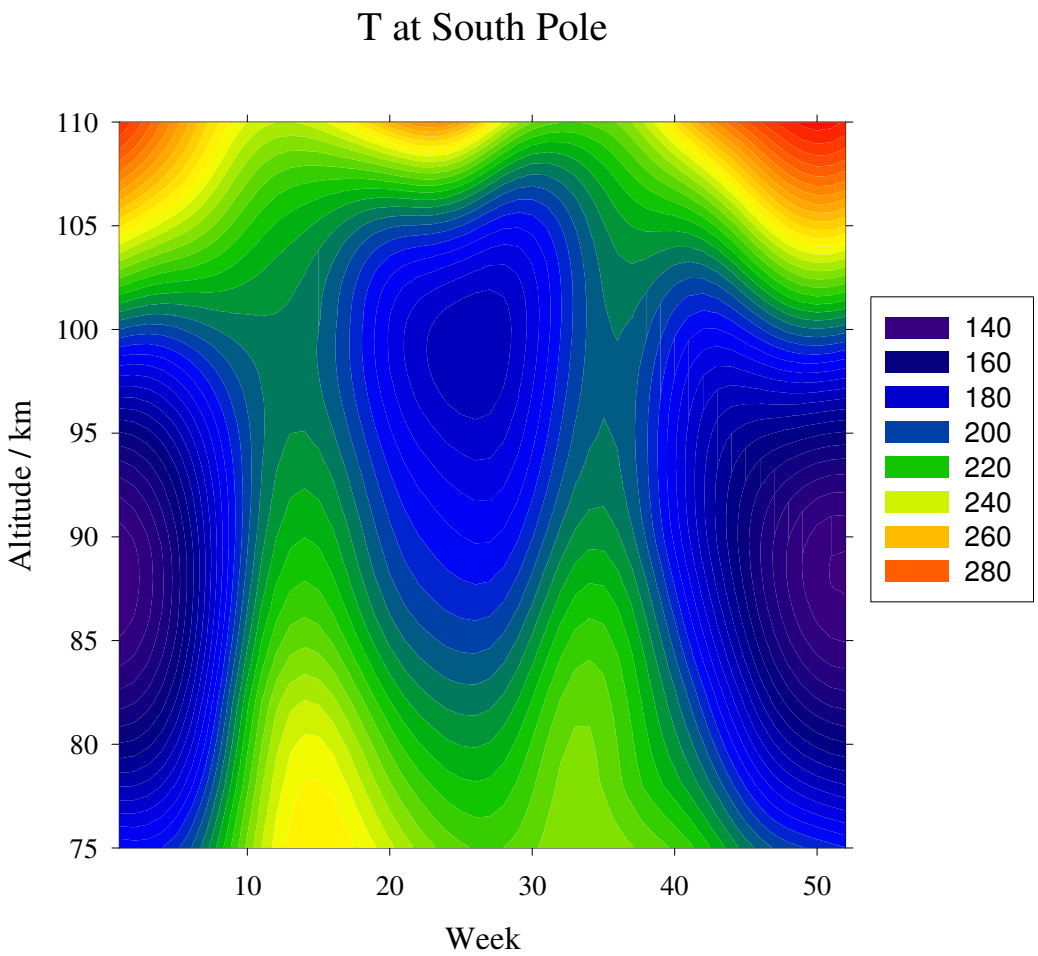

Gardner *et al.*, *JGR*, **110**, art. no. D1030210 (2005)

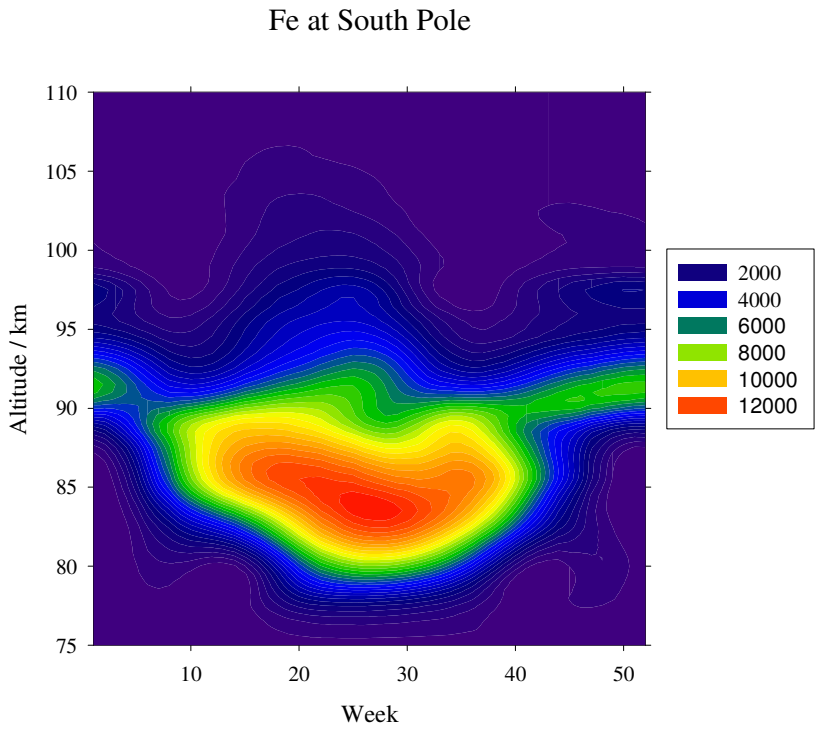
Fe at South Pole
Altitude / km
Week
110
105
100
95
90
85
80
75
10
20
30
40
50
2000
4000
6000
8000
10000
12000

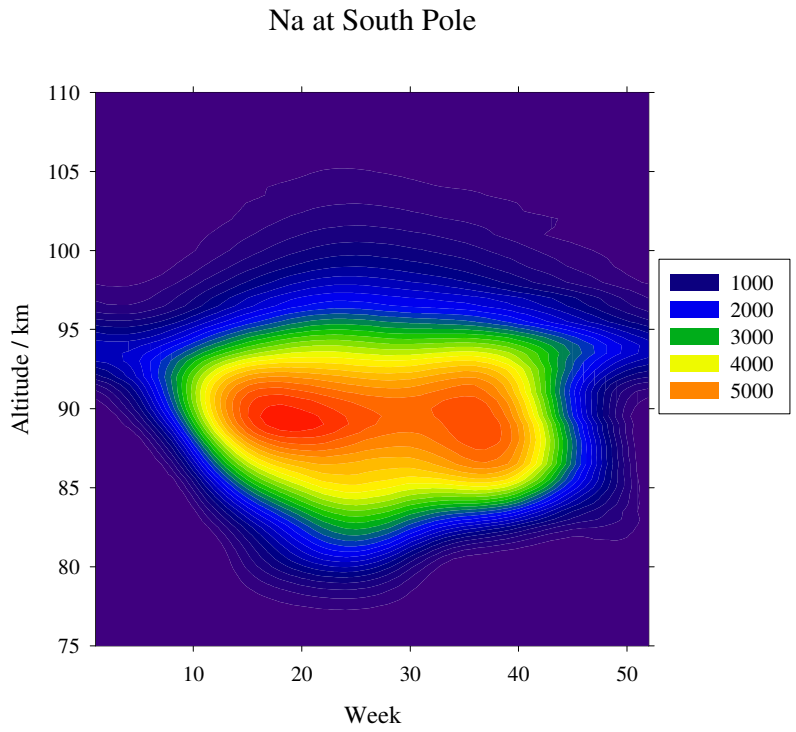
Na at South Pole
Altitude / km
Week
110
105
100
95
90
85
80
75
10
20
30
40
50
1000
2000
3000
4000
5000

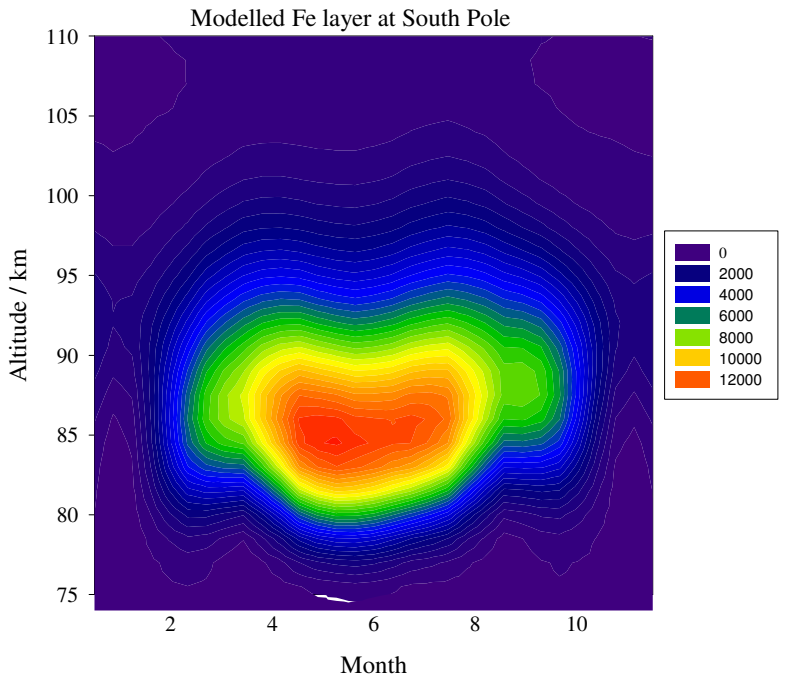
Modelled Fe layer at South Pole
Altitude / km
Month
110
105
100
95
90
85
80
75
2
4
6
8
10
0
2000
4000
6000
8000
10000
12000

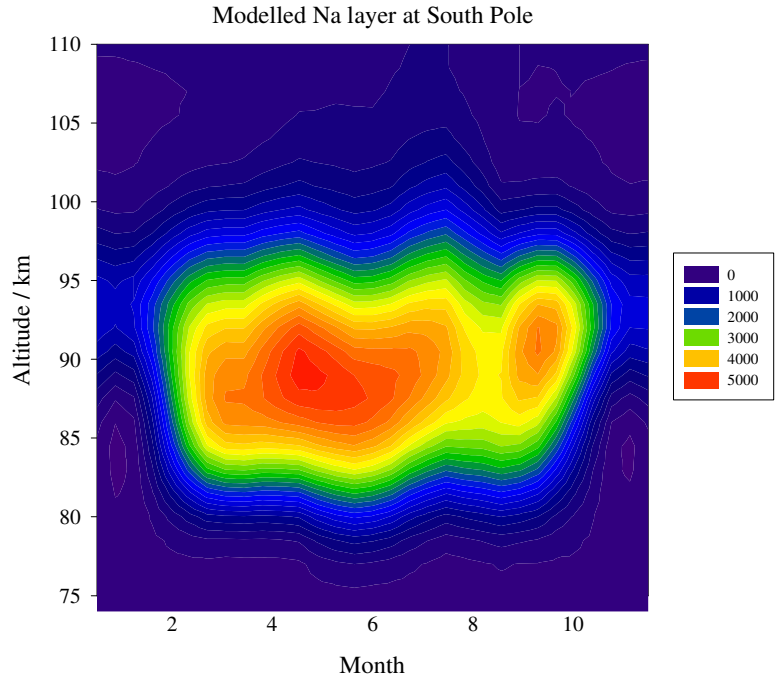
Modelled Na layer at South Pole
Altitude / km
Month
110
105
100
95
90
85
80
75
2
4
6
8
10
0
1000
2000
3000
4000
5000

What happens when ice particles become coated with metal atoms?

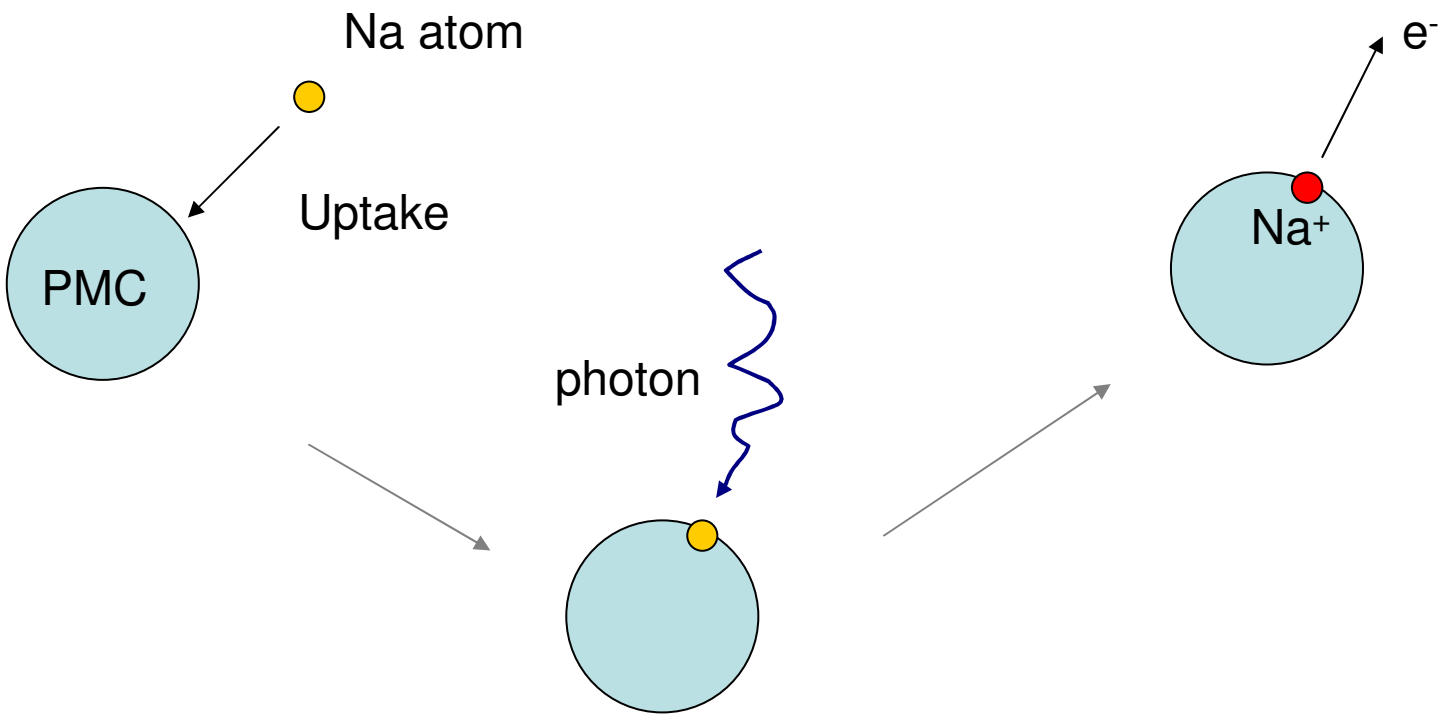

Rocket-borne instruments sometimes find positively-charged ice particles.

Is photo-electric emission the explanation?

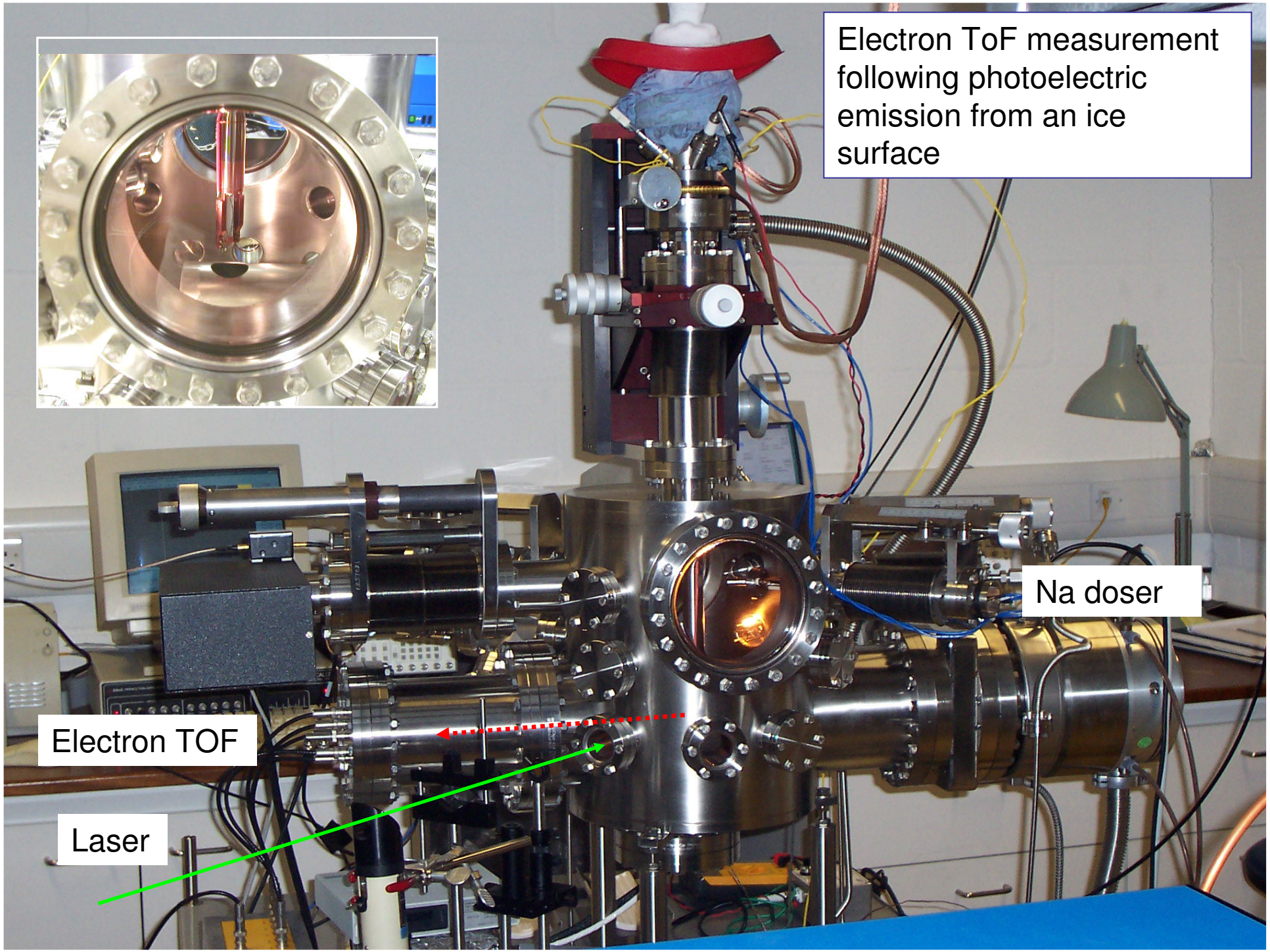
Electron ToF measurement following photoelectric emission from an ice surface
Na doser
Electron TOF
Laser

Spectrum of the photo-ionization cross-section for Na adsorbed on cubic crystalline ice

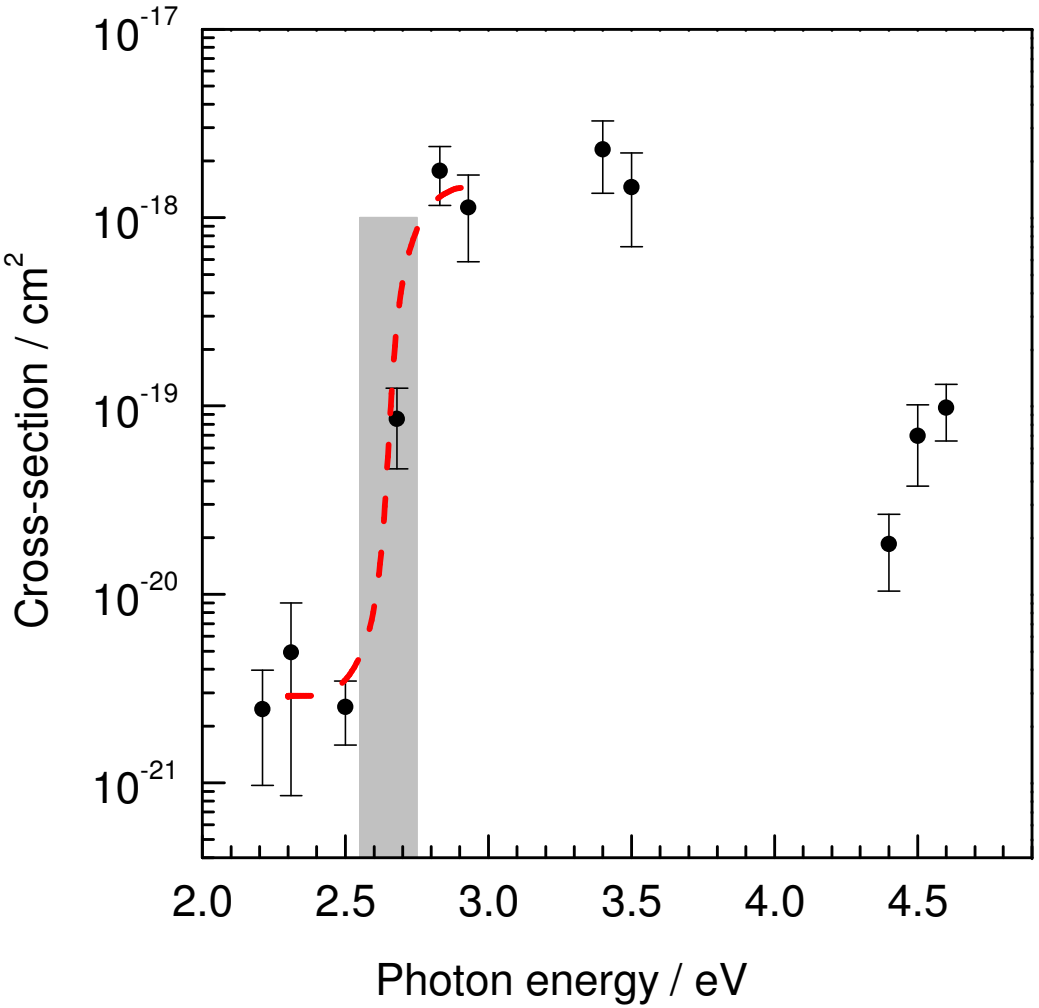

Absolute cross-section computed by estimating the total yield of photoelectrons produced from the measured laser energy impinging on a known ice surface coverage of Na (2×10^{13} cm^{-2})

Vondrak et al., *J. Phys. Chem. B* 110, 3860-3863 (2006).

NaI Photoionization Cross Section

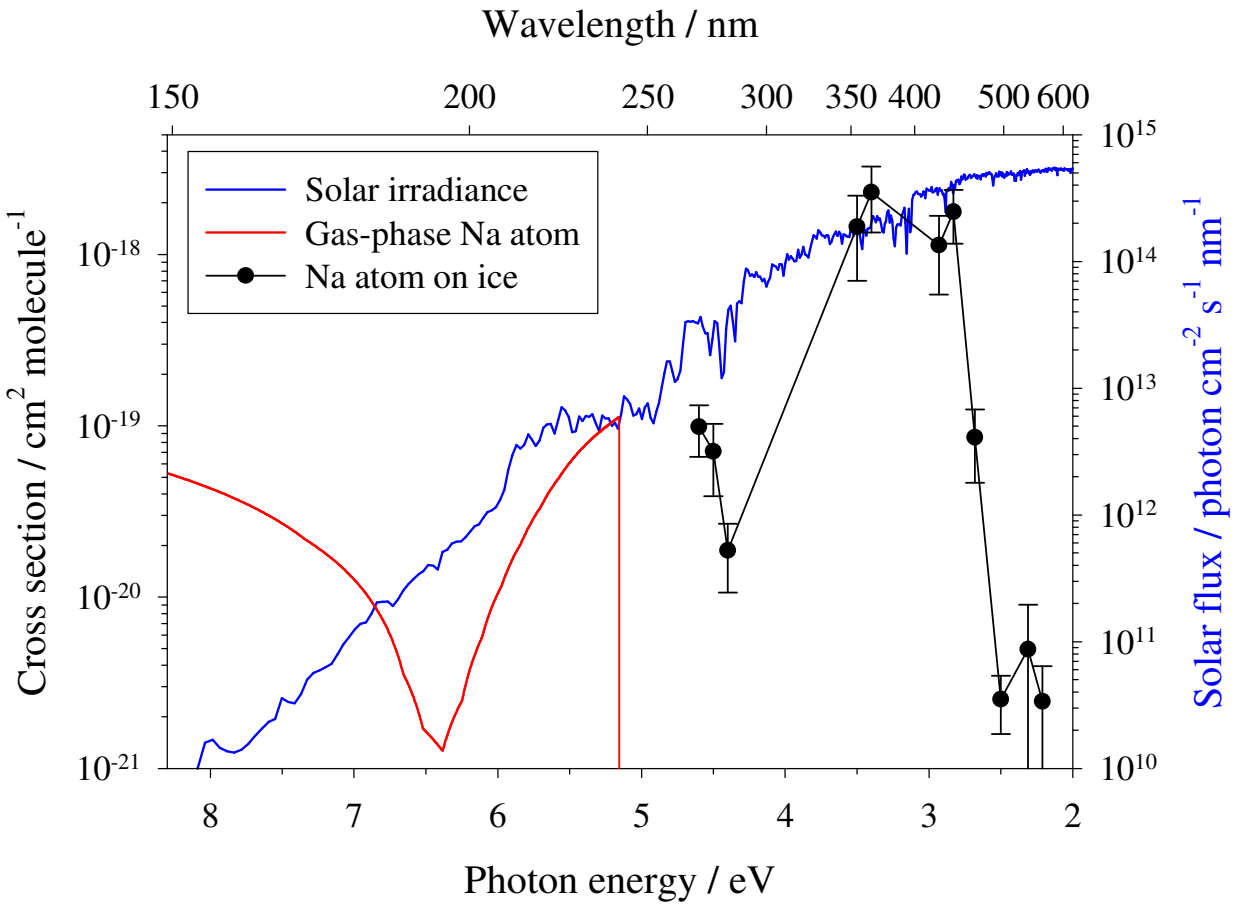

The rate of photo-ionization of a Na atom on a mesospheric ice particle is 0.06 s^{-1} i.e. lifetime is 18 seconds.

Compare with 50,000 seconds in the gas-phase!

Shuttle plume chemistry

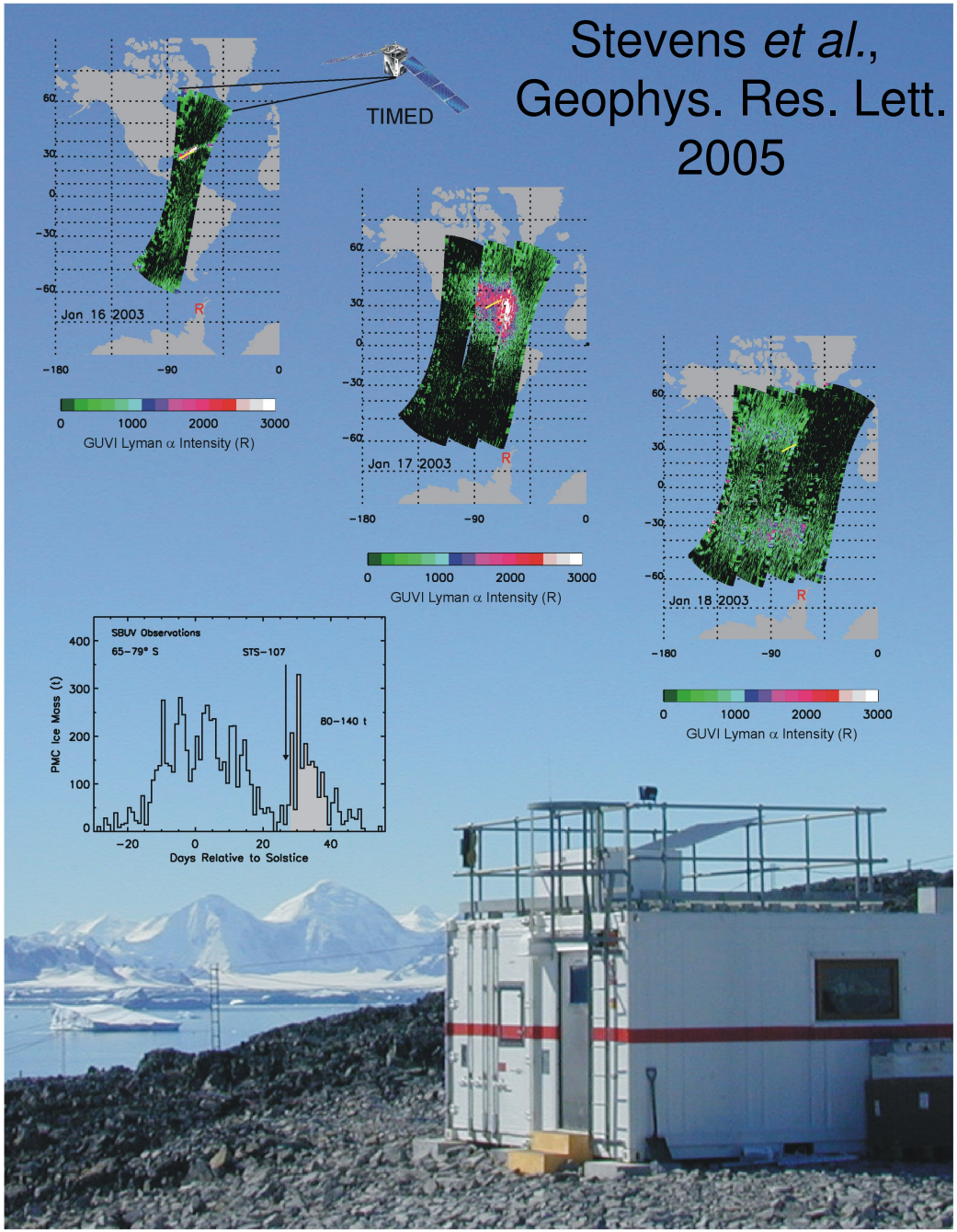

The ascent profile of STS-107 on 16 January, 2003

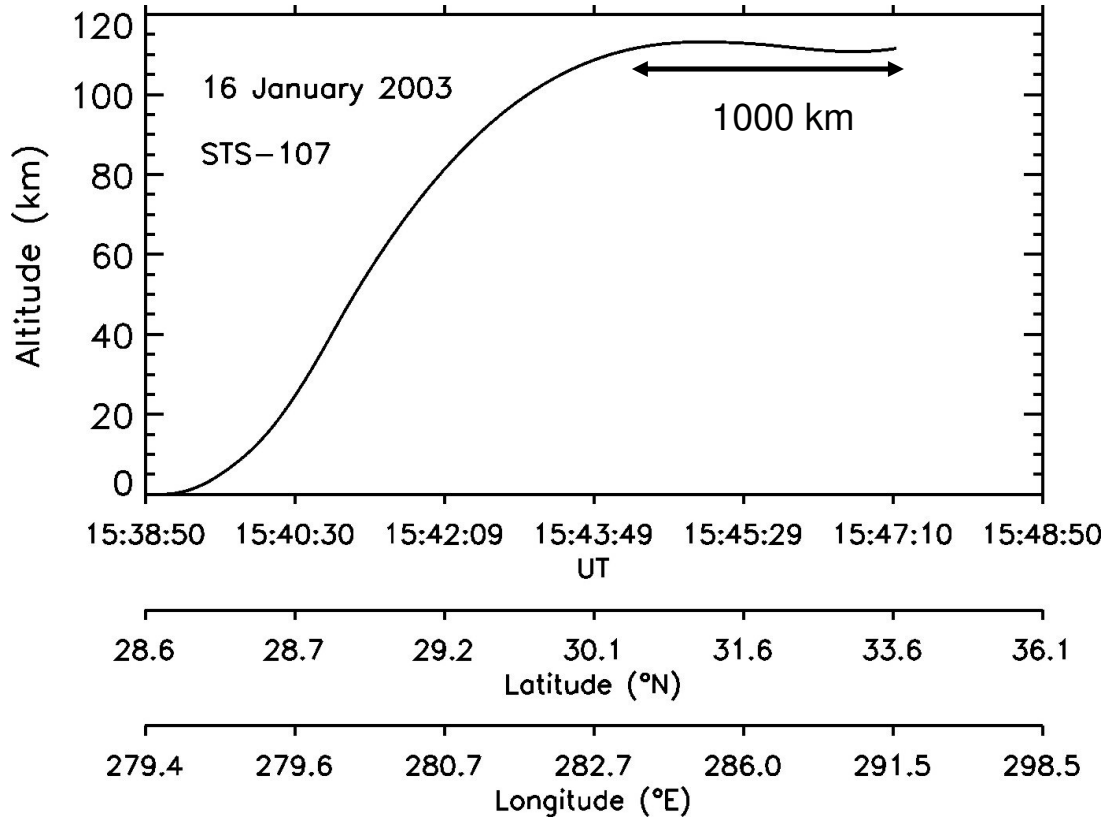

350 tonnes of water vapor are injected in the exhaust of the main engines between 100-115 km.

H_2O is photolysed by Lyman α (121.6 nm) to produce H atoms. These can be detected from a satellite by resonance fluorescence in the VUV

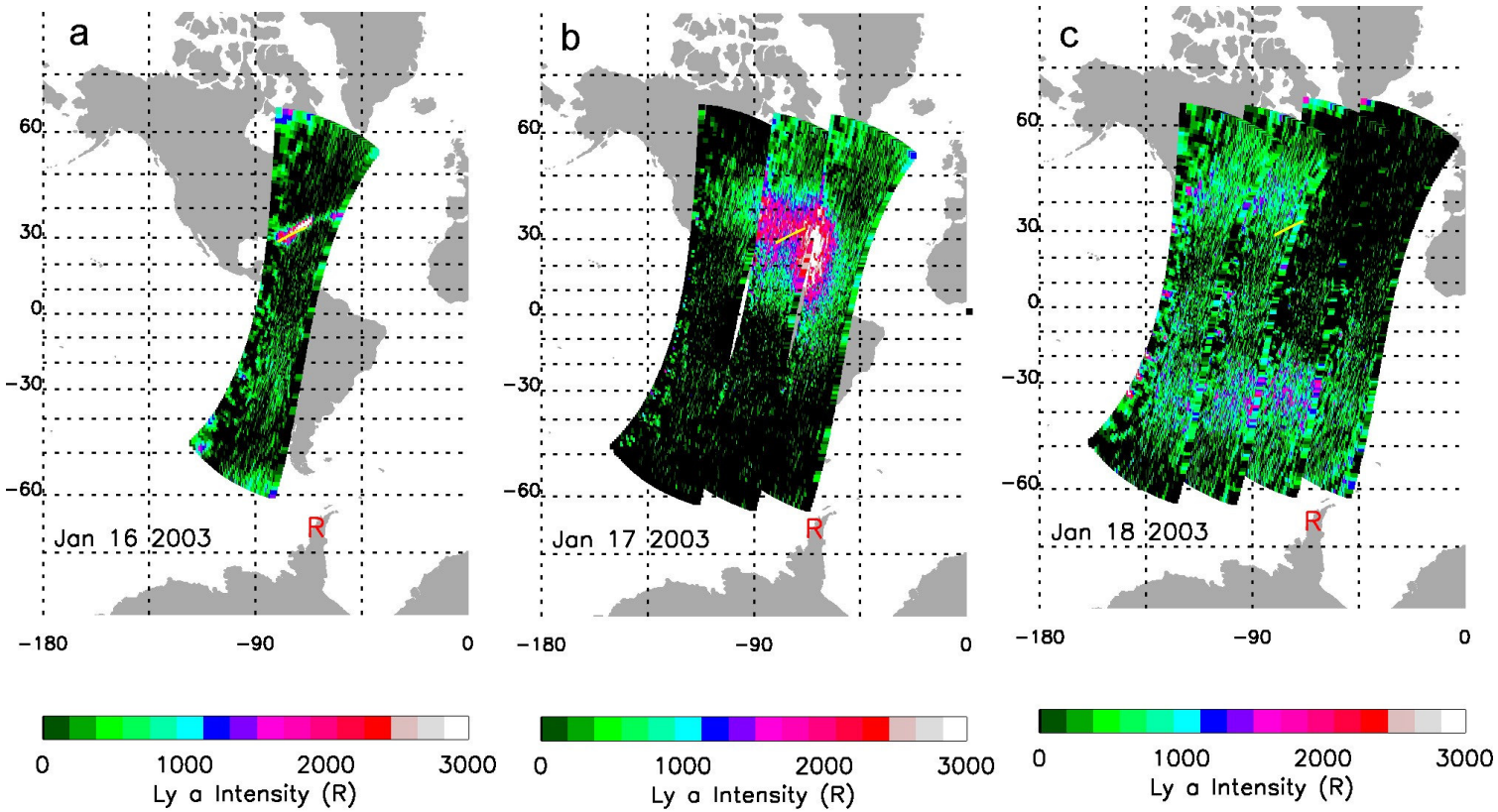

GUVI observations of Lyman α disk emission on 16 January, 2003. The streak of emission off the east coast of the United States is adjacent to the STS-107 ground-track, indicated in black. The ground-based lidar in Rothera, Antarctica at 67.6° S is indicated by the letter “R”.

The southward meridional wind is ~ 150 km h^{-1}

Fe densities measured by ground-based U. Illinois Boltzmann lidar at Rothera, Antarctica on 19-20 January, 2003.

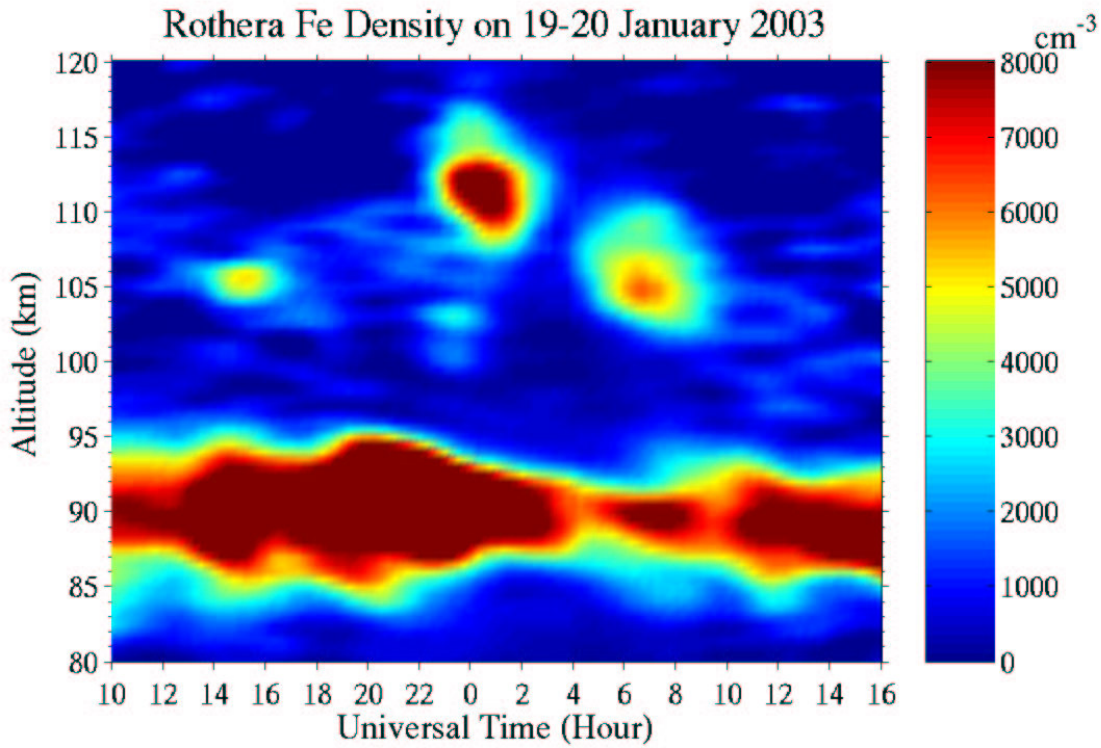

The layers between 105-110 km are highly unusual. Evidence that they are produced from degradation of the shuttle main engine components:

1. The layers appear at the same altitudes as the shuttle flies during main engine burn

2. The layers appear at Rothera at the same time as inferred from the GUVI satellite observations of the plume.

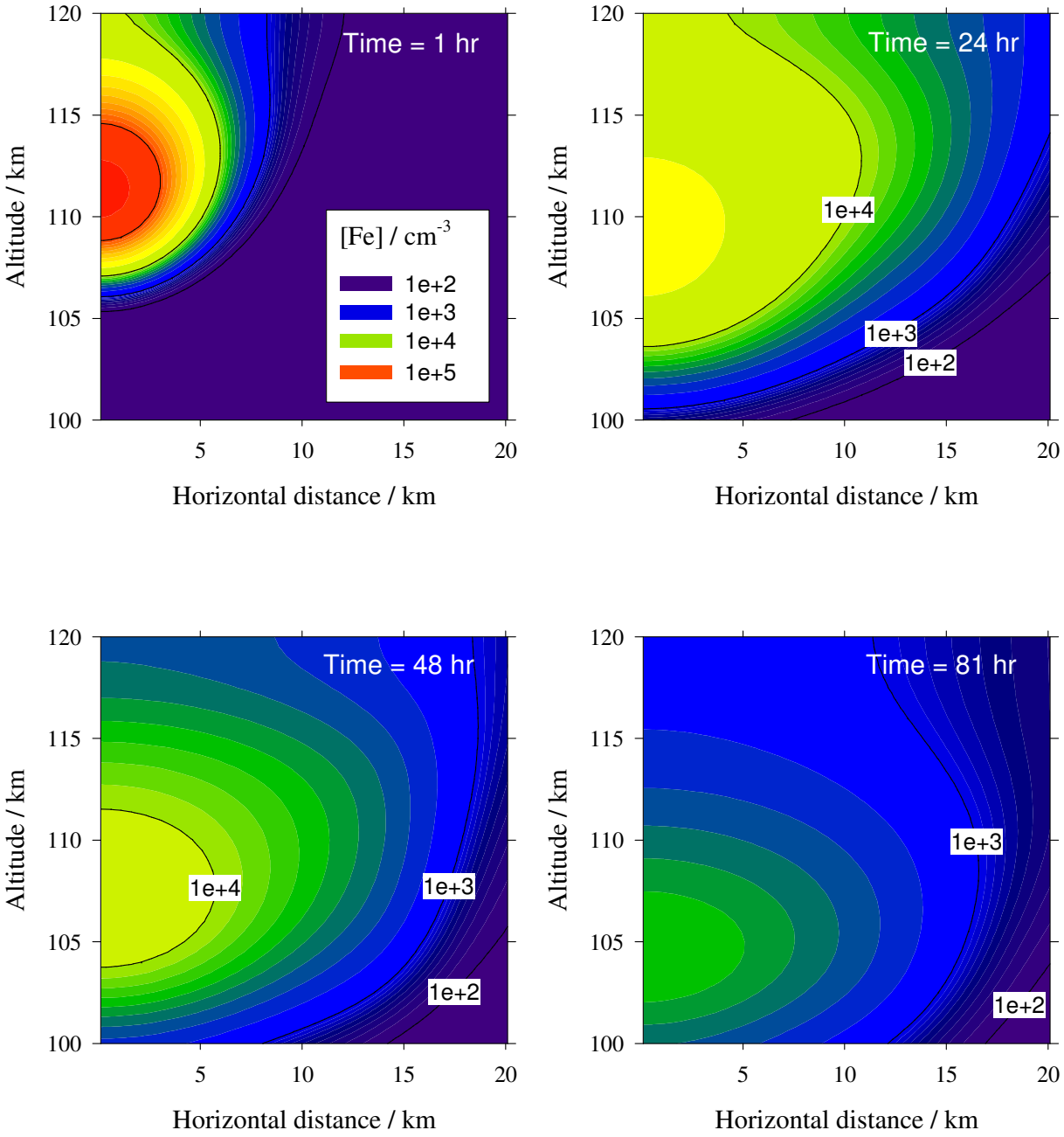

Cross sections through the plume showing the predicted Fe density (in atom cm^{-3}) at 1, 24, 48 and 81 hrs during transit to Antarctica.

The lifetime of atomic Fe against ionization is ~ 3 hrs at 110 km.

How does the Fe survive so long in the plume?

The H_2O in the plume is optically thick in the VUV.

How much Fe was produced by the shuttle?

The model plume requires 850 g of Fe ablated uniformly along the 1000 km track, to produce the observed [Fe] at Rothera after 81 hrs.

cf. ground-based studies of the shuttle's main engines indicate < 125 g [Madzsar et al., 1992].

There are two possible explanations for the discrepancy:

1. Most of the iron is emitted from the engine as FeOH, $Fe(OH)_2$ which is not detected.
2. The degradation of the engine components is considerably faster than predicted by the engineers.

Heavy rocket launches make a substantial contribution to the total H_2O in the MLT

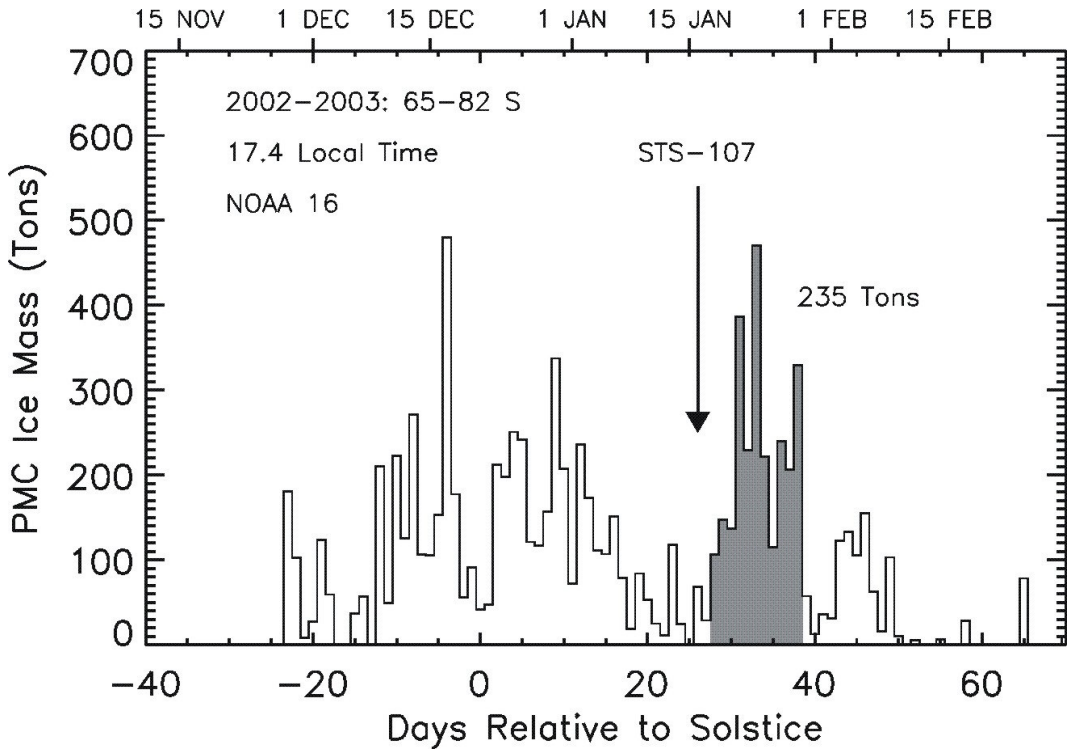

SBUV observations of the PMC ice mass during the southern summer of 2002-2003. Between 65-82° S, SBUV observed on average 235 tons of ice for 14 days following launch of STS-107. This is 18-27% of the entire mass observed for the season.

What happens to the metal compounds below 85 km?

Formation of “Meteoric Smoke”

736 JOURNAL OF METEOROLOGY VOLUME 18

SECONDARY PARTICULATE MATTER FROM METEOR VAPORS

J. Rosinski and R. H. Snow

Armour Research Foundation, Chicago.

(Manuscript received 15 March 1961)

ABSTRACT

The size distribution of secondary particulate matter, formed from condensing vapors in meteoric trains in the meteoric evaporating zone, was calculated. The diameters of the particles were found to be approximately proportional to the size of the meteor. The particles were calculated to be below 100 A in diameter, and the median volume diameters ranged from 4.5 to 80 A one min after evaporation. The average concentration of secondary particles formed from meteoric showers was found to be higher than the concentration from the steady-state influx of sporadic meteors.

From these results, the majority of the freezing nuclei in Bowen's hypothesis might be interpreted to be connected with the secondary particles formed in meteoric trails. If these particles serve as freezing nuclei, then freezing nuclei should be of similar chemical composition. The presence of larger secondary particles in the wakes of very bright meteors may contribute to the formation of noctilucent clouds.

Bowen's hypothesis should be re-evaluated and the role of the secondary meteoric matter in the earth's atmosphere clarified.

Subsequent modelling and laboratory papers

Hunten, D.M., R.P., Turco, and O.B. Toon (1980), Smoke and dust particles of meteoric origin in the mesosphere and stratosphere, *J. Atmos. Sci.*, *37*, 1342-1357.

Kalashnikova, O., M. Horanyi, G.E. Thomas, and O.B. Toon (2000), Meteoric smoke production in the atmosphere, *Geophys. Res. Lett.*, *27*, 3293-3296.

Megner, L., M. Rapp, and J. Gumbel, Distribution of meteoric smoke – sensitivity to microphysical properties and atmospheric conditions, *Atmos. Chem. Phys.*, *6*, 4415-4426 (2006).

Saunders, R. W., and J. M. C. Plane, A laboratory study of meteor smoke analogues: Composition, optical properties and growth kinetics, *J. Atmos. Sol.-Terr. Phys.*, 68, 2182-2202 (2006).

Saunders, R. W., P. M. Forster, and J. M.C. Plane, Potential climatic effects of meteoric smoke in the Earth's paleo-atmosphere, *Geophys. Res. Lett.*, under review.

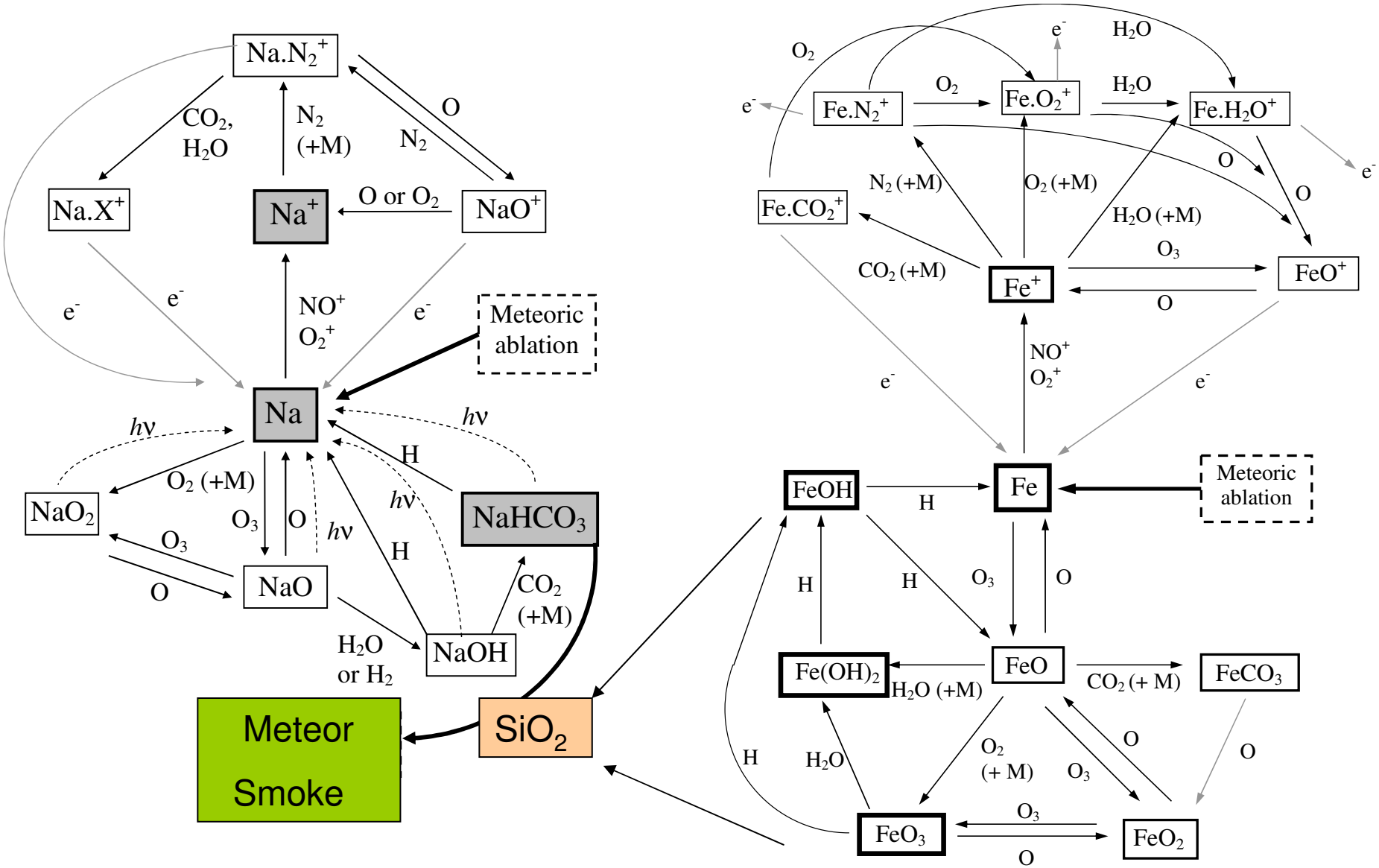

Meteor smoke is formed from metal oxides, hydroxides and carbonates and SiO_2 polymerize over about 10 days to form nanometre-size particles.

Laboratory simulation of meteoric smoke formation

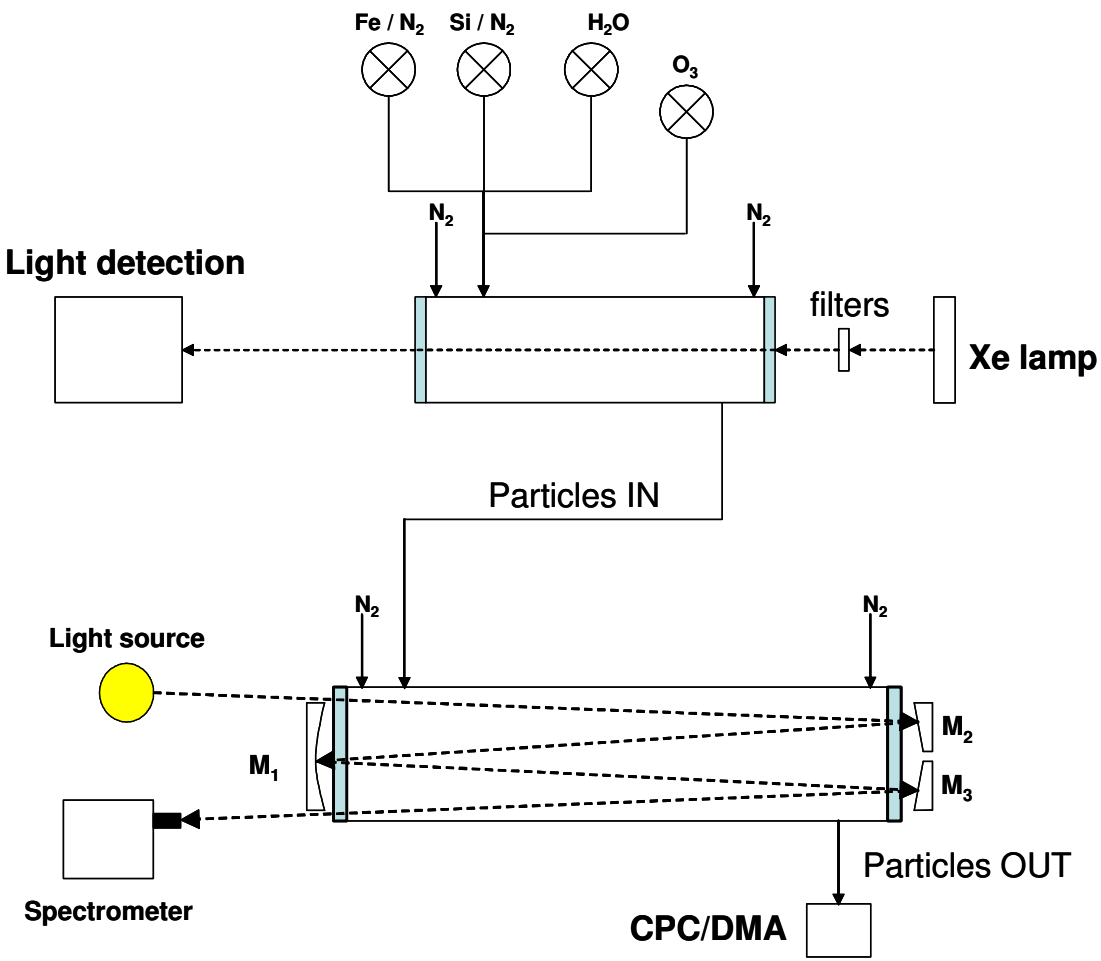

Photochemical reactor

Measure:

Particle size distribution

Optical extinction

Morphology & composition

Photochemical precursors: For Silicon, tetra-ethyl orthosilane or TEOS

For Fe, iron pentacarbonyl

The Iron / silicon / oxygen system

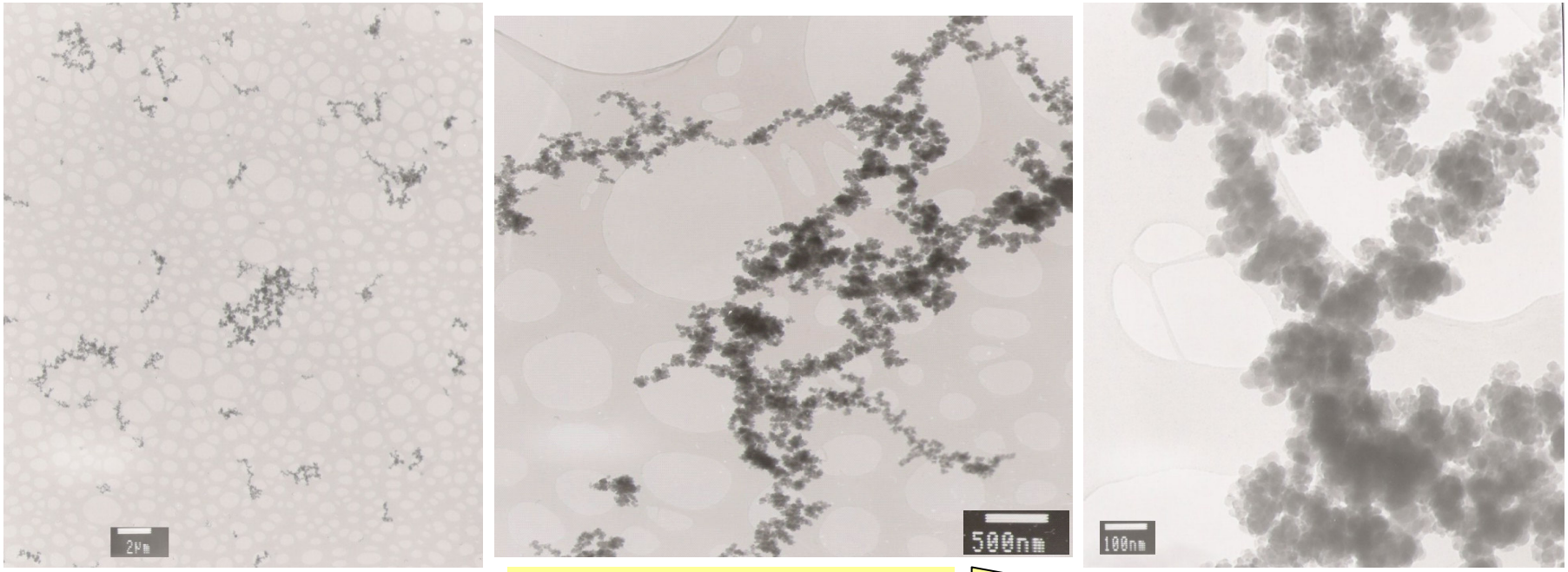

Increasing magnification

Conclusions:

1. Laboratory smoke particles form **fractal aggregates** with *huge surface areas*.
2. EDX, EELS and electron diffraction analysis shows the dark particles are amorphous fayalite (Fe_2SiO_4).
3. These particles agglomerate very aggressively due to **magnetic dipole attraction**.

The Iron / hydrogen / oxygen system

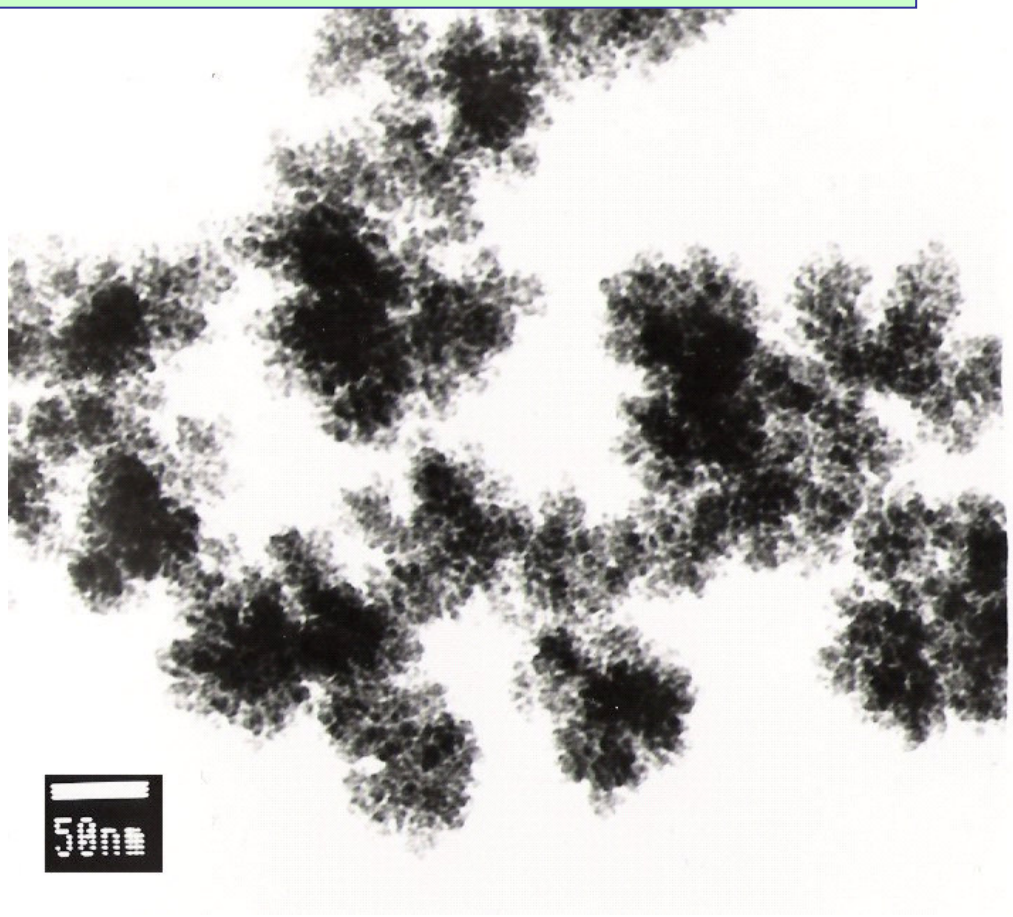

Images of particles produced from Fe + O_3 + H_2O.
Average O:Fe ratio is **1.91± 0.11**.
This suggests iron hydroxide ($Fe(OH)_2$) or goethite (FeOOH).

Aerosol kinetics reactor

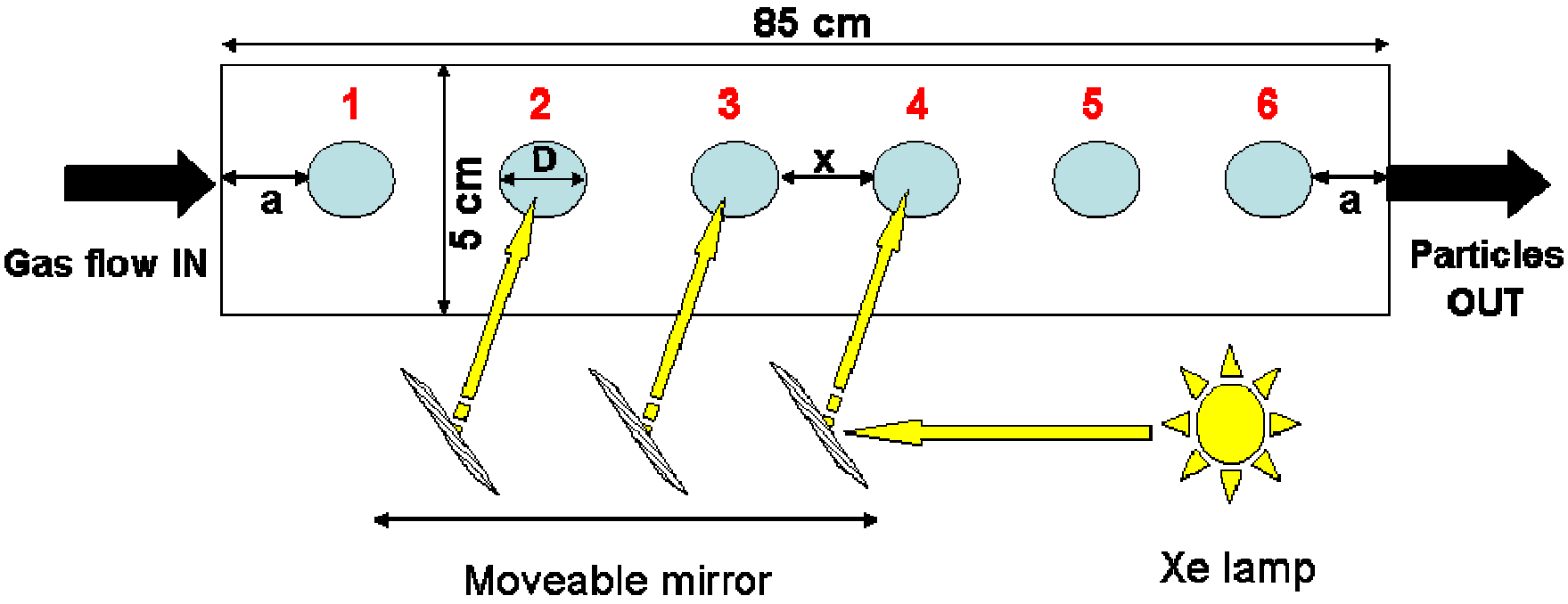

a = 10 cm, D = 2.5 cm, x = 10 cm

Formation of magnetic fayalite monomers

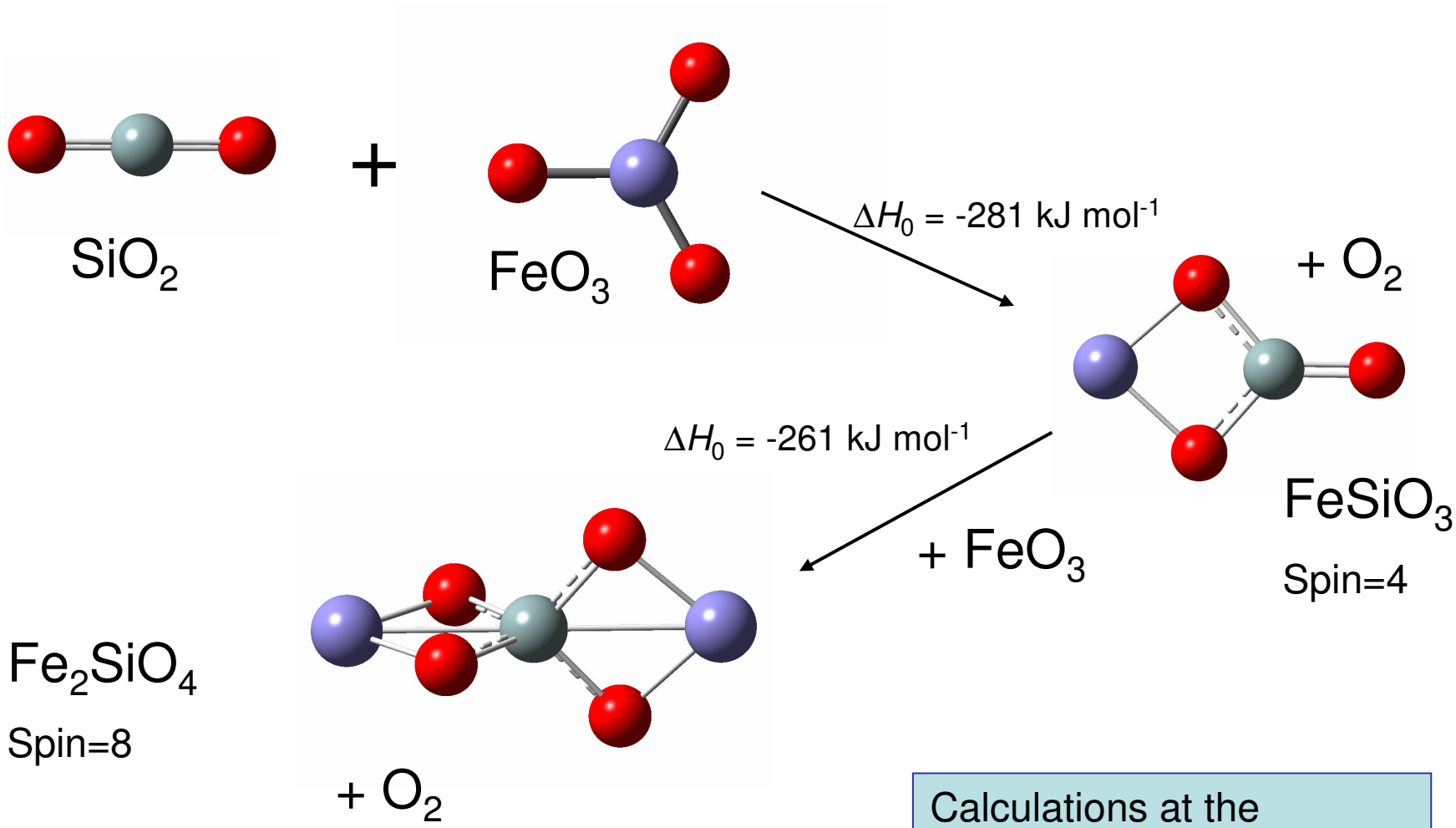

Calculations at the B3LYP/6-311+g(2d,p) level

Coagulation between fayalite particles governed by long-range magnetic dipole attraction

Collision kernels between two particles of radius *r*

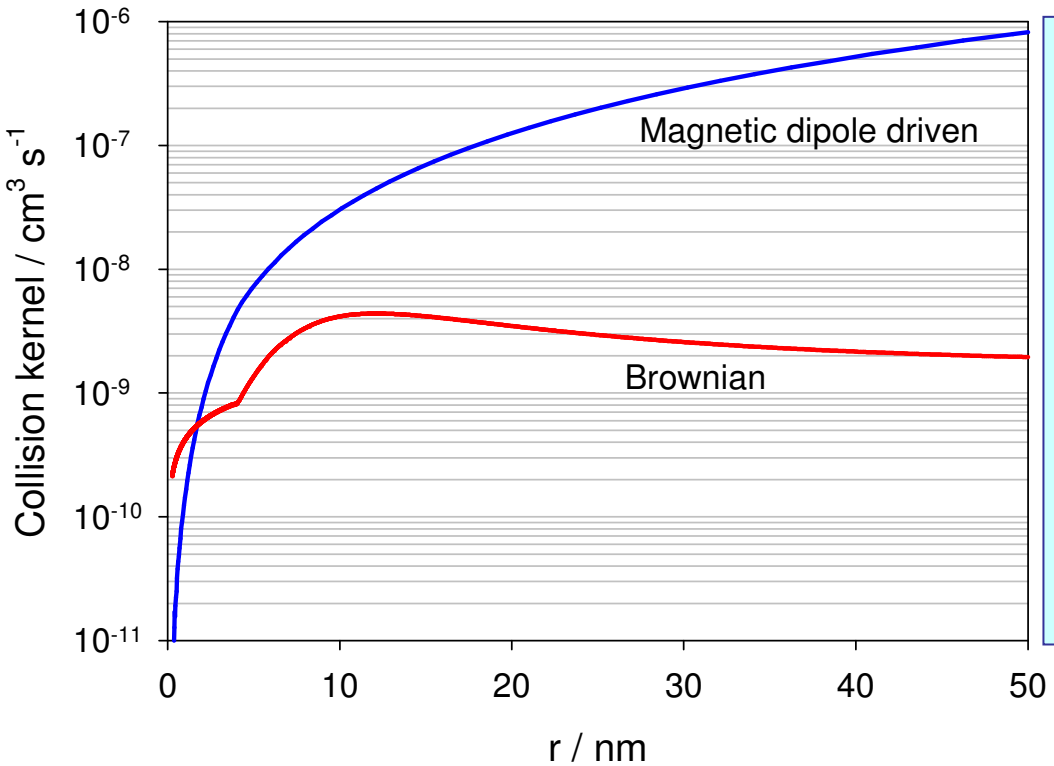

Applying the orbiting criterion on the effective potential energy surface yields:

$$\beta_{i,j}^{Mag}(T) = \pi \left(\frac{8k_B T}{\pi \mu} \right)^{1/2} \left(\frac{2C}{k_B T} \right)^{1/3} \times \Gamma\left(\frac{2}{3} \right)$$

$$\text{where } C = \frac{2}{3} \frac{(\mu_i \mu_j \mu_0)^2}{k_B T}$$

Saunders and Plane, *JASTP,* 68, 2182-2202 (2006)

Fit to experimental kinetic data

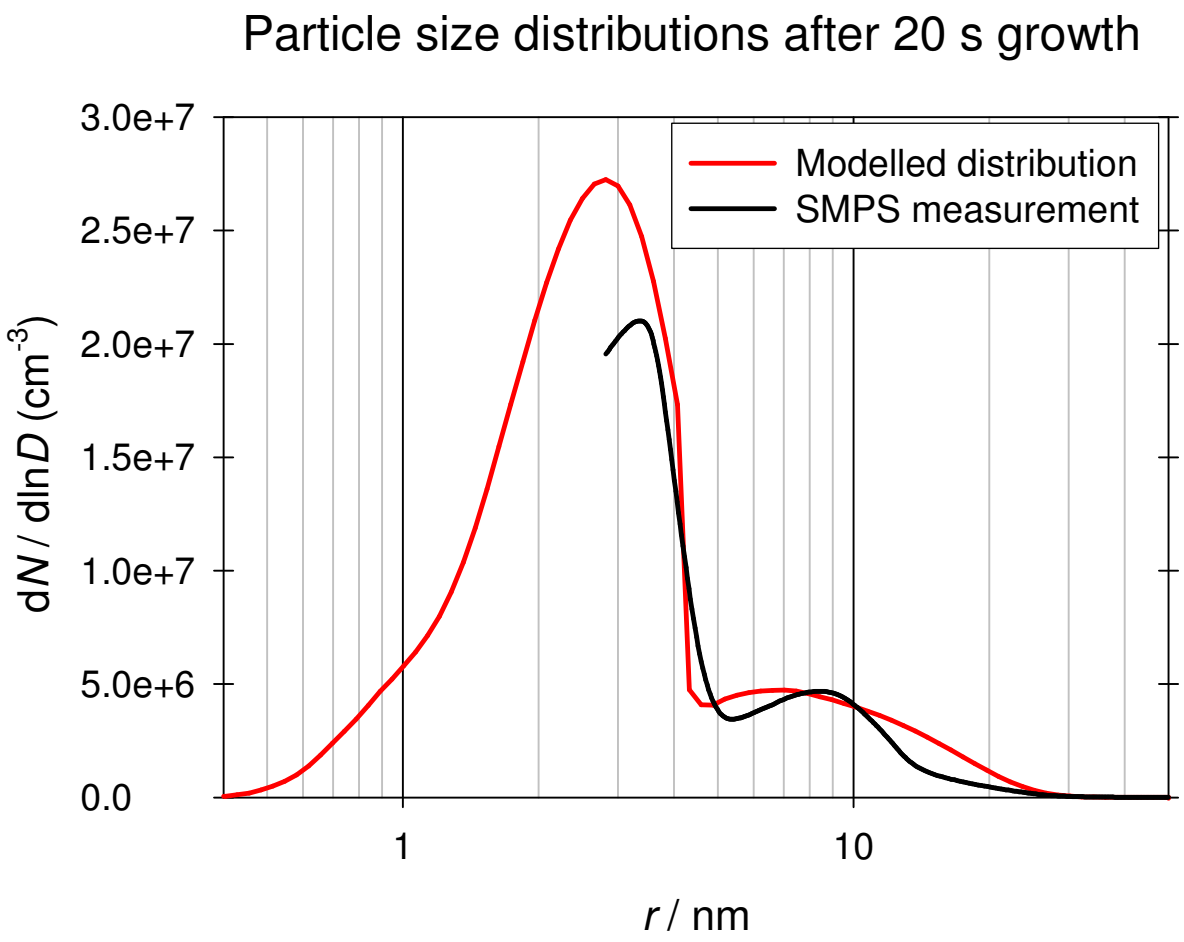

Model uses the <u>measured</u> rate of Fe_2SiO_4 production

Fitted parameters:

D_f = 1.75

p_{prim} = 4.1 nm

Fraction of aligned magnetic dipoles = 0.31

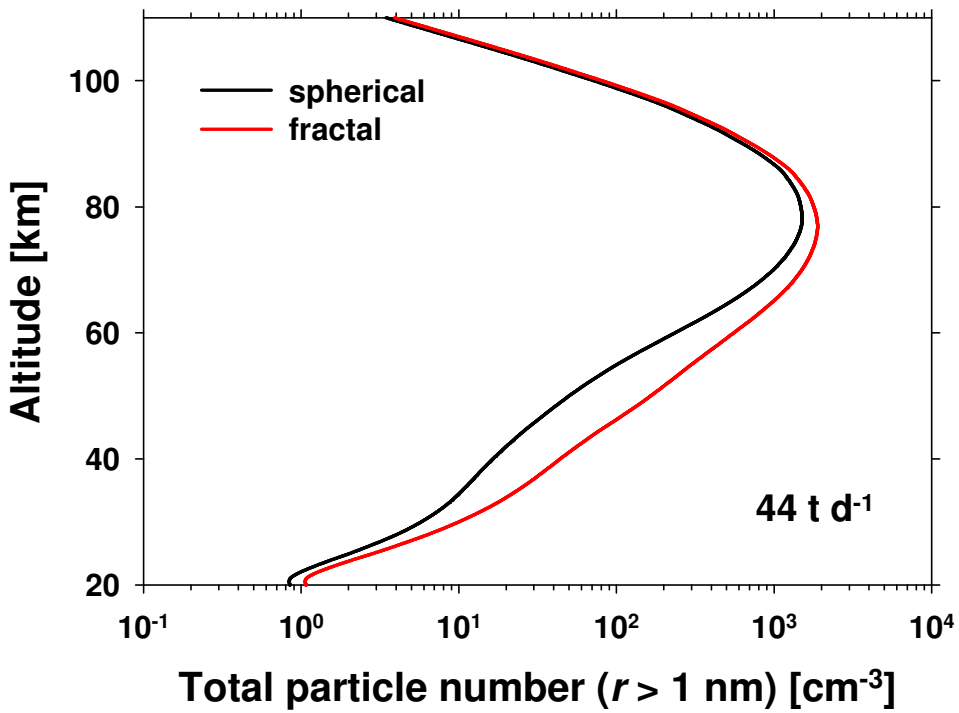

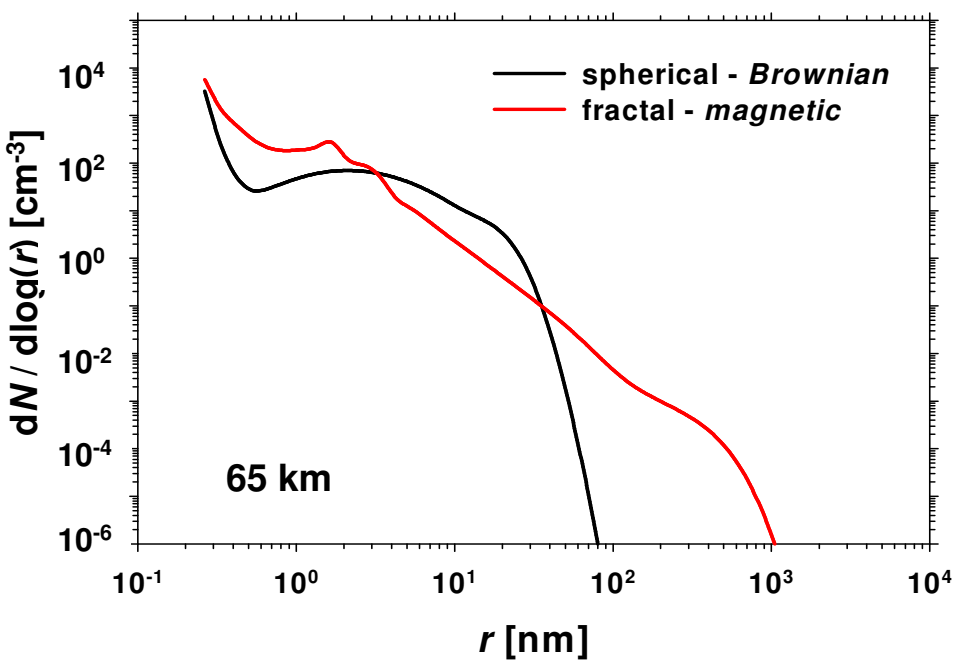

1 D model predictions of smoke profiles for the spherical and fractal cases.

The model contains:

Meteor ablation

Nucleation

Condensation

Agglomerative coagulation

Sedimentation

- Laboratory simulations show that meteoric smoke should consist of hematite (Fe_2O_3) and fayalite (Fe_2SiO_4) with smaller quantities of other metals and SiO_2
- The magnetic dipoles from the high spin states of Fe will cause long-range attraction between particles, causing rapid agglomerative coagulation and highly fractal particles ($D_f < 2$)
- The concentration of these “fluffy” particles could exceed 10 cm^{-3} in the middle mesosphere
- Because of their huge large surface area / mass ratios, these particles sediment slowly and should have unusual properties as ice nuclei and sites for heterogeneous chemistry

Are MSPs able to nucleate ice clouds?

46 JOURNAL OF THE ATMOSPHERIC SCIENCES VOLUME 24

Ice Nucleating Properties of Meteoritic Material

E. K. BIGG
Radiophysics Laboratory, CSIRO, Sydney, Australia

AND J. GIUTRONICH
University of New South Wales, Australia

(Manuscript received 26 September 1966)

ABSTRACT

A description is given of an attempt to duplicate the small particles formed by evaporation and recondensation during the flight of meteors in the atmosphere by heating meteors at a low pressure.

A metallic meteorite produced entirely shiny spherules, almost all of which were in the size range 5 to 25 μ diameter, while a stony meteorite produced only irregular aggregates of tiny particles whose maximum dimensions were 0.1 to 0.2 μ. At water saturation and -10C, it is estimated that the iron meteorite creates about 10^6–10^8 ice nuclei per gram and the stony meteorite about 10^6–10^9. It is concluded that sufficient ice nuclei active at -15C are produced to explain observed concentrations in the troposphere.

Future experiments at the AIDA chamber, Karlsruhe

http://www.mpi-hd.mpg.de/mauersberger/schreiner/PictureGal_AIDA.htm

Experiments with meteoric smoke scheduled for June 2008

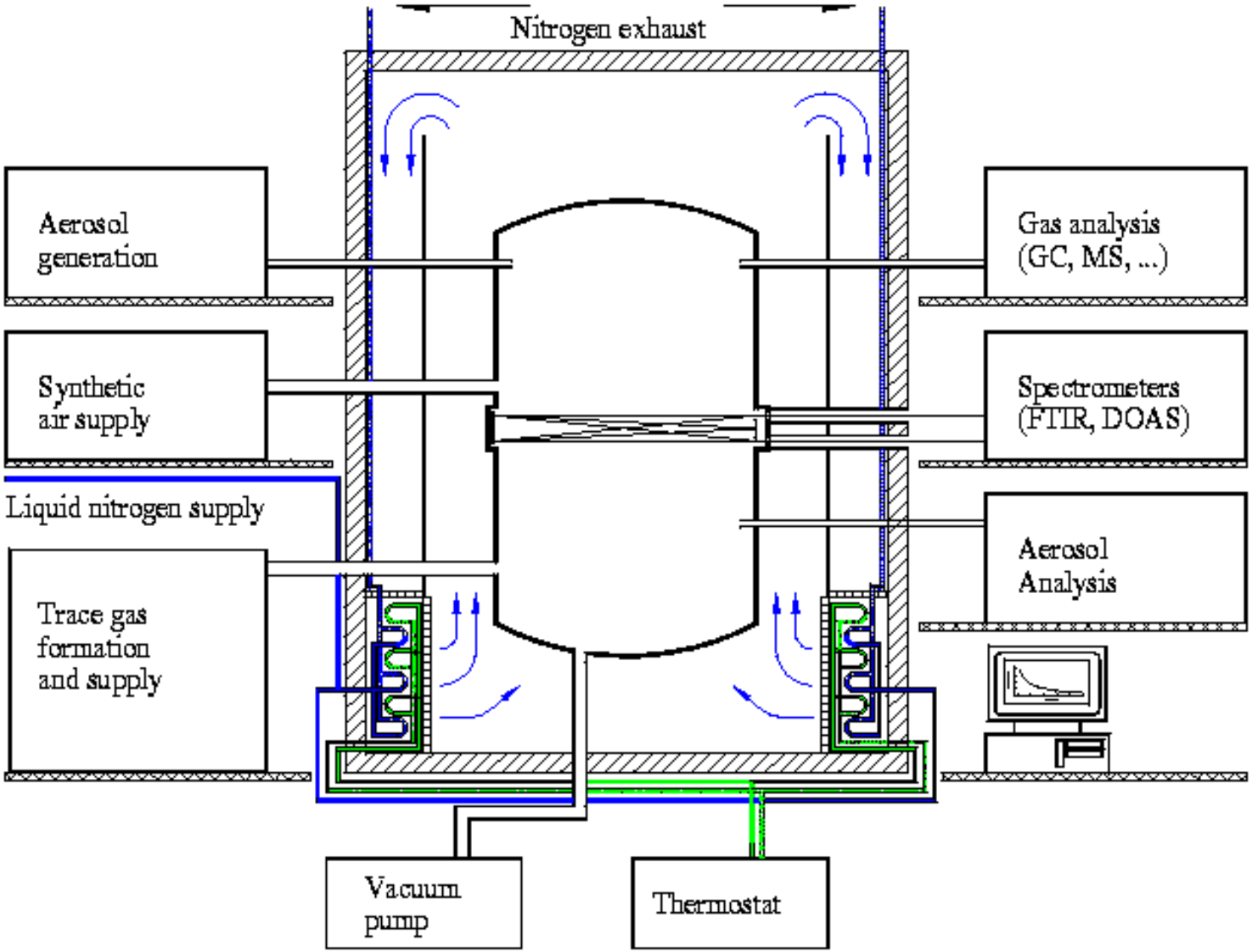

Is there any evidence of meteoric smoke in the mesosphere?

Dust detectors on rockets see very heavy charged ions with masses > 4000 amu [e.g., Gelinas *et al*., *JGR* 2006]. However, these measurements are hard to interpret *quantitatively* for two reasons:

1. The ramming effect of the rocket can create charge by impact fragmentation (e.g., Bariatya, A., and C. M. Swenson, *GRL* (2006)).
2. The fraction of small dust particles that are charged in a weak plasma is still the subject of debate. Estimates range from 6 – 92 % around 85 km in the atmosphere. Even the sign of the charge can be a surprise [Rapp et al., *GRL* 2005].

So, what about capturing some nano-particles from a rocket …

The MAGIC rocket payload is a development between the Naval Research Laboratory (US), Department of Meteorology (U. Stockholm), MPI Jena, and U. of Leeds. The PI is Frank Giovanni (NRL).

The objective is to capture meteoric smoke directly in the mesosphere, for the first time, and return it to earth for analysis.

Since the particles are only expected to be up to 3 nm diameter, aerodynamics is a very important consideration and the sampling pin needs to have a diameter of ~ 3mm

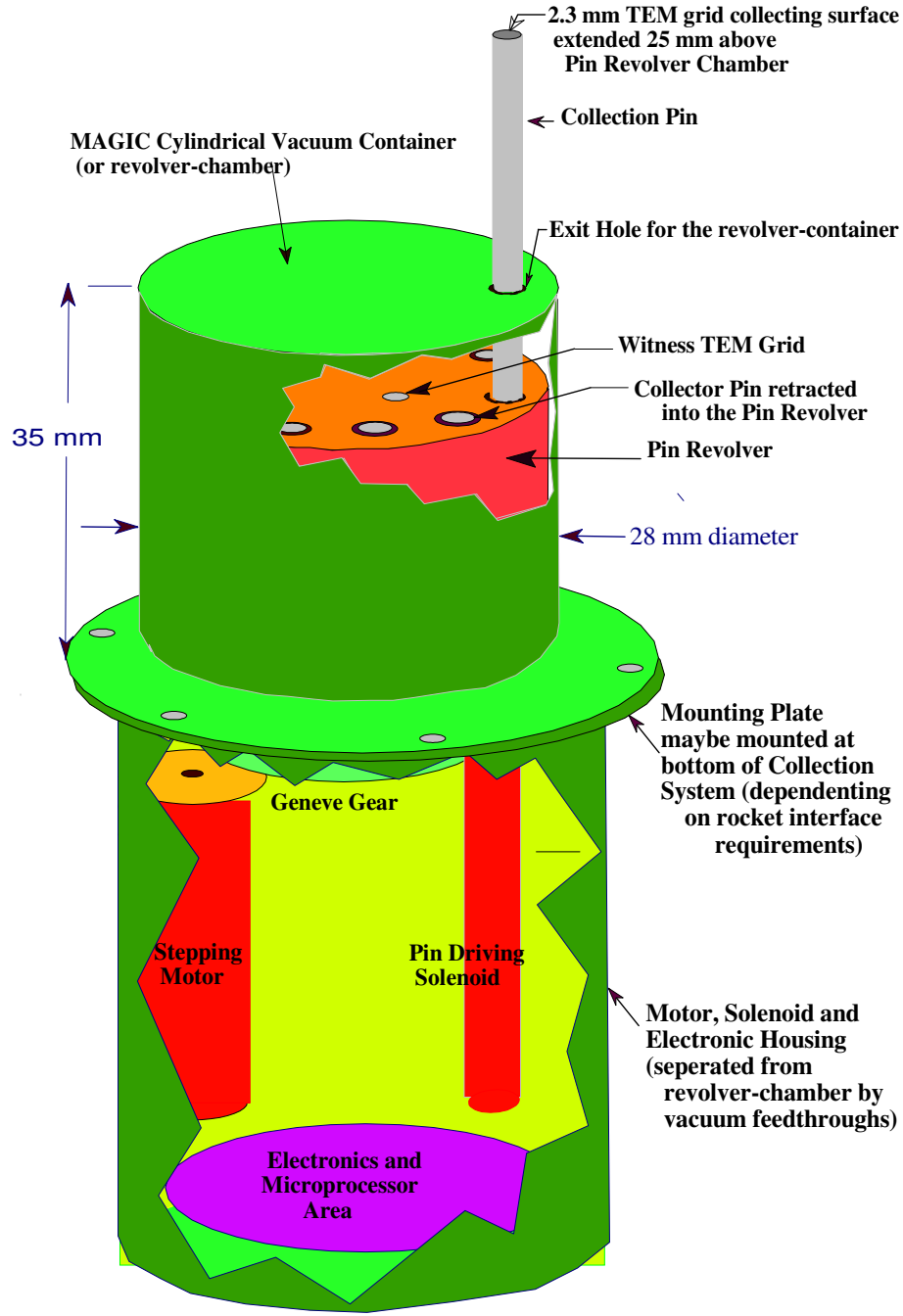

The MAGIC payload has now been launched and retrieved successfully from Kiruna (Sweden), Wallops Island (U.S.) and Andøya (Norway)

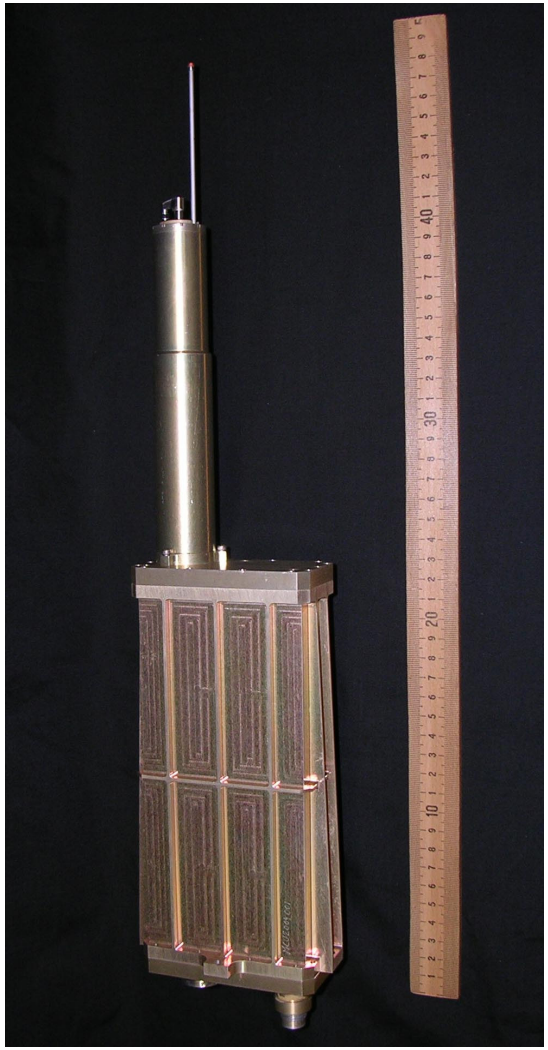

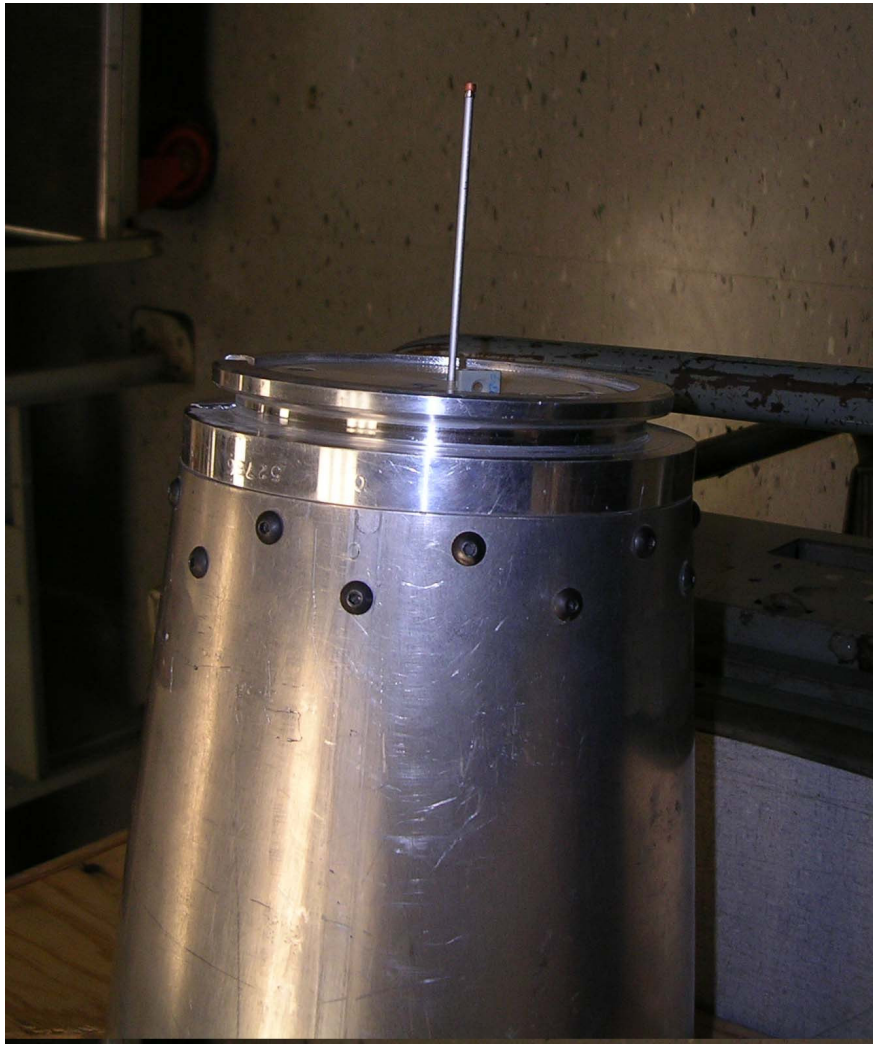

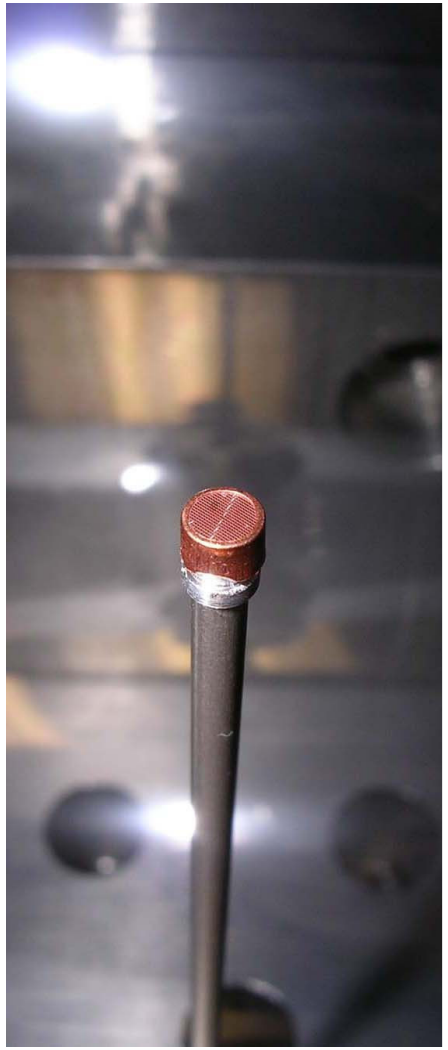

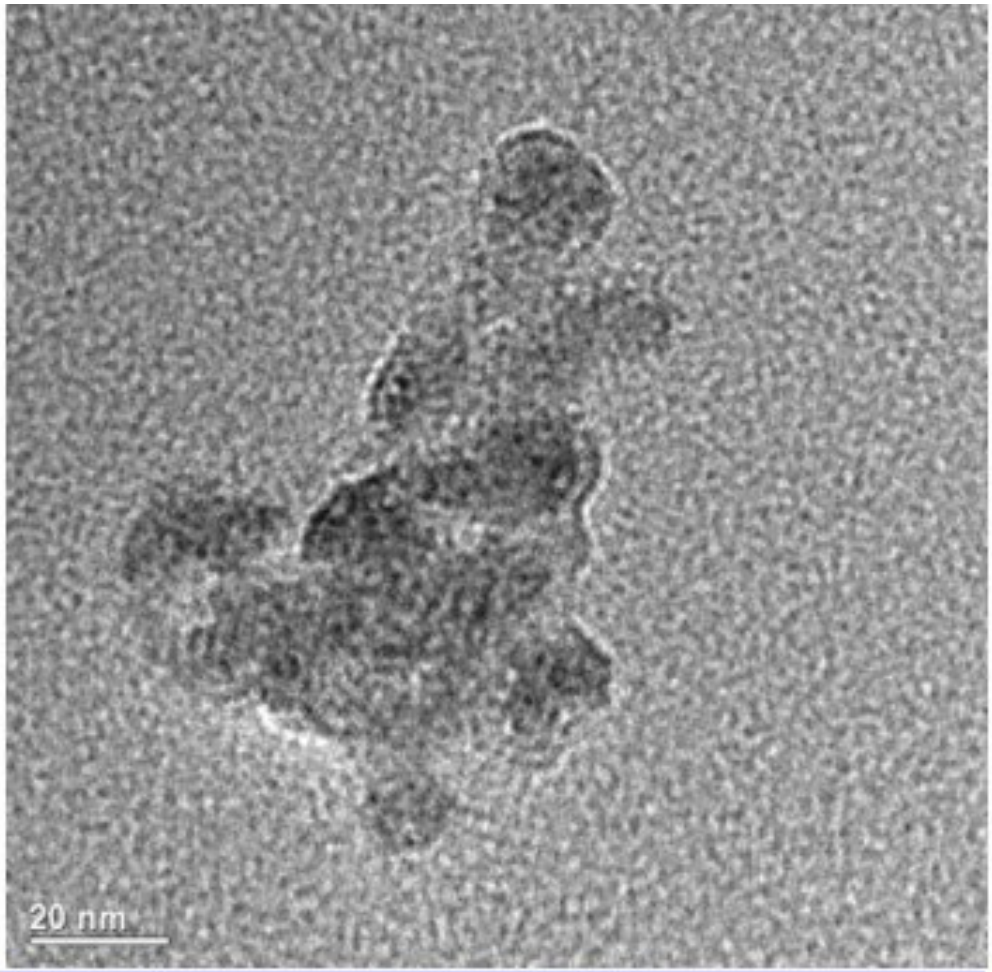

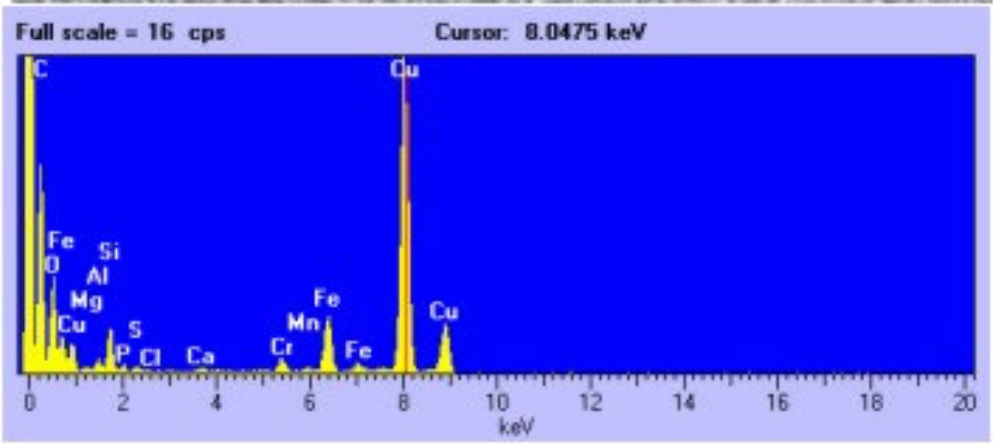

TEM image and xray analysis of a meteoric smoke particle retrieved by a MAGIC instrument at 70 km. Analysis performed by Rik Brydson at U. Leeds.

The elemental analysis shows the particle is mostly Fe, Si and O, with some Mg (Cu and C are grid substrate materials).

Unfortunately, there is also about 10 x too much Cr!!

Incoherent scatter radar measurements of meteoric smoke

The additional narrow line is caused by a second diffusion mode in the plasma due to coupling between electrons and charged MSPs

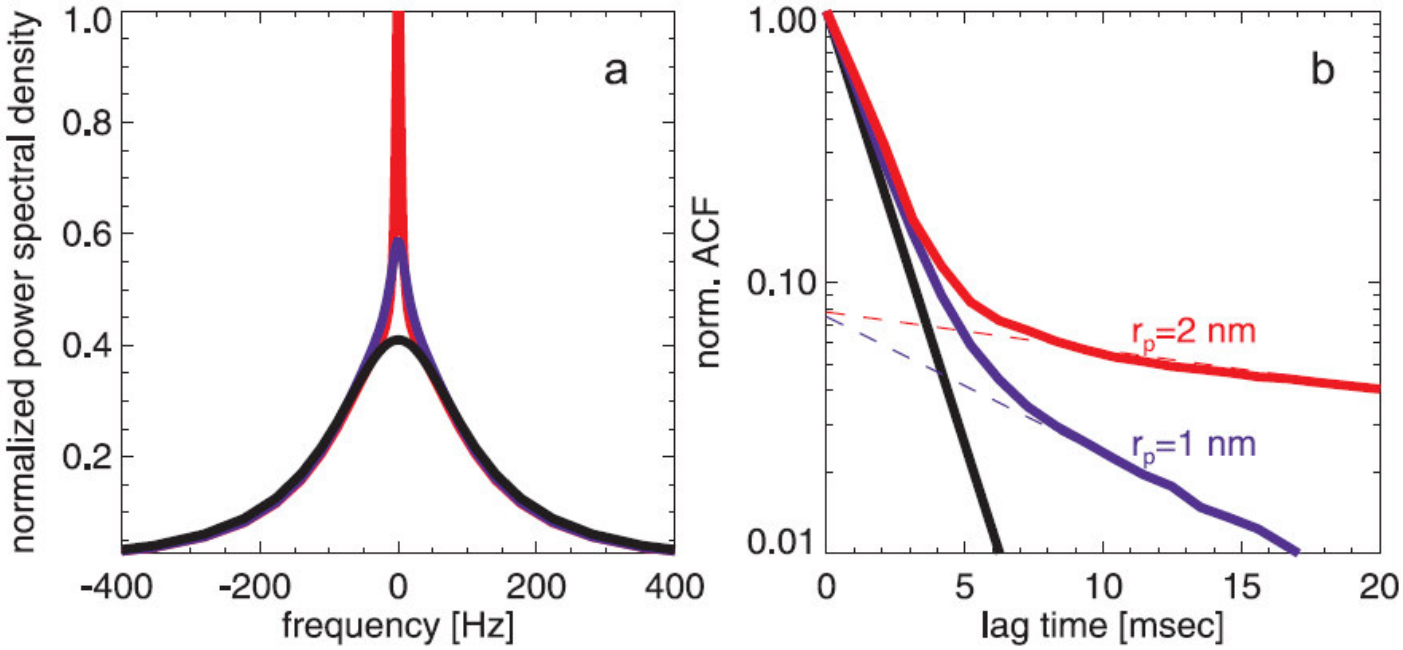

(a) Modelled ISR spectra and (b) the corresponding autocorrelation functions without charged particles (black line) and with 1 nm (blue) and 2 nm (red) particles. Based on theory of Cho et al. (1998).

Strelnikova et al., Meteor smoke particle properties derived from Arecibo incoherent scatter radar measurements, submitted to *GRL* [courtesy of Markus Rapp]

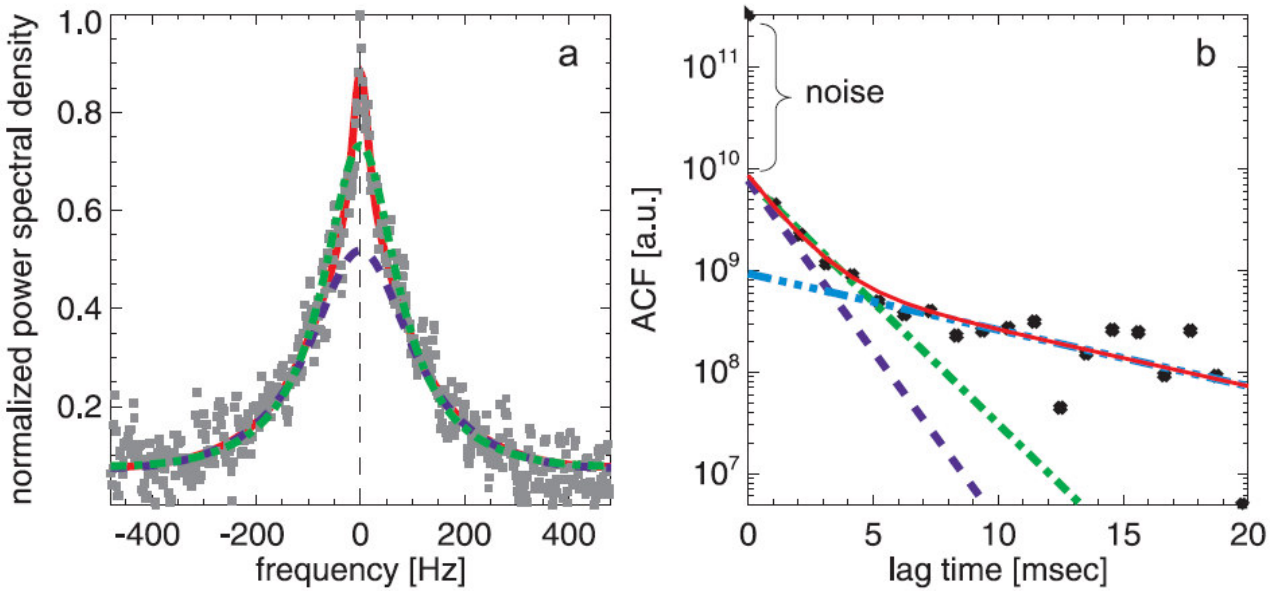

Measurements at 88km from the Arecibo radar show clear evidence for a second diffusion mode due to charged particles

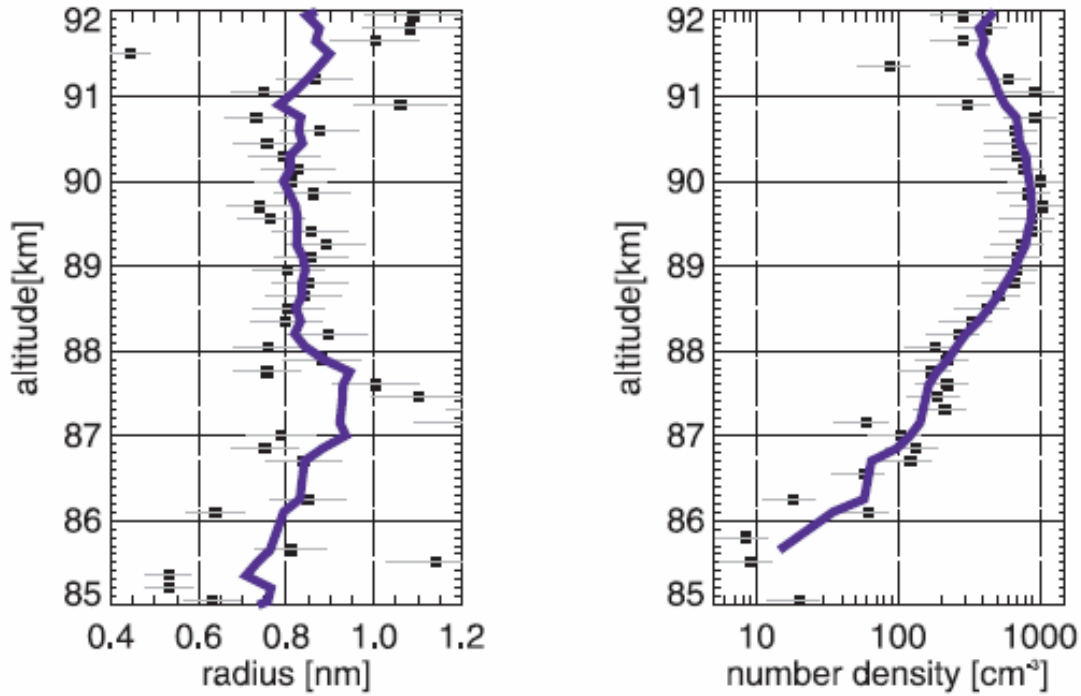

The retrieved particle size and number distribution are in accord with models.

Note that these are POSITIVELY charged particles

What evidence is there for meteoric smoke particles in the middle atmosphere?

Within the last 5 years …

1. Substantial concentrations of meteoric metals in Junge layer aerosols [Cziczo *et al.*, *Science*, 2001]
2. Enhanced metal concentrations in stratospheric aerosols inside the polar vortex ⇒ implications for aerosol nucleation [Curtius *et al.*, *ACP*, 2005]
3. Polar winter radar echoes [Stebel *et al.*, *JASTP*, 2004]
4. Lidar observations of dust descending dust layers in winter polar vortex from 25 – 40 km [Gerding *et al., Ann. Geophys.*, 2003]
5. Enhanced H_2O layer above 50 km [Siskind *et al., GRL* 1999]
6. H_2SO_4 removed in the polar stratosphere above 40 km [Mills *et al.*, *JGR*, 2005]
7. Enhanced HNO_3 in polar stratosphere above 30 km [Stiller *et al.*, *JGR*, 2005]

What evidence is there for meteoric smoke particles in the middle atmosphere?

Within the last 5 years …

1. Substantial concentrations of meteoric metals in Junge layer aerosols [Cziczo *et al.*, *Science*, 2001]
2. Enhanced metal concentrations in stratospheric aerosols inside the polar vortex ⇒ implications for aerosol nucleation [Curtius *et al.*, *ACP*, 2005]
3. Polar winter radar echoes [Stebel *et al.*, *JASTP*, 2004]
4. Lidar observations of dust descending dust layers in winter polar vortex from 25 – 40 km [Gerding *et al., Ann. Geophys.*, 2003]
5. Enhanced H_2O layer above 50 km [Siskind *et al., GRL* 1999]
6. H_2SO_4 removed in the polar stratosphere above 40 km [Mills *et al.*, *JGR*, 2005]
7. Enhanced HNO_3 in polar stratosphere above 30 km [Stiller *et al.*, *JGR*, 2005]

What evidence is there for meteoric smoke particles in the middle atmosphere?

Within the last 5 years …

1. Substantial concentrations of meteoric metals in Junge layer aerosols [Cziczo *et al.*, *Science*, 2001]
2. Enhanced metal concentrations in stratospheric aerosols inside the polar vortex ⇒ implications for aerosol nucleation [Curtius *et al.*, *ACP*, 2005]
3. Polar winter radar echoes [Stebel *et al.*, *JASTP*, 2004]
4. Lidar observations of dust descending dust layers in winter polar vortex from 25 – 40 km [Gerding *et al., Ann. Geophys.*, 2003]
5. Enhanced H_2O layer above 50 km [Siskind *et al., GRL* 1999]
6. H_2SO_4 removed in the polar stratosphere above 40 km [Mills *et al.*, *JGR*, 2005]
7. Enhanced HNO_3 in polar stratosphere above 30 km [Stiller *et al.*, *JGR*, 2005]

What evidence is there for meteoric smoke particles in the middle atmosphere?

Within the last 5 years …

1. Substantial concentrations of meteoric metals in Junge layer aerosols [Cziczo *et al.*, *Science*, 2001]
2. Enhanced metal concentrations in stratospheric aerosols inside the polar vortex ⇒ implications for aerosol nucleation [Curtius *et al.*, *ACP*, 2005]
3. Polar winter radar echoes [Stebel *et al.*, *JASTP*, 2004]
4. Lidar observations of dust descending dust layers in winter polar vortex from 25 – 40 km [Gerding *et al., Ann. Geophys.*, 2003]
5. Enhanced H_2O layer above 50 km [Siskind *et al., GRL* 1999]
6. H_2SO_4 removed in the polar stratosphere above 40 km [Mills *et al.*, *JGR*, 2005]
7. Enhanced HNO_3 in polar stratosphere above 30 km [Stiller *et al.*, *JGR*, 2005]

What evidence is there for meteoric smoke particles in the middle atmosphere?

Within the last 5 years …

1. Substantial concentrations of meteoric metals in Junge layer aerosols [Cziczo *et al.*, *Science*, 2001]
2. Enhanced metal concentrations in stratospheric aerosols inside the polar vortex ⇒ implications for aerosol nucleation [Curtius *et al.*, *ACP*, 2005]
3. Polar winter radar echoes [Stebel *et al.*, *JASTP*, 2004]
4. Lidar observations of dust descending dust layers in winter polar vortex from 25 – 40 km [Gerding *et al., Ann. Geophys.*, 2003]
5. Enhanced H_2O layer above 50 km [Siskind *et al., GRL* 1999]
6. H_2SO_4 removed in the polar stratosphere above 40 km [Mills *et al.*, *JGR*, 2005]
7. Enhanced HNO_3 in polar stratosphere above 30 km [Stiller *et al.*, *JGR*, 2005]

What evidence is there for meteoric smoke particles in the middle atmosphere?

Within the last 5 years …

1. Substantial concentrations of meteoric metals in Junge layer aerosols [Cziczo *et al.*, *Science*, 2001]
2. Enhanced metal concentrations in stratospheric aerosols inside the polar vortex ⇒ implications for aerosol nucleation [Curtius *et al.*, *ACP*, 2005]
3. Polar winter radar echoes [Stebel *et al.*, *JASTP*, 2004]
4. Lidar observations of dust descending dust layers in winter polar vortex from 25 – 40 km [Gerding *et al., Ann. Geophys.*, 2003]
5. Enhanced H_2O layer above 50 km [Siskind *et al., GRL* 1999]
6. H_2SO_4 removed in the polar stratosphere above 40 km [Mills *et al.*, *JGR*, 2005]
7. Enhanced HNO_3 in polar stratosphere above 30 km [Stiller *et al.*, *JGR*, 2005]

What evidence is there for meteoric smoke particles in the middle atmosphere?

Within the last 5 years …

1. Substantial concentrations of meteoric metals in Junge layer aerosols [Cziczo *et al.*, *Science*, 2001]
2. Enhanced metal concentrations in stratospheric aerosols inside the polar vortex ⇒ implications for aerosol nucleation [Curtius *et al.*, *ACP*, 2005]
3. Polar winter radar echoes [Stebel *et al.*, *JASTP*, 2004]
4. Lidar observations of dust descending dust layers in winter polar vortex from 25 – 40 km [Gerding *et al., Ann. Geophys.*, 2003]
5. Enhanced H_2O layer above 50 km [Siskind *et al., GRL* 1999]
6. H_2SO_4 removed in the polar stratosphere above 40 km [Mills *et al.*, *JGR*, 2005]
7. Enhanced HNO_3 in polar stratosphere above 30 km [Stiller *et al.*, *JGR*, 2005]

Can meteoric smoke be detected by Rayleigh/Raman lidars ?

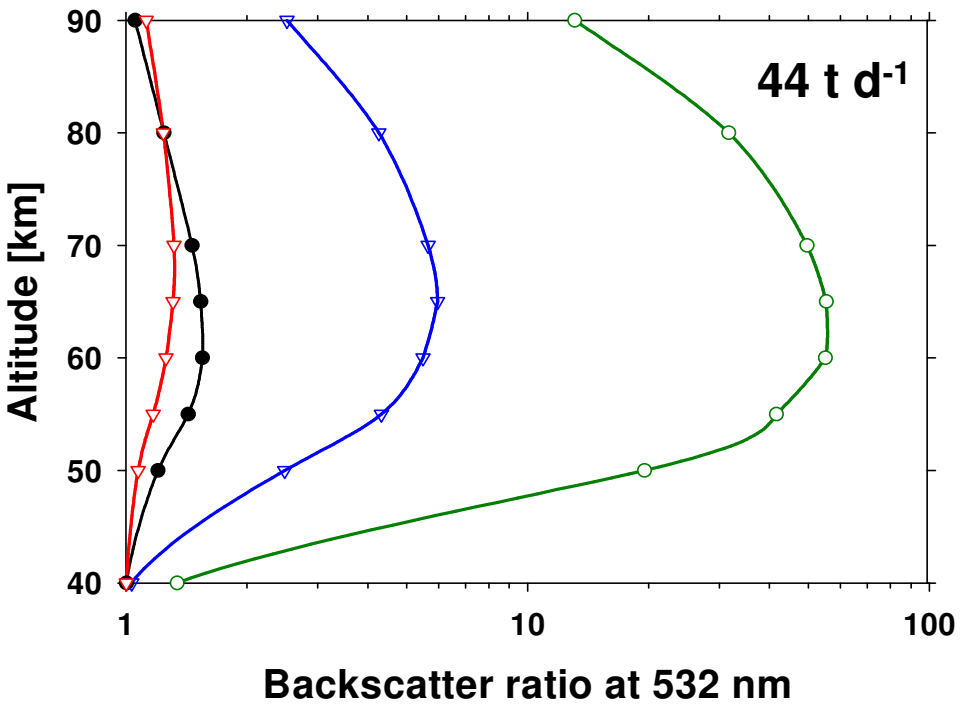

Calculated backscatter eatio using the Leeds 1D model prediction of MSP size distribution profiles

Simultaneous Raman measurements would distinguish MSPs from cold layers with enhanced Rayleigh scatter

- **Spherical, non-magnetic particles**
- **Fractal, magnetic particles / Porosity = 0.5**
- **Fractal, magnetic particles / Porosity = 0.75**
- **Fractal, magnetic particles / Porosity = 0.9**

Fluffy particles

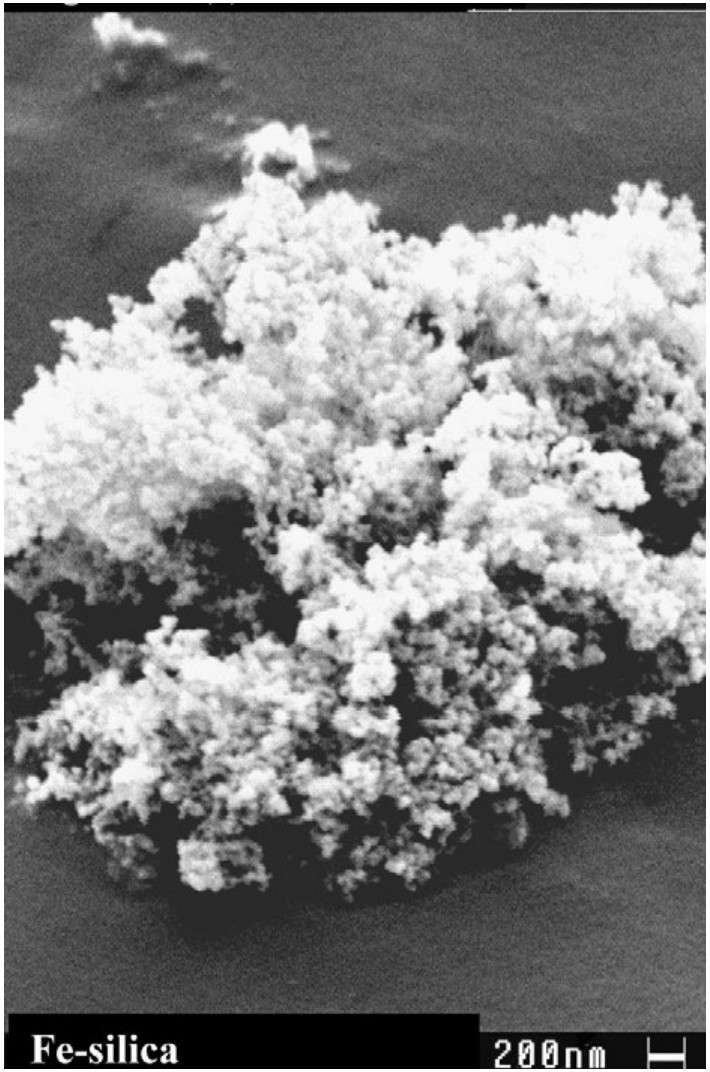

Laboratory generated
(Hadamcik *et al*., 2007)

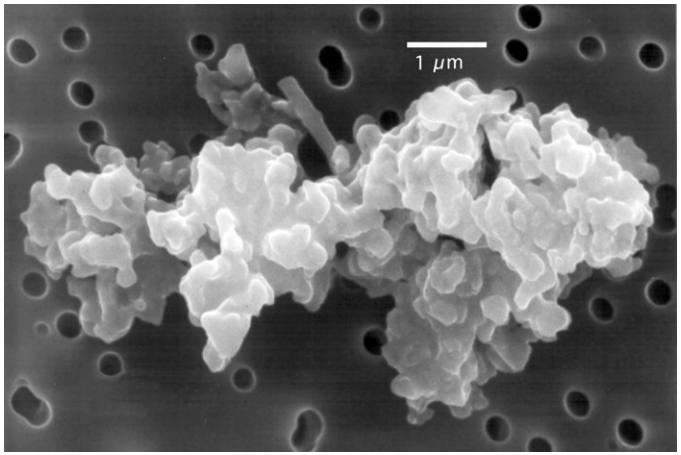

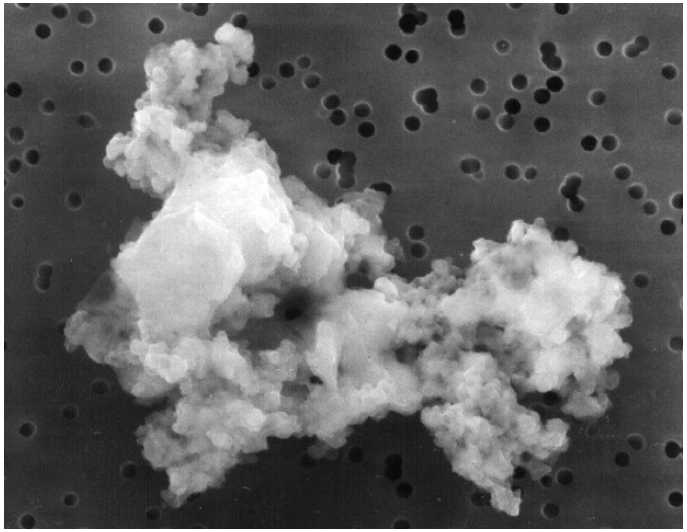

Chondritic IDP's sampled
from stratosphere
(NASA – *Cosmic Dust Lab* website)

‘Equivalent porous sphere’ + Effective medium theory

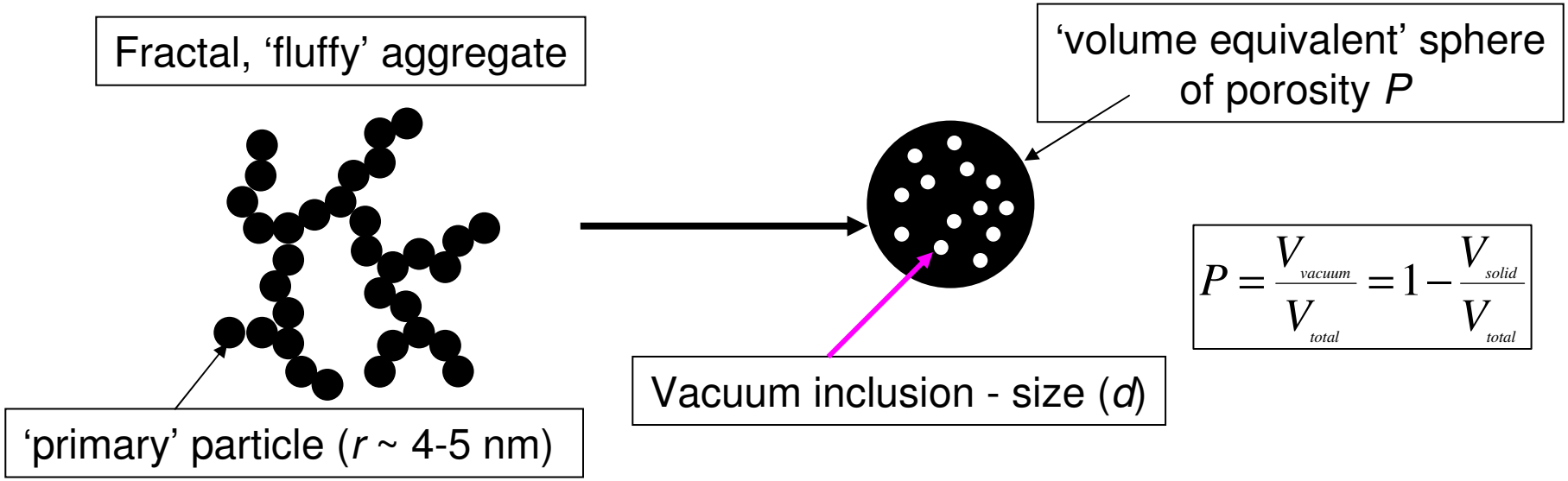

$$P = \frac{V_{vacuum}}{V_{total}} = 1 - \frac{V_{solid}}{V_{total}}$$

Maxwell-Garnett mixing rule: For $d << \lambda$,

$$\varepsilon_{eff} = \varepsilon_2 \left[1 + \frac{3 f_i \dfrac{\varepsilon_1 - \varepsilon_2}{\varepsilon_1 + 2\varepsilon_2}}{1 - f_i \dfrac{\varepsilon_1 - \varepsilon_2}{\varepsilon_1 + 2\varepsilon_2}} \right]$$

ε_{eff} is the ‘average’ dielectric function of the porous particle
ε_2 is the dielectric function of the particle material
ε_1 is the dielectric function of the inclusion (i.e. vacuum)
f_i is the volume fraction taken up by vacuum (i.e. the porosity)

$$\varepsilon_{eff} = \varepsilon' - i\varepsilon'' = m^2 = n^2 - 2i(nk) - k^2$$

m is the complex refractive index (RF) of the particle
n is the real part of RF
k is the imaginary part of RF

Therefore
$$\boxed{\begin{aligned} \varepsilon' &= n^2 - k^2 \\ \varepsilon'' &= 2nk \end{aligned}}$$

$n,k \rightarrow$ Mie calculations of particle backscatter

Why are smoke layers rarely observed?

- Meteoric flux << 44 t d^{-1}
- Fractal agglomerative coagulation is prevented by particles being charged

Need to carry out combined Rayleigh *and* Raman lidar measurements

Particle optical extinction

Meteoric smoke may have played a role in:

- the **early evolution of the atmosphere** (screening near-UV before the O_3 layer formed)
- two **"snowball earth" episodes** when the solar system moved through spiral arms of the galaxy [Pavlov et al., *GRL*, 2005]

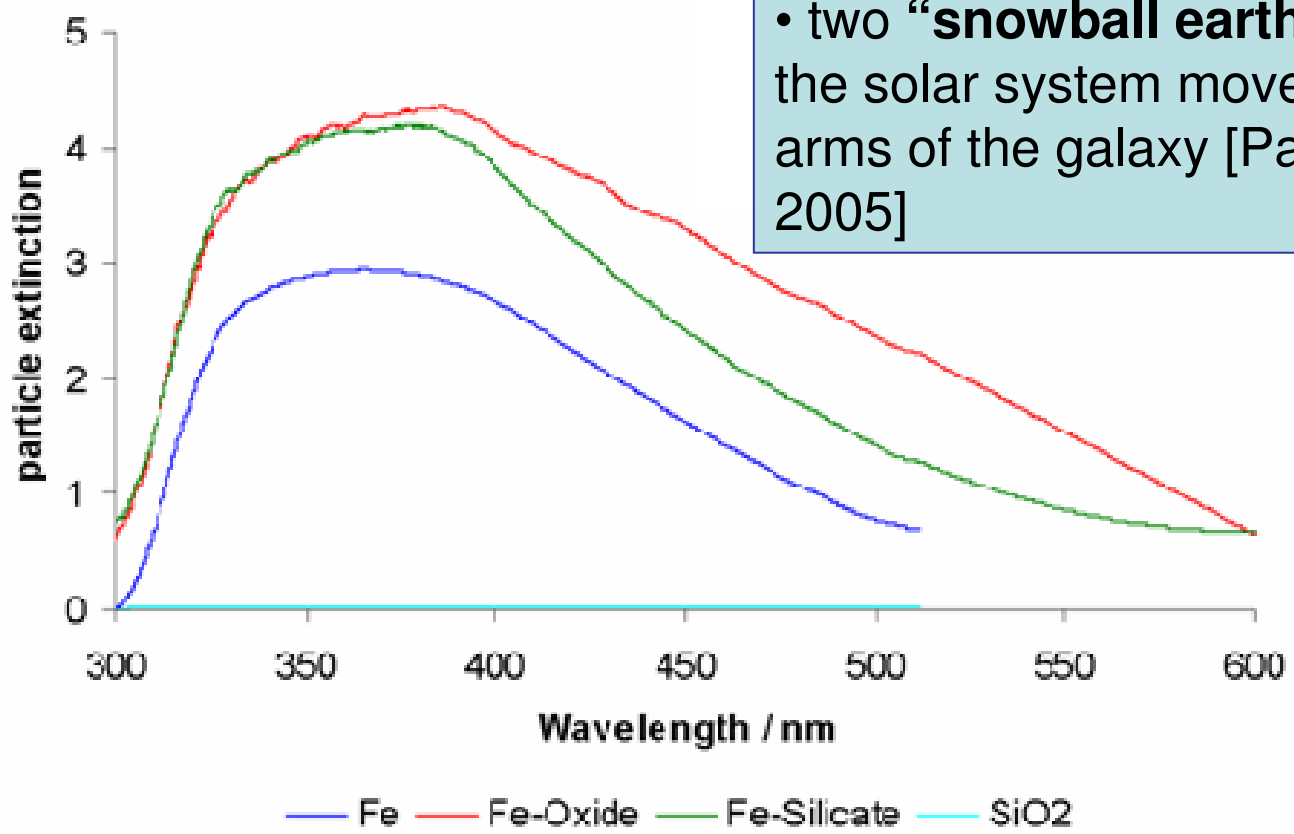

Radiative forcing of meteor smoke as a function of IDP flux

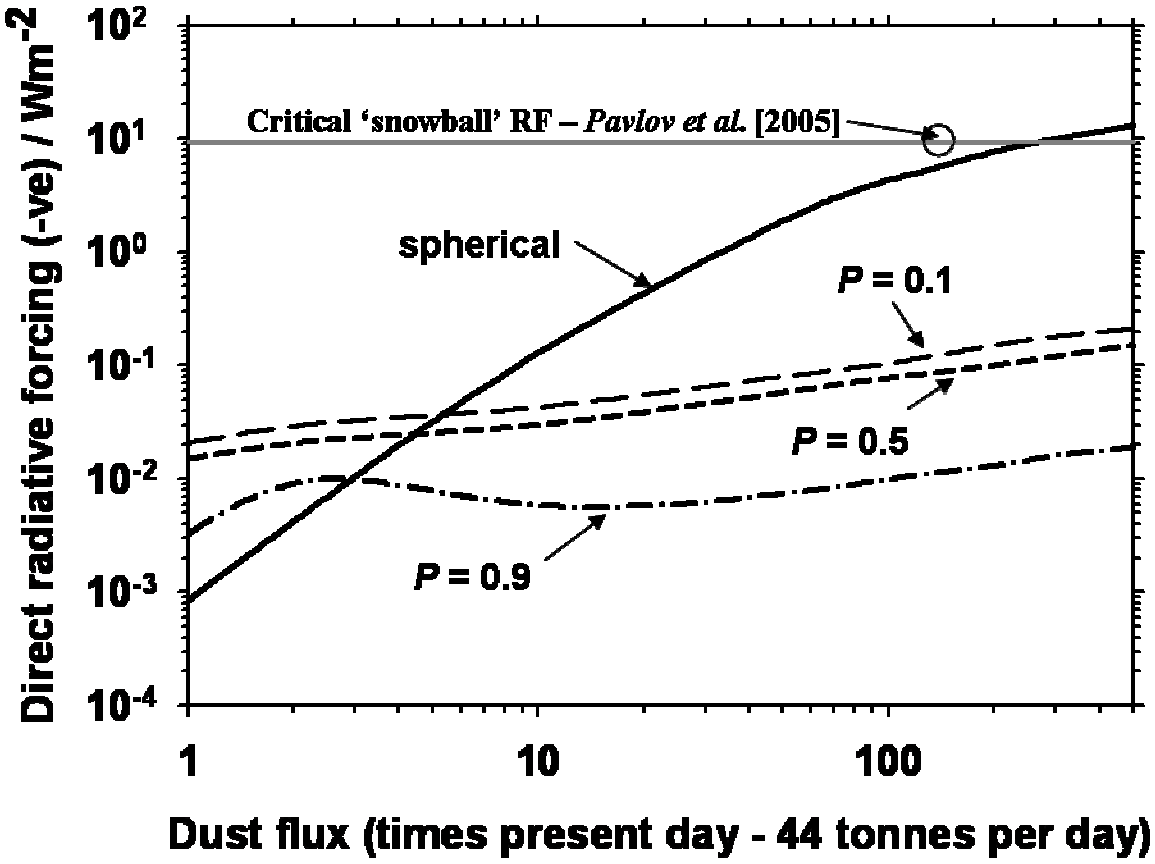

Conclusion: the required cooling of -9.3 Wm^{-2} is only reached with a massive increase in the flux to 250 times present day, *and* assuming that the smoke consists of compact spheres.

For fractal particles, sufficient cooling is never achieved because magnetic agglomeration leads to a few very large particles.

Saunders, R. W., P. M. Forster, and J. M.C. Plane, Potential climatic effects of meteoric smoke in the Earth's paleo-atmosphere, *Geophys. Res. Lett.*, under review.

Meteoric smoke

Produced from the ablation of interplanetary dust

Global layers of metal atoms

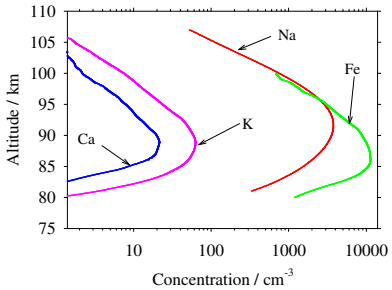

Noctilucent clouds

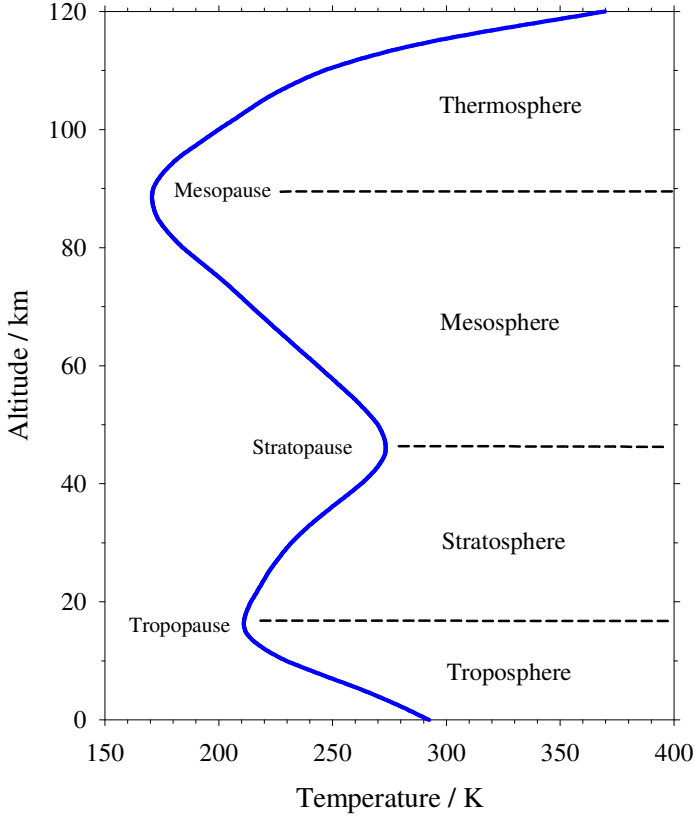

Heterogeneous reactions:

$O + H_2 \rightarrow H_2O$

$N_2O_5 \rightarrow HNO_3$

Removal of H_2SO_4 and HNO_3

Polar stratospheric clouds

Ice-core record of extra-terrestrial input over 700 kyr

Measure Ir and Pt in polar ice cores

A collaboration with Paolo Gabrielli, Claude Boutron (Grenoble) and Carlo Brabante (Venice)

Ice core collected from the Greenland ice core project (GRIP) at Summit.

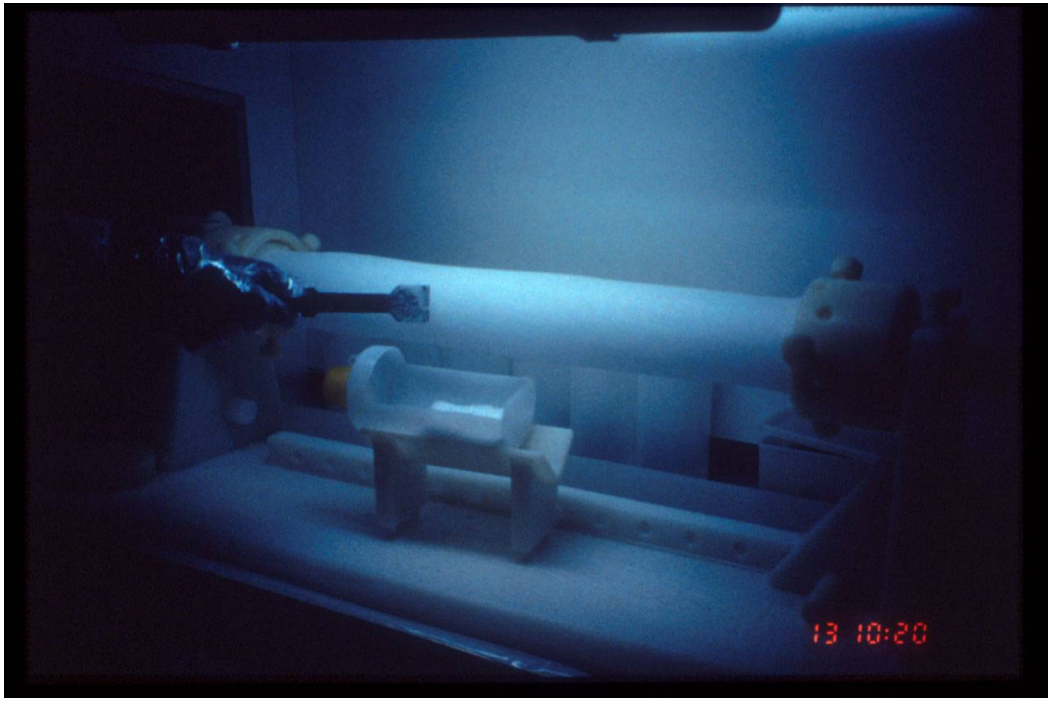

Decontamination: chiselling ice cores in a clean bench (Class 100) under laminar flow conditions at -15°C

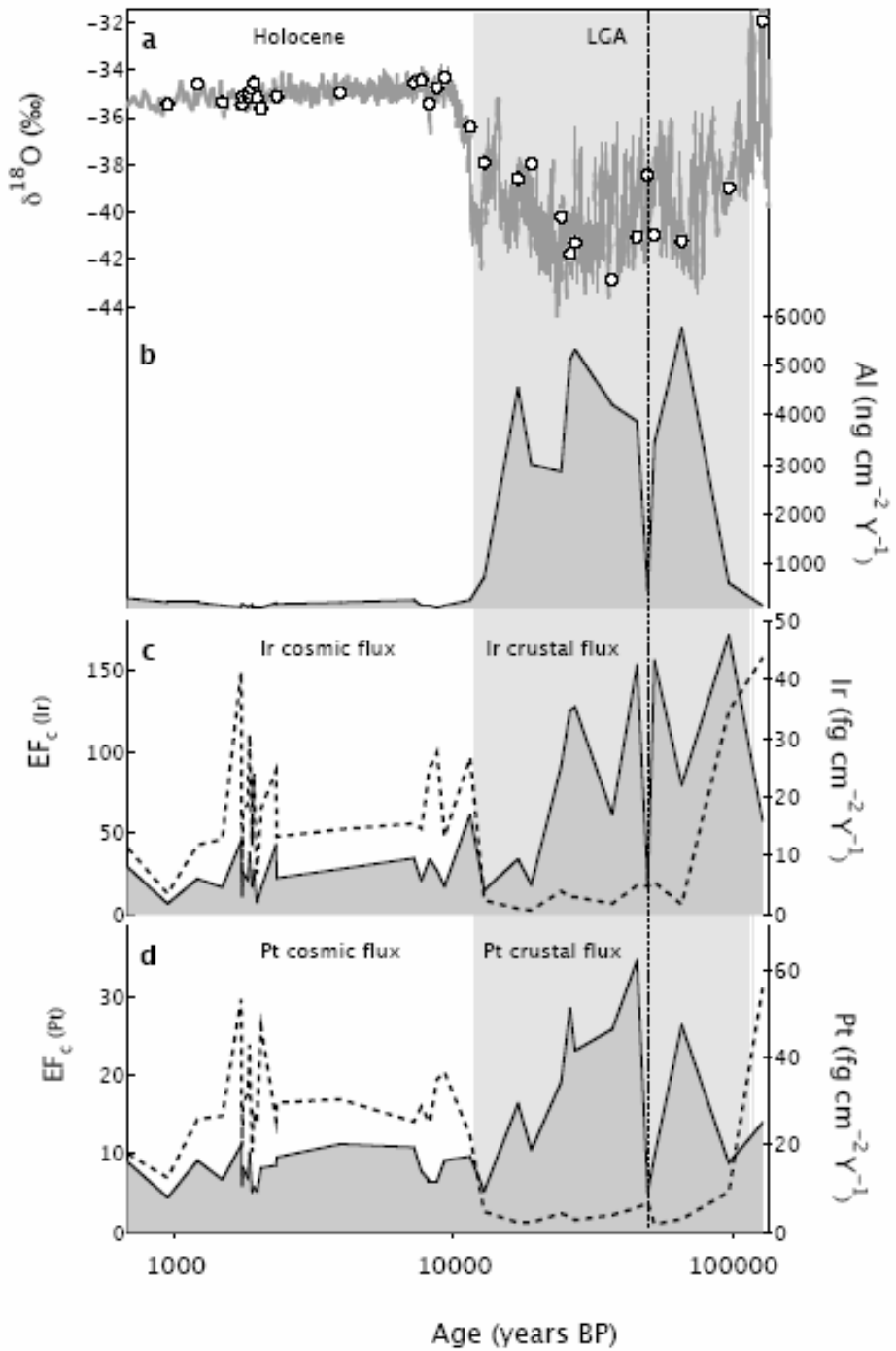

Measurements of Iridium and Platinum in an ice core from the Greenland ice core project (GRIP) at Summit.

By calculating Enrichment Factors (EF_c) with respect to Al, the record shows that the major source of Ir and Pt during the Holocene was interplanetary dust

Ultra-trace quantities of Ir and Pt in the GRIP ice core from central Greenland enable us to estimate the daily influx of interplanetary dust over the Holocene.

Gabrielli et al., *Nature* (2004)

GEOPHYSICAL RESEARCH LETTERS, VOL. 33, L13308, doi:10.1029/2006GL026480, 2006

Click Here for Full Article

Meteoric smoke fallout revealed by superparamagnetism in Greenland ice

L. Lanci[1] and D. V. Kent[2,3]

Measurements of remanent magnetization distinguish magnetic particles of extraterrestrial origin

⇒ confirms laboratory finding that the particles should be highly magnetic

Interplanetary dust flux in very good accord with estimate from Ir/Pt measurements

The particles are in the size range 7 – 17 nm.

Antarctic measurements of meteoric smoke

Gabrielli et al., *Earth and Planetary Science Letters*, 250, 459-469 (2006).

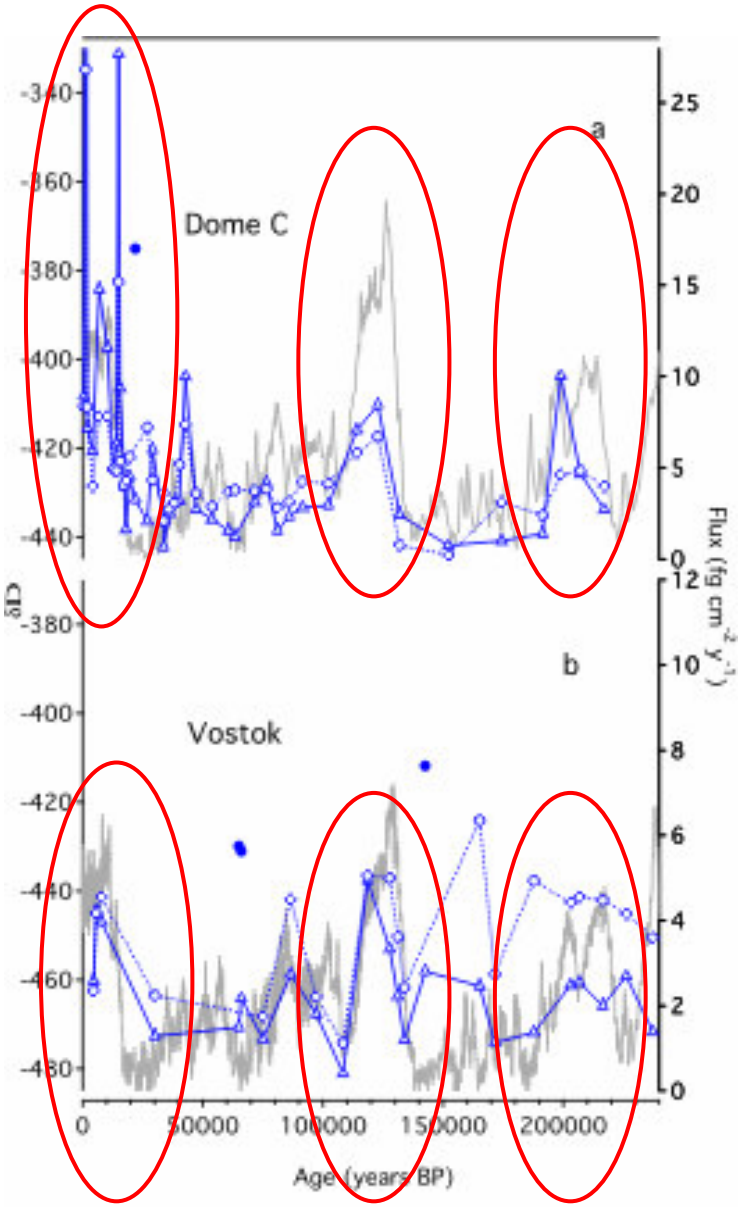

Chondritic ratio

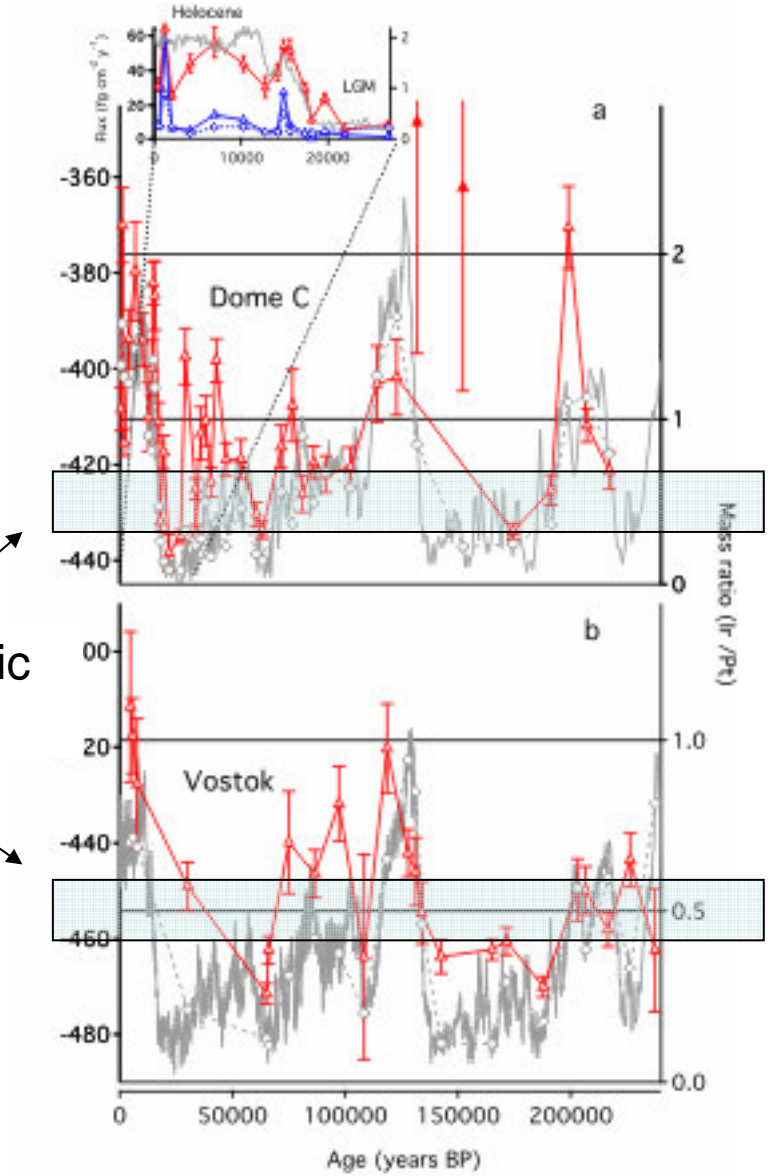

Global meteor input rate (tons day^{-1})

Gabrielli *et al.* (2004)	214 ± 82 (ice cores – Ir/Pt)
Lanci *et al.* (2006)	175 ± 55 (ice cores - Fe)
Kerner *et al*. (2003)	0.6 ± 0.3 (micrometeoroids
Rasmussen *et al*. (1995)	38 in ice >0.45 μm)
Rocchia *et al*. (1990)	27
Love *et al*. (1993)	110 ± 55 (LDEF)
Peucker *et al*. (1996)	101 ± 36 (sediment cores)
Mathews *et al*. (2001)	7 – 10 (ISR)
Plane (2003)	12 – 30 (Na model)

The impact of meteor smoke will be greatest in the winter polar vortex because the entire mesosphere is “flushed” within 3 weeks by the very strong meridional circulation from the summer to winter pole

Assuming smoke deposited at latitudes > 50°, then

global IDP flux = ice core smoke flux / 5

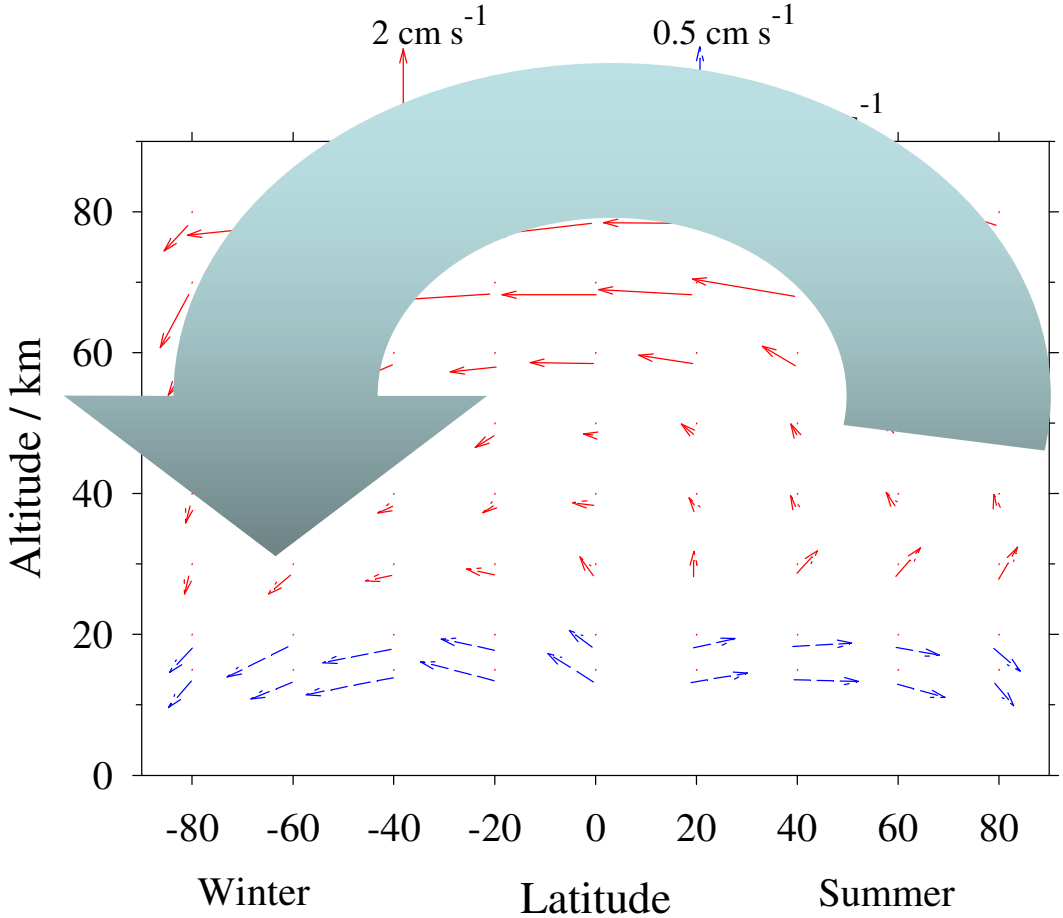

Global meteor input rate (tons day^{-1})

Gabrielli *et al.* (2004)	40 ± 16 (ice cores – Ir/Pt) / 5
Lanci *et al.* (2006)	35 ± 10 (ice cores - Fe) / 5
Kerner *et al*. (2003)	0.6 ± 0.3 (micrometeoroids
Rasmussen *et al*. (1995)	38 in ice >0.45 μm)
Rocchia *et al*. (1990)	27
Love *et al*. (1993)	110 ± 55 (LDEF)
Peucker *et al*. (1996)	101 ± 36 (sediment cores)
Mathews *et al*. (2001)	7 – 10 (ISR)
Plane (2003)	12 – 30 (Na model)

Conclusion: there is plenty of work still to do

In the meantime, here is a movie of meteoric smoke in the upper mesosphere (well, sort of …)

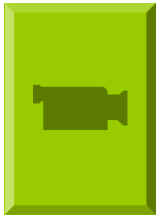

The End